1999

Algorithms on determining the correlation laws between ultrasonic images and quality of spot welds.

Hsu-Tung Lee
University of Windsor

Algorithms on Determining the Correlation Laws between Ultrasonic Images and Quality of Spot Welds

By

Hsu-Tung Lee

A Dissertation
Submitted to the Faculty of Graduate Studies and Research
through Industrial and Manufacturing Systems Engineering
in Partial Fulfilment of the requirements for
the Degree of Doctor of Philosophy at the
University of Windsor

Windsor, Ontario, Canada

1999

Your file Votre référence
ISBN: 0-494-00167-4
Our file Notre référence
ISBN: 0-494-00167-4

Abstract

Conventional quality control devices for spot welding cannot perform on-line inspection and provide feedback to the welding control system. In this way, the traditional quality control systems are similar to statistical welding parameters monitoring systems. It is imperative to combine the idea of on-line quality inspection with closed-loop feedback control in a robust control system. However, there is no single acoustic method to date capable of manipulating real-time control and on-line quality inspection, concurrently, since specific procedures (e.g. scanning time and adjustment time) need to be adopted by traditional acoustic microscopes to retrieve proper information, and these procedures tend to disable the real-time and on-line capability of acoustic microscopy.

With recent hardware improvements, the novel portable acoustic device is able to reduce the scanning time to real-time fashion without losing any significant data. On the other hand, the adjustment time of the portable acoustic device can be reduced noticeably by employing intelligent control software instead of human operators. This new hardware-software configuration will be an ideal approach to the on-line, real-time nondestructive inspection of spot welds. The primary goal of this research is to develop an intelligent system to accomplish the on-line, real-time nondestructive inspection for spot welds. The following objectives were fulfilled to reach the final goal.

- Classification of the acoustic images of spot welds.
- Quantification of acoustic information as parameters.

- The study of the influence of each parameter on the strength of spot welds.
- Identification of important and significant parameters.
- Integration of these parameters into the knowledge base of the software.

The system developed can be an on-line advisor that is capable of providing critical information about the quality of spot welds during the process. Furthermore, this system is able to render warning signals to the process control unit to prevent further mistakes.

DEDICATION

To my family

ACKNOWLEDGEMENTS

I would like to take this opportunity to express my sincere gratitude toward Dr. R. Maev and Dr. M. Wang, my dissertation advisor, for their support and guidance. I would like to thank my committee members, Dr. M. W. Lu, Dr. G. Rankin, Dr. F. Salustri, and Dr. S. Taboun for their helpful advice and well wishing.

I would like to express my sincere thanks to Dr. E. Maeva for her constantly encouragement and precious suggestions during the preparations of this dissertation. I would also like to thank to all the members of Center for Imaging Research and Advanced Materials Characterization for their support.

I would like to thank my friends, all the graduate students of the Industrial, Manufacturing and Systems Engineering for their friendship and companionship.

Finally, to my parents, my wife and our families, I owe the most sincere debt of gratitude for their support, encouragement, and help.

Contents

LIST OF TABLES

LIST OF FIGURES

NOMENCLATURE

I: current

R: resistance

t: time

$[\tau]$: stress matrix

$[\varepsilon]$: strain matrix

C_{ijkl}: second-order elastic constant

λ and μ: Lamé constant

E: Young's modulus

G: Shear modulus

ν: Poisson ratio

u: particle displacement vector

ρ: density

λ: eigenvalue

p: polarization vector of acoustic waves

d: propagation unit vector of acoustic waves

A: amplitude

ω: angular frequency

k: wave vector

l, m, n : propagation unit vectors

γ: Texture anisotropy factor

$\oplus$: operator for dilation

Θ: operator for erosion

AWS: American Welding Society

NDT: Nondestructive Testing

NDE: Nondestructive Evaluation

SPSAM: ultra-Short Pulse Scanning reflection Acoustic Microscope

SAM: Scanning Acoustic Microscope

ANOVA: Analysis of Variance

ASQC: American Society of Quality Control

SQC: Statistical Quality Control

GTAW: Gas Tungsten Arc Welding

SNT, ASNT: American Society for Nondestructive Testing

HAZ: Heat Affected Zone

ANN: Artificial Neural Networks

Chapter 1

Introduction

Sheet metal joining processes are widely used in many industries, such as the aerospace and automotive industries. Among these processes, resistance spot welding is the most common procedure used to join metal sheets because it has high process speed and is easily adopted in mass production lines. As these industries grow, the quality control of spot welds becomes an important issue for manufacturers eager to improve their output commodity. The quality of the spot weld is affected by welding processes and the design of the joint. Many factors have to be taken into account, such as metallurgic reactions, thermal behaviors, chemical composition and condition of the base metal, welding conditions, and the welding equipment. Furthermore, the intricate relationship between these factors makes it more difficult to control the quality of spot welds. Numerous efforts have been made to improve weld quality through different approaches; nevertheless, most of them are not overall solutions due to the lack of adequate equipment and efficient algorithms to inspect these improvements.

A conventional strategy for spot weld quality control inspection usually consists of: 1) an on-line weld current/resistance monitoring system to maintain consistent welding parameters, and 2) a spot weld examination standard set up by the American Welding Society (AWS) or the industries themselves. A spot weld examination standard includes visual inspection of the weld surface and destructive testing of collected weldment. The most important indicators of weld quality are the following [20]:

1. Surface appearance (by visual inspection);
2. Weld size (by visual/destructive inspection);
3. Penetration (by destructive inspection);
4. Strength and ductility (by destructive inspection);
5. Internal discontinuities (by destructive inspection);
6. Sheet separation and expulsion (by destructive inspection);
7. Weld consistency (by monitoring welding parameters).

The welding quality indicators listed above are vague due to the insufficient quantified description. To apply these specifications in practical manufacturing cases, these indicators must be converted to quantified inspection standards. From the Welding Handbook [20] and the Resistance Welding Manual [73], some of those quantified indicators are itemized in Table 1.1.

Table 1.1 Welding quality specifications

Weld Quality	Specifications from welding handbook	Industries' quantified standard
Surface appearance	Free from fusion, electrode deposit, pits, cracks, excessive indentation	Free from weld flash, sharp protrusions, and other surface distortion Surface indentation is less than 30% of the thinner base metal thickness
Weld size	Minimum nugget diameter of 3.5 to 4 times the thickness of the thinner outside part	Nugget diameter depends on the thickness of base metals Tabular for different conditions
Penetration	Minimum penetration: 20% of thinner outside piece Maximum penetration: 80% of thinner outside piece	Shall not be less than 20% of the original sheet thickness
Strength and ductility	1. At or close to the tensile strength of base metal 2. Minimum ductility ratio: 25%	Min. tensile strength = (3.14) x (min. tensile strength of base metals) x (required nugget size) x (thinner metal thickness)
Internal discontinuities	No defects should occur at the periphery of a weld	Ultrasonic or Eddy current method Metallographic method
Others	Sheet separation and expulsion	Destructive test frequency, distortion, nondestructive wedge and bend test

In reference to the table above, the spot weld quality control relies mainly on an on-line supervising unit to monitor welding parameters, on-line inspectors to perform visual inspection, and statistical sampling techniques for off-line destructive testing.

It is obvious that the aforementioned conditions are mostly for visual inspection and destructive testing which do not take into account the combined effect of those indicators. Furthermore, the true quality of the spot weld, i.e. its strength, is only presumed by off-line destructive sample tests. Unless every spot weld is examined, there is no certainty that the required strength has been met.

The acoustic microscopy method is one of the extensively used nondestructive testing (NDT) methods and has been used for various inspection applications. Unlike other non-destructive methods, the acoustic method provides both surface and internal information. Moreover, the acoustic method stipulates deeper penetration into specimens and higher sensitivity to small discontinuities. By utilizing the acoustic nondestructive method, the internal structure of spot welds can be represented as acoustic images for further studies. However, acoustic methods are not flawless, and the nature of acoustic methods confines the applications of acoustic microscopy. The most common limitations of the acoustic method are:

1. Couplant fluid (propagating medium) is required for acoustic wave propagation between the acoustic probe and the test specimen; and
2. Skillful operators are needed to operate devices and to analyze the information.

The first limitation does not cause much difficulty in examining spot welds since the materials for joining in the automotive and aerospace industries are usually galvanized or coated. Thus, applying couplant fluid on surfaces to be examined will not damage the product. For the second limitation, manufacturers have to set up standards or training programs for the inspection personnel to ensure accurate NDT results. This limitation makes the on-line inspection of spot welds difficult because it is not economical to train every worker in the plant to be a tester/analyzer/operator. Besides, the nature of the acoustic method limits its practicality in on-line applications.

The acoustic method, unlike the optical or X-ray method which receives two-dimensional information through one process, has to go through point-to-point scanning procedures to obtain two-dimensional information. There are several ways to display acoustic information, and they can be categorized by the information obtained. The most common ones are A, B, and C scans that can be selected to show the internal defects as required [84].

A-scan:

The A-scan is the simplest presentation. It shows the amplitude of the echoes, or the reflection, as a function of time at a selected point of the work surface. The duration of time between different peaks represents the time needed for acoustic waves to travel between discontinuities.

B-scan:

The B-scan follows the same procedure as the A-scan but repeats the signal-catching procedures while the lens scans along the X-direction. Hence, an image of the cross-section of a component is built up. The measured amplitude is displayed as a colored dot on the monitor and its coordinate is defined by the position of the lens (X-coordinate) and the acoustic pulse's traveling time (Y-coordinate).

C-scan:

If the amplitude of a particular echo is monitored at each point on certain depth of the workpiece, a C-scan can be formed. Measurements at each point are taken using scanning and electronic gate mechanisms that produces a plan for the level of the defects. This scan only gives the information at the preset depth of the electronic gate.

Among these three types of scans, the C-scan provides the richest information and is therefore more desirable for our quality control purpose; however, it is also the most time-consuming scan.

The primary goal of this research is to develop a rapid and robust algorithm for the software of the acoustic microscope to reduce the role of experienced microscopy operators involved in spot weld inspection. By employing the recently developed ultra-Short Pulse Scanning reflection Acoustic Microscope (SPSAM) system, designed by the Center For Imaging Research and Advanced Materials Characterization, a large amount of acoustic information can be retrieved, processed, and represented in a short period of time. This state-of-the-art hardware design facilitates on-line acoustic non-destructive inspection for spot welds. To adapt this hardware for use in industrial plants, the accompanying software is equipped with algorithms that can help analyze the information acquired by the acoustic device, and is capable of providing the go/no-go responses to on-line workers in a real-time fashion. Furthermore, feedback can be provided to the welding control unit during the inspection process.

The major contribution of this study is the development of software for an on-line feedback system for spot weld quality control. This developed system overcomes the limitations of the acoustic microscope and complements the acoustic spot weld inspection instrument to a closed-loop, feedback quality advisor system. Once the acoustic inspection system detects defects or inconsistent weld strength, the system will be able to provide advice for the welding unit. This system will render more accurate feedback than the traditional current/resistance monitoring system. Besides, this system can achieve the goal that old monitoring systems cannot, that is, to give on-line feedback of the weld quality and to perform inspections based on the internal structure of welds. This system functions as a complementary tool to the design unit since the integrity of any given weld can be predicted based on acoustic information. This helps designers to reduce the total number of spot welds and thereby reduces manufacturing costs.

The steps to achieve this goal are as followed.

Step One: Study of acoustic wave propagation in anisotropic, textured structures including alloy and weld metals

The spot weld nugget is an anisotropic material with microstructures different from its base metal. The study of acoustic wave propagation in the weld nugget includes metallurgical analysis and characterization by the acoustic microscope. The aim of this step was to study the mechanical and physical properties of weld nuggets including dendrite structures and ferrous areas. The propagation and interaction of focused acoustic beams inside spot welds is also studied. This step provides the fundamental understanding of the connection between weld nugget structures and the associated acoustic images.

Step Two: Quantitative study of acoustic information

The relationship between the acoustic information of spot welds and the quality of spot welds takes further efforts to clarify. Through the study of acoustic images, information such as the profile of surfaces, shape and size of weld nuggets, and size of defects are quantified. Afterward, this quantified information was formulated as the quality index of spot welds. The objective here is to analyze the acoustic image and to extract desired information. The procedures for this task are:

- **Mathematical morphology**: This procedure improves the acoustic images by eliminating noise, improving geometrical shape, and reshaping important objects inside the spot welds. By using morphology techniques such as dilation and erosion, some porosity is grouped geometrically and the joint effect of grouped porosity is studied.
- **Segmentation image**: This procedure uses a thresholding technique to distinguish desirable objects from noise. Thus, important information is left for further study. The threshold that separates the peaks on a color/gray level histogram is selected based on the knowledge gained from the previous step.
- **Edge detection**: At this stage, the task is to differentiate discontinuity information inside the nugget from the nugget area, and to build up clear and continuous boundaries for those objects.

- **Area calculation**: The task involved is to use the boundaries obtained in edge detection to quantify the desired information for later study.

Details of these procedures are listed in Chapter 4.

Step Three: Destructive examination of specimens

Destructive testing of the samples will establish quality indexes for spot welds. These quality indexes could be the strength of the weld, the nugget size, and a good/bad quality judgment from experts. Later, the result is correlated with acoustic image parameters.

Step Four: Parameters study

Two approaches are used for this stage. The first task is the statistical analysis of the parameters through an ANalysis Of VAriance (ANOVA) method. This task will contribute to the selection of significant parameters to build up the quality index for welds. After the ANOVA analysis, a mathematical relationship is built between the weld index and the quantified information established in Step Two. The second task is to establish the relationship between the weld quality and screened parameters provided in the first task by artificial neural networks and non-linear regression methods. The first method is aimed at determining the weld index as a good/bad judgement, and establishing the relationship between these non-quantified judgments and quantified weld index information. The latter method targets simpler weld quality indicators, e.g. the size of welds, and builds mathematical relationship between weld indices obtained in the first task and the quality indicator. Details of both methods are listed in Chapter 4.

Step Five: Integrate knowledge into software

The integration of knowledge is the last part of this research, and the most important part. By importing the extracted knowledge into its control mechanism, the portable acoustic device becomes an intelligent device for spot weld inspection. Both quality evaluation methods developed in Step Four show promising results. The statistical method is applied as a nugget diameter predictor, and the neural network model is employed in order to determine nugget integrity. Regardless of which model is adapted in the final hardware product, the knowledge accompanying the software will serve as an on-line advisor for workers, and will provide closed-loop feedback to the robot welding control system.

Chapter 2 presents a literature review of the spot weld process, spot weld metallurgy, and major studies on spot weld quality control. Review of the applications, historical development, and the advantages of acoustic microscopes are then introduced. **Chapter 3** provides a general description of an acoustic device, its theory and the acoustic wave propagation inside spot welds. **Chapter 4** describes the procedures for quantitative analysis of the acoustic information and establishes the relationship between this information and weld quality. Four steps are proposed in order to obtain a systematic result from analyzing acoustic images. Two methods are proposed to build the relationship between these parameters and the weld quality indexes. **Chapter 5** is a report of experimental results. **Chapter 6** is the conclusion.

Chapter 2

Literature review

2.1 Spot weld quality control

The American Welding Society (AWS) has established a standard method for testing resistance welds. The standard method describes five types of resistance weld processes including spot welds, roll spot welds, seam welds, project welds, and flash welds. Among them, there are 11 general test methods for spot welds. However, it is noted [20] that, "In general, the lack of nondestructive tests for resistance welds makes it necessary to depend largely upon sampling testing for the control of weld quality." Thus, the standard employs the control chart methods, developed by the American Society of Quality Control (ASQC) to evaluate weld consistency.

This off-line, statistical quality control (SQC) method does not meet the requirement of mass production industries simply because it cannot offer the timely feedback for their products. Hence, many industries tend to use on-line monitoring systems to accomplish the real time feedback inspection. Some systems include the automatic current and voltage control system, the voltage and current integrator monitor, the expansion rate monitor, the expansion correction system, and the resistance correction system. Johnson [50] reviews these techniques and their progress in his paper published in 1975.

As industries expand, resistance spot welding becomes more important because it is a widely accepted joining process for mass production with high process speed. As a result, more studies have been devoted to spot weld process characterization to improve the quality of spot welds. Previous research about spot welds can be divided into three main groups: studies on the modeling of spot weld processes, studies on the welding characteristics by different materials, and studies on welding quality control by controlling certain weld parameters.

Greenwood [39] uses exact geometric models and numerical methods to study the temperature of spot welds on mild steel. Gould [37] examines nugget development on AISI 1008 steel using an experimental technique which studies a metallographic of the nugget's microstructure and an analytic model which determines the heat required to melt the base metal, and for heat transfer in liquid. Cho *et al.*[18] establish a model to predict nugget growth, nugget penetration and temperature distribution on mild steel by taking into account factors such as heat generation from electric current, thermal conductivity, and the phase change from solid to liquid. Neid [67] and Tsai *et al.* [81][82] develop finite element analysis models for simulating the thermal exchange and the pressure of electrodes. Vlahopoulos *et al.* [87] develop the finite element analysis method based on formulating the governing differential equations with respect to the energy variable. Hirsch [42], Bertram [7], and Fuerschbach [30] establish mathematical models based on different considerations for spot welding processes.

Aluminum welding has become an innovative application in recent years because of its light weight. Irving [46] discusses the welding techniques used in the four most common aluminum alloys, namely, Alloys 6061, 5083, 5052, and 5454. Gerry [32] from Texas Instruments develops an alternate method to join aluminum and steel. Browne *et al.* [11][12] develop a computer-based model to include the elastic-plastic mechanical deformation and the thermal conduction in aluminum resistance spot welding. Roset and Rager [72] study the welding parameter profile of aluminum spot welds. In the aspects of welding processes of various materials, Lin and Duh [60] examine the spot weld parameters on the Fe-Mn-Al-Cr alloy. Acoff and Thompson [2] study the weld heat treatment on the Ti-14Al-21Nb alloy by Gas Tungsten Arc Welding (GTAW). De *et al.* [21] conduct a series of experiments of resistance spot welding in 1- mm thick St1203 low carbon steel sheet.

The welding parameters of spot welds are welding current, weld holding time, and electrode pressure. Controlling these parameters may help to manufacture a good spot weld. Experiments show a range of current values over which a given material may be successfully spot-welded. Many studies have focused on managing these parameters to produce indexes for good quality welds. In the 1960's and 70's, a large amount of research was done on monitoring single or multi-welding parameter(s) to achieve quality control of spot welds. Recently, mathematical or finite element models were adopted to simulate the welding process in verifying the theoretical solutions to the experimental data. Snee and Taylor [77] provide an experimental study of an infra-red monitoring system for resistance spot weld. In their study, infra-red signal amplitude is used to study the development of a weld. Bhattacharya *et al.* [8] develop an in-process quality control technique of spot welding by monitoring the dynamic resistance during weld development. Dickinson *et al.* [24] characterize spot welding behaviors by monitoring dynamic resistance and critical expulsion energy. Taylor [80] develops a monitoring system by exploring the relationship between electrode displacement and expansion rate. Chang *et al.* [17] carry out a control method to track the movement of a desired electrode curve and to adjust the input voltage for an ideal weld. Tsai *et al.* [83] develop a single parameter, in-process and feedback control system on spot welds by using finite element analysis. Howe [44] uses the ANOVA method to analyze a series of experimental data produced by specimens of different thicknesses and materials with respect to different welding parameters. Pal and Cronin [70] characterize spot welded sheet metal beams with static and dynamic tests. Other parameters have been studied for their on-line monitor possibility. Beersiek *et al.* [5] use penetration depth as the control parameter in on-line monitoring laser beam welding. Nava-Rudiger and Houlot [66] develop an integrated real-time system using infrared photodiodes to detect the appearance of geometric defects such as sagging or misalignment during laser beam welding.

There is, as yet, no comprehensive mathematical model for spot weld processes because of the variety of factors involved, e.g., different surface roughnesses, diverse material coatings, various material compositions, and human error. Furthermore, the traditional mathematical methods cannot handle chemical reaction, thermal behavior, electrical and mechanical conducts simultaneously in a single model. By implementing new modeling techniques such as fuzzy control and neural networks, it is possible to solve this complicated problem through different approaches. Much work has been done in this area. In one case, Jou *et al.* [51] introduce a fuzzy control system for spot welds based on neural network models. Spinella [79] develops a fuzzy logic model to determine the operation parameters of aluminum spot welding. Nevertheless, these methods are still dealing with the task of optimizing welding parameters alone and are unable to provide accurate indicators of the on-line quality of spot welds.

2.2 Spot weld metallurgy

This literature review section is devoted to the fundamental study of spot welds, especially for its microstructure and acoustic properties. The structure of weld nuggets directly affects the propagation of acoustic waves. Moreover, the non-homogeneous elastic properties inside spot welds affect the contrast of acoustic images. Thus, it is essential to understand the spot weld nugget structure before further inspection. A great deal of literature, e. g. Lancaster [58], Linnert [61], Bruckner [13], Séférian [74] and Easterling [26], discuss metallurgy in welding. Dix *et al.* [25] use an experimental method to study two phenomena: nugget formation and stuck welds in the spot weld process. Ledbetter [59] studies the mono-crystal elastic constants in a weld by the ultrasonic method. However, only a few of them are concentrated on the acoustic properties of weldment.

2.2.1 General metallurgy of spot weld

The idea behind a resistance spot weld is to join two or more parts by applying clamping pressure and high electrical current. The clamping pressure is applied during the welding process to provide the required intimacy of contact between faying surfaces and to confine melted liquid. Liquid metal is melted by the welding heat generated by the resistance of the metal at the site where electric current flows. The liquid metal serves as the joining bridge between surfaces.

The amount of heat produced is dependent upon the value of I (current), R (resistance) and t (the time during which the current flows). The heat generated is given by the equation

heat produced $= I^2Rt$ joules

where I is in amperes, R is in ohms, and t is in seconds.

There are different kinds of resistance involved in spot welding, and they are shown in Figure 2.1.

Case 1. Electrical resistance of the electrode material.

Case 2. Contact resistance between sheets.

Case 3. Interface resistance at the location where the weld is to be formed.

Case 4. Contact resistance between the electrode and sheet material.

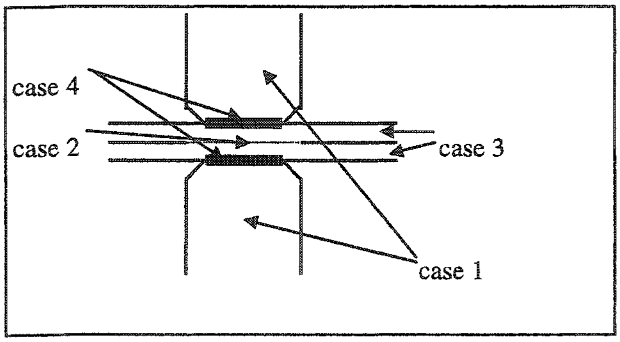

Figure 2.1 Type of resistances in spot weld

There are two stages, heating and cooling, when a spot weld is deposited. During the heating stage, the resistance in the path of the current flow does not remain constant. First, the contact resistance between sheets vanishes in the melted region. Then the resistance diverts the electrical current to the still solid metal surrounding the melted region. The diverted electrical current raises the temperature nearby and increases the volume of melted metal as the bridge of the weld bonds. When the temperature cools down, the melted region begins to solidify. The processes for solidification are:

1. Nuclei begin to form at preferred sites.
2. Individual nuclei grow into large, solid particles called grains. The orientation of the grain lattice differs from one grain to another.
3. Grains grow larger and meet at an irregular boundary called the grain boundary. The grain boundary forms a continuous network throughout the metal. The physical properties are often different at the grain boundary from elsewhere between grains.

The abstract interior structure of a spot weld after cooling is shown in Figure 2.2.

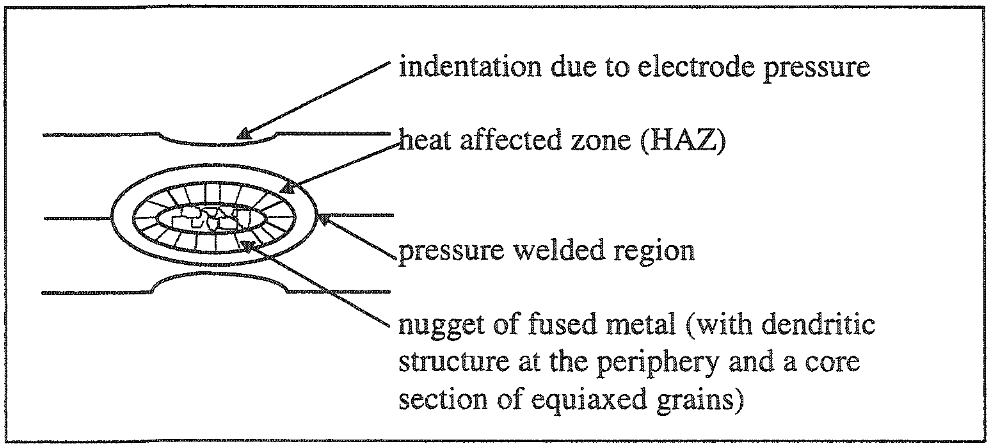

Figure 2.2 Diagram of resistance spot weld (following Lancaster [58])

There are some factors which will affect the formulation of spot welds, and they are:

1. Effect of welding current: The welding current has a greater influence on welding heat generation than resistance and time because it is in square form in the heat generation formula. A minimum current density is required for overcoming the heat conduction/ radiation loss and generating the efficient heat input to produce fusion at the interface. The maximum current density has to be limited because excessive heat input causes the expulsion of molten metal or a deep indentation on welding surfaces.
2. Effect of welding time: The heat input is proportional to the welding time. A minimum time is required to reach melting temperature at each current density. If the welding time exceeds the maximum, not only will expulsion or deep indentation occur, but the heat affect zone (HAZ) will be oversized as well, which results in certain metallurgy changes in the base metal.
3. Effect of welding pressure: The resistance is influenced by welding pressure which keeps the faying surfaces in contact.
4. Other factors: The presence of electrodes, surface conditions and metal composition are other factors that influence the welding process; however, these factors are taken into account in the welding design process.

2.2.2 Metallurgy in nugget area

When a weld is deposited, the first grains to solidify are nucleated by the un-melted base metal, and the orientation of crystal grains is in the same direction toward the steepest temperature gradient. While solidifying, metals grow more rapidly in certain crystallographic directions, and the direction of crystal growth is perpendicular to the isotherms. Hence, favorably oriented grains grow faster for substantial distances, while the faster growing grains block the growth of others in a non-favorable orientation. The aforementioned favorable crystallographic direction is the [100] direction in cubic crystals, such as body central cubic or face central cubic, the [100] direction being the least closely packed direction in cubic crystals. The [100] crystals' growth direction and the direction of the steepest temperature gradient is the same in a spot weld because there is no welding speed involved.

Because of the crystals' growth directions, weld pools solidify in a cellular or dendritic growth mode depending on the composition and solidification rates. Both modes cause micro-segregation of alloying elements. As a result, the weld metal may be less homogeneous than the base metal. During the welding solidification, three stages of microstructure formulations can be found.

First stage: Because the temperature differences inside a weld range have an extensive range, epitaxial growth from the base metal is likely to occur initially in the planar growth front.

Second stage: During further cooling, the temperature gradient decreases, resulting in a planar to cellular microstructure transition.

Third stage: When the temperature gradient further changes, the primary cellular microstructures become unstable, and develop secondary arms called dendritic structure.

Although the dendrite structure is not yet fully understood, from experimental observation (Easterling [26]), the dendrite arm spacing decreases as the cooling rate increases. This fact that the dendrite direction does affect acoustic propagation contributes to later study. The following cause-effect table draws the microstructures and properties of the weld roughly.

Table 2.1 Cause-effects of the formulation of weld microstructure

CAUSE	EFFECTS
welding process design (weld tip size, current, time)	weld pool size and geometry
composition of the melt metal (base metal, coating material, air)	constitutional supercooling and segregation
weld thermal cycle	microstructural coarseness and type of transformation product during cooling

2.2.3 Metallurgy in the Heat Affected Zone (HAZ)

The heat affected zone (HAZ) is adjacent to the weld metal. The HAZ is the portion of the base metal that has not been melted, but whose mechanical properties or microstructure have been changed by the heat of welding. Depending on the base metal's characteristics, the HAZ has been recrystallized, transformed, or tempered. The material properties and the prior thermal/mechanical history of the metal also play an important role in the formulation of HAZ. These different factors, in addition to the post-weld heat treatment, control the properties of spot welds. HAZ can be divided into several sub-zones whose microstructures are different due to the temperature gradient during welding. A schematic plot of welding sub-zones is shown in Figure 2.3.

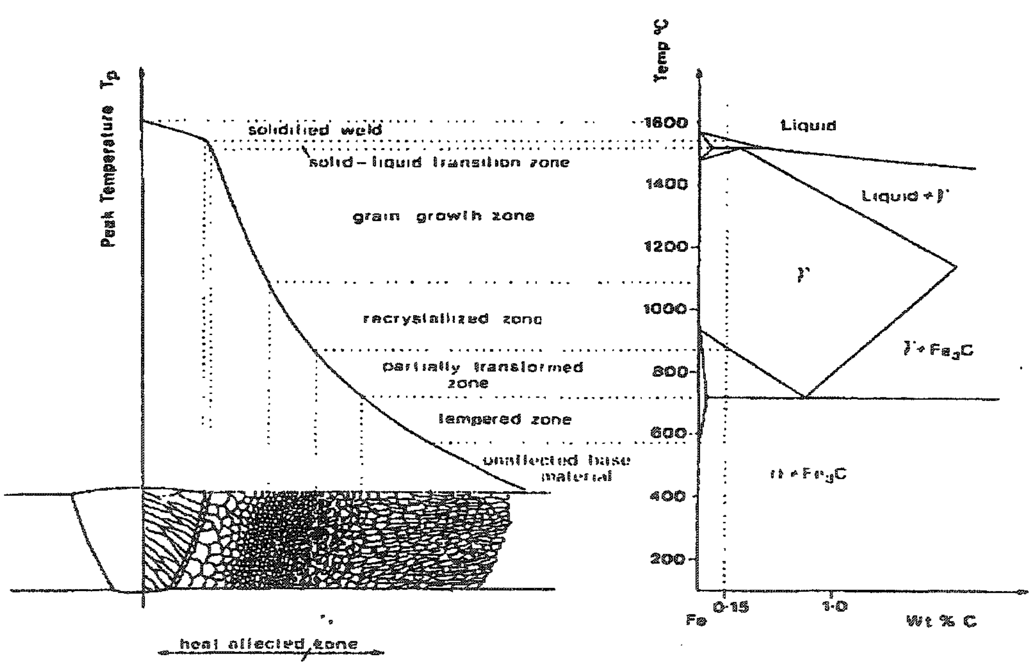

Figure 2.3 The sub-zones in resistance spot weld (following Easterlin [26])

Analyzing the formulation procedures of HAZ will help us to understand its microstructure and the propagating manners of acoustic waves through welds. Some characteristics directly affect the microstructure of HAZ and these are shown in the following table.

Table 2.2 Weld characters and their effects on the formulation of HAZ

WELD CHARACTERISTICS	EXAMPLES
Base metal	1. For a plain carbon as-rolled steel, the heat of welding has little influence on those regions heated to less than 1350° F (700° C). 2. For a heat-treated steel quenched to martensite and tempered at 600 ° F (315 ° C), heating above 600 ° F will change the mechanical properties of the metal. 3. For a heat-treated aluminum alloy age hardened at 250 ° F (120 ° C), any portion of a welded joint heated above this temperature is in the heat affected zone.
Mechanical history	1. Alloys that are strengthened by solid solution, 2. Alloys that are strengthened by cold work, 3. Alloys that are strengthened by precipitation hardening, and 4. Alloys that are strengthened by transformation (martensite).
thermal cycle	1. Temperature of recrystallization, 2. The rate of coarsening of carbides and nitrides, 3. The temperature of the solution of carbides and nitrides, 4. The main proportion of grain growth, and 5. The degree of superheating.

2.3 Applications of scanning acoustic microscopes

Scanning acoustic microscopes are scientific instruments which use the characteristics of acoustic wave propagation to image the elastic variations of materials. Unlike optical and electron microscopes, the acoustic microscope can examine the internal structure of objects, and this advantage makes acoustic microscopes suitable for inspections where internal information is important. This instrument is now widely used in scientific, medical, biological, and industrial settings. Some of the applications are:

- Industrial applications in the non-destructive evaluation of internal structures such as: welds, composite structures, various joint systems, multi-layer structures and electrical chips.
- Scientific applications in determining the properties of new materials, such as ceramics or composite materials.
- Medical diagnosis of dental implants, and soft and hard tissues.
- Biological study of bio-cells, bio-structures, and their behaviors and dynamics.

2.3.1 The development of the acoustic microscope

The acoustic microscope was independently introduced in 1929 by both Sokolov and Muhlhauser. Sokolov proposed the first application of ultrasound radiation to visualize the mechanical structure of various objects and he named the application "acoustic visualization". Thereafter, researchers began to expand the field of ultrasound studies, with the development of higher frequency acoustic waves, different resolutions of acoustic images, or the application of acoustic microscopy to different areas. The following table shows the milestones of research and development activities involving high frequency acoustic waves for visualizing interior structures [34].

2.3.2 Advantages of the acoustic microscope

The acoustic method has many advantages in nondestructive testing, and it is by far the best solution for spot weld inspection. Some common nondestructive testing methods could not address the nature of spot welds and could not provide the type or amount of information that acoustic methods do. For instance, magnetic particle testing can only give the information near the surface of the specimen, but fails to offer the interior examination for spot welds. Radiographic testing has a higher initial cost and would increase the cost dramatically to inspect each weld. The Eddy Current method, which is the other potential method for examining internal structures, performs well only on flat pipe- or tube-shaped specimens. As a result, it is not a practical method for examining spot welds because the most common location for spot welds is not on flat surfaces. In addition, Utrata *et al.* [85] review various destructive and nondestructive techniques for spot welds evaluation.

Acoustic microscopy can be used to examine the internal structure of objects. It is one of the commonly used nondestructive testing methods and has many advantages. The approach of this method is to generate mechanical vibrations, to guide the vibrations through the desired examining specimen, then to receive the acoustic signals. The

Table 2.3 Milestone of development of acoustic microscopes

Year	Event
1929	Muhlhauser and Sokolov independently propose ultrasonic waves for materials evaluation. Scanned imaging is suggested outright in manuscripts by both.
1931	Muhlhauser obtains German patent for ultrasonic testing of materials using continuous wave transmission.
1936	Sokolov proposes acoustic visualization of the electric-charge distribution on a piezoelectric disk as a receiver.
1937	Bergmann writes Ultraschall with ~600 references. Pohlman transforms sound pressure into visible images.
1940	Pulse-echo ultrasonic testing is invented by Firestone Inc. (USA), Sproule (England), and Kruse (Germany) independently. SNT (later ASNT) chartered to provide a professional forum for NDT.
1943	The first commercial apparatus for using pulse-echo method in industrial application.
1947	First time this method is used as medical diagnostic tool.
1945 to 1958	Sperry acquires Firestone patent (ultrasonic reflectoscope). Erdman, Krautkramer, Pringle, and Smack develop ultrasonic C-scan equipment. Hasting, using an Erdman system, makes gray-scale C-scan image.
1959	First ASNT handbook by McMaster. C-scans, focused probe, scanned image, CRT grayscale C-scan image.
1963	Jacobs adds electron multiplier to Sokolov Tube.
1966	Korpel *et al.* at Zenith Corp. invent scanning laser acoustic microscope.
1967	First international symposium on acoustic holography.
1969	Batalle founded Holotron Inc., later Holosonics Inc., to market acoustic holography systems.
1971	Fowler at Panametrics Inc. introduces and markets a quartz buffer-rod-lens focused 50 MHz transducer.
1973	Lemons and Quate invent and introduce 1 GHz SAM. Stanford group includes G. Kino, P. Khuri-Yakub, and B. Auld.
1974	Sonoscan Inc. founded by L. Kessler to market SAM. E. Ash builds SAM group at University College, London, UK, that includes C. Tsai and H. Wickramasinghe.
1977	Tsai builds second SAM in US at Carnegie Mellon University.
1978	Weglein and Wilson develop the first theory for quantitative characterization of the contrast response in reflection acoustic microscope.
1980	Leitz Inc. and Olympus Ltd. introduce scanning acoustic microscopes to international market. Imaging is now seeing rapid growth.
1982	Kushibiki and Chubachi develop the cylindrical lens excites Rayleigh waves in one direction which can be applied as an effective instrument for anisotropic materials study.
1983	Stanford University builds the prototype of cryogen scanning acoustic microscope at frequency of up to 6 GHz.
1988	Maev *et al.* develop device for polymer and medical diagnosis of transmission microscope with 500 MHz frequency.
1990's	More than 30 firms manufacture industrial acoustic imaging/microscopy systems for an international market.

acoustic wave propagation can be affected by various conditions such as the velocities of acoustic waves traveling in materials, the frequency of the acoustic wave, and the focusing of the acoustic beam. These various conditions increase the flexibility of acoustic nondestructive testing, and these advantages are summarized in reference [84].

Versatility

The acoustic method permits testing on objects of a wide range of sizes and geometries. The technique detects internal, hidden discontinuities that may be deep below the surface. Applications range from thickness measurement, and porous detection to residual stress detection.

Sensitivity

The use of a high frequency, well-defined beam of sound permits detection of the smallest critical discontinuities. In terms of detection sensitivity, disk shapes and cracks of almost zero thickness can be detected. In terms of the location of discontinuities, the depth of the cracks can be measured within millimeters.

Safety and Convenience

There is no hazard to the operator or to nearby personnel during the use of acoustic equipment. Acoustic devices can be used in shops, laboratories, warehouses, or open fields (allowing on-site tests). Moderate power is needed from an alternating current line or a small generator.

Many studies have been done concerning the application of the acoustic method in different areas. Lott [62] uses ultrasound to detect the molten/solid interface of Gas Tungsten Arc Welding (GTAW) pools. Ogilvy [68] studies the ultrasonic beam profile and beam propagation in austenitic welds by using a ray tracing model. Veidt and Sachse [86] use a point-source/point receiver technique to measure the mechanical properties of the {111} p-type semiconductor. Gilmore *et al.* [33] study ultrasonic images through the non-destructive examination of structural materials. In their studies, they establish accuracy by calibrating information from some known targets with which the flaw size and shape, and spacing between flaws can be imaged. Yuasa and Masazumi [88] designed a device with linear array type inspection to examine the spot weld nugget diameter and thickness. Maev [64] *et al.* have developed a high resolution ultrasonic welding inspection device with a wide-field, short-pulse acoustic microscope at operating frequencies of 25, 50, and 100 MHz. Sokolowski *et al.* [78] use acoustic microscopy to study the internal structures of aluminum 318 casting.

Acoustic waves propagating through anisotropic materials is a very complicated phenomenon and it is a material-dependent problem. Many researchers have studied this issue, especially in the area of composite materials. Briggs [10] examines ceramic fiber composites under scanning acoustic microscopy. Lee *et al.* [57] use line focus acoustic microscopy to examine the reflect function of layered anisotropic materials. Deschamp and Som [22] utilize scanning reflection acoustic microscopy to obtain high resolution acoustic images and perform a trial on anisotropic materials. These studies are all focused on composite materials. Adler *et al.* [3] characterize gas porosity in aluminum alloy casting with ultrasonic experiments. Dewey *et al.* [23] use the ultrasonic method and the tensile testing method to measure the anisotropic elastic constants of 308 stainless steel welds. Kupperman and Reimann [56] study the wave propagation and anisotropy in austenitic stainless steel weld metal. Gornaja and Aljoshin [35] use the Born approximation to solve the problem of planar ultrasonic wave scattering in an anisotropic polycrystal medium.

The acoustic method is widely applied in many engineering areas including the spot weld integrity examination. One example is illustrated in the Ultrasonic Testing Handbook [84]. However, most commercial acoustic testing devices use A-scans representation for off-line quality control. These devices present acoustic information by A-scans, about which there is not enough information for us to understand the true quality of a given spot weld. To build the next generation of on-line devices with the ability to process more acoustic information in a short period of time becomes critically important.

Chapter 3

Overview of the theory of acoustic nondestructive testing method

3.1 Fundamentals of the acoustic microscope

Ultrasonic testing is one of the nondestructive testing methods which is widely accepted as a substantial technique for inspecting industrial products, biological tissue, and construction sites. The subsequent development of the Scanning Acoustic Microscope (SAM) has enlarged the capability of acoustic microscopes from one-dimensional to three-dimensional. This development provides higher resolution and makes the acoustic microscope another testing option distinct from the traditional optical and electron microscopic methods. The basic features of SAM are:

1. Acoustic pulse receiver and generator

   The pulse generator generates an acoustic wave, and the pulse receiver collects it. The acoustic wave generated can be a continuous pulse or a short pulse, depending on the system requirements.

2. Focus transducer

   Most focus transducers use a piezomaterial element with an optical quality ground lens to provide the desired quality of acoustic beam alignment and focusing. The material of the acoustic lens should have low attenuation and a high velocity to minimize aberrations. The lens can thereby focus the acoustic beam into various frequencies from 5MHz to 2GHz. The focus transducer converts electric pulses into mechanical vibrations or vice versa. Sapphire is a superior material for the lens in both respects. The precision of the acoustic beam focus primarily depends on spherical aberration; consequently, the spherical aberration itself depends on the ratio of the ultrasound propagation velocities in liquid and the velocities inside the sound-guide in the transducer.

3. Coupling fluid

   Acoustic waves need a medium to support their propagation. Between the acoustic probe and the test specimen, the medium must be a fluid to allow the scanning procedure. Two major concerns in choosing a couplant fluid are the fluid's attenuation to acoustic waves and its applicability to the test specimen. The performance varies under different coupling fluids and different temperatures. Of all the coupling fluids, water and ethanol are the most preferred.

Basically, a SAM is a computer-controlled ultrasonic scanning system designed for examining the detailed internal structure of a wide range of parts. A SAM system usually consists of:

1) a piezoelectric transducer to generate a high radio frequency acoustical pulse,
2) a focusing acoustic lens, with a liquid coupling medium for the pulse to propagate through,
3) a scanning system that can relate to the desired region in reliable steps,
4) a memory unit to store the achieved signal step by step,
5) an analog to digital converter to transfer signals to images, and
6) a monitor to display images.

The performance of a SAM system depends on the frequency of the ultrasound wave, the lens of the system, the nature of the immersion medium, and the properties of the investigating materials. The nature of the frequency of ultrasound effects the resolution of microscopic imaging and the depth of penetration, but in a contrary way. A higher frequency of ultrasound offers a better resolution microscopic image, but shallower penetration of the testing samples. Thus, to choose a proper frequency of ultrasound for a particular testing example requires a compromise between the resolving power and the degree of penetration.

3.2 Acoustic waves propagate through solid materials

Acoustics is the study of time-varying deformations or vibrations in elastic media. As discussed in Chapter 2, the microstructure of the nugget region of a spot weld is considered as an anisotropic region. It is crucial to formulate the phenomenon of acoustic waves propagation in anisotropic materials for this study. This section begins with a brief review of acoustic wave propagating in isotropic materials (with 2 elastic constants). Then a primitive anisotropic case (cubic symmetric case with 3 elastic constants) is introduced for a better understanding for the idea of "anisotropy". In the next section, the wave propagation in the nugget of a spot weld (hexagonal symmetric case with 5 elastic constants) will be studied.

The acoustic wave propagation theory from the literature (e.g. Achenback [1] and Briggs [10]) is summarized as:

The mechanism for acoustic wave propagating is governed by Newton's Third Law and the stress-strain relation. In general, the displacement-strain relation is defined by the symmetric gradient operator which excludes rotation.

$$\varepsilon_{ij} = \frac{1}{2}\left(\frac{\partial u_i}{\partial x_j} + \frac{\partial u_j}{\partial x_i}\right) \qquad \textbf{(3.1)}$$

For a non-rotational system, the independent strain components are:

$$\begin{bmatrix} \varepsilon_{11} \\ \varepsilon_{22} \\ \varepsilon_{33} \\ \varepsilon_{13} \\ \varepsilon_{23} \\ \varepsilon_{31} \end{bmatrix} = \begin{bmatrix} \partial u_1 / \partial x_1 \\ \partial u_2 / \partial x_2 \\ \partial u_3 / \partial x_3 \\ 1/2 (\partial u_1 / \partial x_2 + \partial u_2 / \partial x_1) \\ 1/2 (\partial u_2 / \partial x_3 + \partial u_3 / \partial x_2) \\ 1/2 (\partial u_3 / \partial x_1 + \partial u_1 / \partial x_3) \end{bmatrix} \quad \text{...............(3.2)}$$

For the stress-strain relation (constitutive equation):

$$\tau_{ijkl} = C_{ijkl}\varepsilon_{kl} \quad \text{.....................(3.3)}$$

where $i, j, k, l = 1, 2,$ or 3

This equation contains 81 constants. Since [τ] and [ε] matrices are symmetric, the following conditions are applicable:

For a rotation free system, $C_{ijkl} = C_{jikl} = C_{ijlk} = C_{jilk}$; and

for reciprocity, $C_{ijkl} = C_{klij}$.

The constants in the constitutive equation are now reduced to 36.

Then we can reduce the 4th rank tensor to a 2nd rank tensor by mutating *ij* and *kj*. Let *ij* or *kl* be represented by the following:

11 ⇒ 1; 22 ⇒ 2; 33⇒ 3;

23⇒ 4; 31⇒ 5; and 12⇒ 6,

The constitutive equation can be rewritten in the following matrix form:

$$\begin{bmatrix} \tau_{11} \\ \tau_{22} \\ \tau_{33} \\ \tau_{23} \\ \tau_{31} \\ \tau_{12} \end{bmatrix} = \begin{bmatrix} C_{11} & C_{12} & C_{13} & C_{14} & C_{15} & C_{16} \\ C_{21} & C_{22} & C_{23} & C_{24} & C_{25} & C_{26} \\ C_{31} & C_{32} & C_{33} & C_{34} & C_{35} & C_{36} \\ C_{41} & C_{42} & C_{43} & C_{44} & C_{45} & C_{46} \\ C_{51} & C_{52} & C_{53} & C_{54} & C_{55} & C_{56} \\ C_{61} & C_{62} & C_{63} & C_{64} & C_{65} & C_{66} \end{bmatrix} \begin{bmatrix} \varepsilon_{11} \\ \varepsilon_{22} \\ \varepsilon_{33} \\ 2\varepsilon_{23} \\ 2\varepsilon_{31} \\ 2\varepsilon_{12} \end{bmatrix} \quad \text{.....................(3.4)}$$

The independent elastic constants can be further simplified:

general anisotropic case:	21 elastic constants
orthorhombic case:	9 constants
hexagonal symmetric case:	5 elastic constants
cubic symmetric case:	3 elastic constants
isotropic case:	2 elastic constants (Lamé constant λ and μ)

For a cubic symmetry, supposing that the symmetry directions coincide with the coordinate axes, the stiffness matrix can be rewritten as:

$$\begin{bmatrix} \tau_{11} \\ \tau_{22} \\ \tau_{33} \\ \tau_{23} \\ \tau_{31} \\ \tau_{12} \end{bmatrix} = \begin{bmatrix} C_{11} & C_{12} & C_{12} & 0 & 0 & 0 \\ C_{12} & C_{11} & C_{12} & 0 & 0 & 0 \\ C_{12} & C_{12} & C_{11} & 0 & 0 & 0 \\ 0 & 0 & 0 & C_{44} & 0 & 0 \\ 0 & 0 & 0 & 0 & C_{44} & 0 \\ 0 & 0 & 0 & 0 & 0 & C_{44} \end{bmatrix} \begin{bmatrix} \varepsilon_{11} \\ \varepsilon_{22} \\ \varepsilon_{33} \\ 2\varepsilon_{23} \\ 2\varepsilon_{31} \\ 2\varepsilon_{12} \end{bmatrix} \quad \text{...................(3.5)}$$

There are three independent elastic constants.

For an isotropic system, the elastic constants can be further reduced to two independent constants, the so-called Lamé constants λ and μ. Where:

$$C_{11} = \lambda + 2\mu$$
$$C_{12} = \lambda \quad \text{..........................(3.6)}$$
$$C_{44} = \mu$$

The relationship between the Lamé constants and the much more familiar elastic constants are:

$$E(Young's\ \text{modulus}) = \frac{\mu(3\lambda + 2\mu)}{\lambda + \mu}$$
$$G(shear\ \text{modulus}) = \mu \quad \text{......................(3.7)}$$
$$\upsilon(Poisson\ ratio) = \frac{\lambda(\lambda + \mu)}{2}$$

The next step is to plug this relationship into a wave equation. The three-dimensional wave equation is:

$$\nabla^2 u = \rho\ddot{u} \quad \text{.....................(3.8)}$$

The plan wave solution for the above equation is:

$$u(x,t) = Ape^{i(\omega t - kx)} \quad \text{..........................(3.9)}$$

where A is the amplitude, ω is the angular frequency, p is the polarization vector, and k is the wave vector.

Rewriting equation 3.9 in detail,

$$u_1 = A_1 p_1 e^{i\omega t} e^{-ik(d_1x_1 + d_2x_2 + d_3x_3)}$$
$$u_2 = A_2 p_2 e^{i\omega t} e^{-ik(d_1x_1 + d_2x_2 + d_3x_3)} \quad \text{..........................(3.10)}$$
$$u_3 = A_3 p_3 e^{i\omega t} e^{-ik(d_1x_1 + d_2x_2 + d_3x_3)}$$

where d is the propagation unit vector.

By substituting the strain-stress matrix (equation 3.5) and the plane wave solution (equation 3.9) into the three-dimensional wave equation (equation 3.8), the Christoffel equation can be obtained. It is customary to denote the direction cosines d_1, d_2, and d_3 by l, m, and n. With l, m, and n, the Christoffel equation can be written as:

$$\begin{bmatrix} \lambda_{11} - \rho c^2 & \lambda_{12} & \lambda_{13} \\ \lambda_{12} & \lambda_{22} - \rho c^2 & \lambda_{23} \\ \lambda_{13} & \lambda_{23} & \lambda_{33} - \rho c^2 \end{bmatrix} \begin{bmatrix} p_1 \\ p_2 \\ p_3 \end{bmatrix} = \begin{bmatrix} 0 \\ 0 \\ 0 \end{bmatrix} \quad \text{......................(3.11)}$$

where

$$\begin{aligned} \lambda_{11} &= l^2 C_{11} + (m^2 + n^2) C_{44} \\ \lambda_{22} &= m^2 C_{11} + (l^2 + n^2) C_{44} \\ \lambda_{33} &= n^2 C_{11} + (l^2 + m^2) C_{44} \\ \lambda_{12} &= ml(C_{12} + C_{44}) \\ \lambda_{13} &= nl(C_{12} + C_{44}) \\ \lambda_{23} &= mn(C_{12} + C_{44}) \end{aligned} \quad \text{..........................(3.12)}$$

The aniostropy of materials results from the orientation-dependence of its elastic modulus. The simplest anisotropic in a cubic symmetric system, where three mutually orthogonal directions of symmetry are equivalent, can be shown in Figure 3.1.

There are three special symmetry directions in the cubic crystal: [100], [110], and [111]. Only in these directions can a pure mode elastic wave propagate. In all other directions, quasi-longitudinal and quasi-transverse waves will propagate.

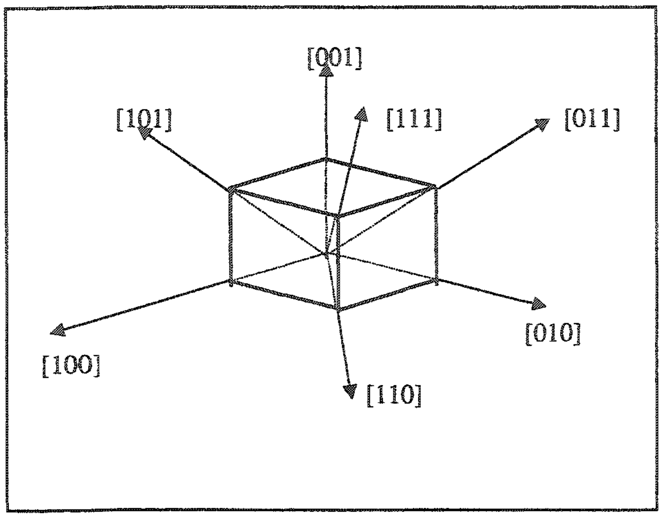

Figure 3.1 Cubic crystal structure

The following table lists the elastic constants in isotropic and cubic symmetric materials.

Table 3.1 Elastic constants in isotropic and cubic symmetric materials [1]

	Isotropic materials	Cubic symmetric materials
Stiffness matrix components	C_{11}, C_{12} $C_{44}=(C_{11}-C_{12})/2$	C_{11}, C_{12}, and C_{44}
Christoffel equation	$\begin{bmatrix} \lambda+2\mu-\rho c^2 & 0 & 0 \\ 0 & \mu-\rho c^2 & 0 \\ 0 & 0 & \mu-\rho c^2 \end{bmatrix}$	$\begin{bmatrix} \lambda_{11}-\rho c^2 & \lambda_{12} & \lambda_{13} \\ \lambda_{12} & \lambda_{22}-\rho c^2 & \lambda_{23} \\ \lambda_{13} & \lambda_{23} & \lambda_{33}-\rho c^2 \end{bmatrix}$
Wave speeds	Longitudinal $c_L=\sqrt{\frac{\lambda+2\mu}{\rho}}$ shear $c_S=\sqrt{\frac{\mu}{\rho}}$	[100] direction $c_1=\sqrt{\frac{C_{11}}{\rho}}$; $c_2=c_3=\sqrt{\frac{C_{44}}{\rho}}$ [110] direction $c_1=\sqrt{\frac{C_{11}+C_{12}+2C_{44}}{2\rho}}$ $c_2=\sqrt{\frac{C_{11}-C_{12}}{2\rho}}$ $c_3=\sqrt{\frac{C_{44}}{\rho}}$ [111] direction $c_1=\sqrt{\frac{C_{11}+2C_{12}+4C_{44}}{3\rho}}$ $c_2=c_3=\sqrt{\frac{C_{11}-C_{12}+C_{44}}{3\rho}}$

For different cases, the independent elastic constants can be shown in Table 3.2.

Table 3.2 Independent elastic constants in different crystal cases [1]

Most general case (Triclinic case)	$\begin{bmatrix} C_{11} & C_{12} & C_{13} & C_{14} & C_{15} & C_{16} \\ C_{12} & C_{22} & C_{23} & C_{24} & C_{25} & C_{26} \\ C_{13} & C_{23} & C_{33} & C_{34} & C_{35} & C_{36} \\ C_{14} & C_{24} & C_{34} & C_{44} & C_{45} & C_{46} \\ C_{15} & C_{25} & C_{35} & C_{45} & C_{55} & C_{56} \\ C_{16} & C_{26} & C_{36} & C_{46} & C_{56} & C_{66} \end{bmatrix}$
Orthorhombic case	$\begin{bmatrix} C_{11} & C_{12} & C_{13} & 0 & 0 & 0 \\ C_{12} & C_{22} & C_{23} & 0 & 0 & 0 \\ C_{13} & C_{23} & C_{33} & 0 & 0 & 0 \\ 0 & 0 & 0 & C_{44} & 0 & 0 \\ 0 & 0 & 0 & 0 & C_{55} & 0 \\ 0 & 0 & 0 & 0 & 0 & C_{66} \end{bmatrix}$
Hexagonal case	$\begin{bmatrix} C_{11} & C_{12} & C_{13} & 0 & 0 & 0 \\ C_{12} & C_{11} & C_{13} & 0 & 0 & 0 \\ C_{13} & C_{13} & C_{33} & 0 & 0 & 0 \\ 0 & 0 & 0 & C_{44} & 0 & 0 \\ 0 & 0 & 0 & 0 & C_{44} & 0 \\ 0 & 0 & 0 & 0 & 0 & \frac{C_{11}-C_{12}}{2} \end{bmatrix}$
Cubic case	$\begin{bmatrix} C_{11} & C_{12} & C_{12} & 0 & 0 & 0 \\ C_{12} & C_{11} & C_{12} & 0 & 0 & 0 \\ C_{12} & C_{12} & C_{11} & 0 & 0 & 0 \\ 0 & 0 & 0 & C_{44} & 0 & 0 \\ 0 & 0 & 0 & 0 & C_{44} & 0 \\ 0 & 0 & 0 & 0 & 0 & C_{44} \end{bmatrix}$

3.3 Acoustic waves propagate in spot welds

3.3.1 Wave propagation in the core of weld nugget

The spot weld nugget is an irregularly shaped artifact with rough surfaces on both sides, and its metallurgical structure is different from the original sheet metal. Moreover, the existence of discontinuities, porosity, and inclusion inside the weld nugget makes the acoustic wave propagation more difficult to study. Numerous studies ([26], [58]) have demonstrated that the solidification processes in welds affect the crystallographic orientation. The direction of the grain growth follows the steepest temperature gradient, and the crystal growth direction is the [100] direction of the cubic crystal [20]. Thus, for a spot weld, the examining acoustic waves are going through the [100] direction of the dendritic crystals [26]. Figures 3.2 and 3.3 (following Bently [6]) demonstrate the temperature distribution in both theoretical and experimental analysis. Figures 3.4 show the possible crystal growth direction in the spot weld nugget, which will be on the equiaxed grain.

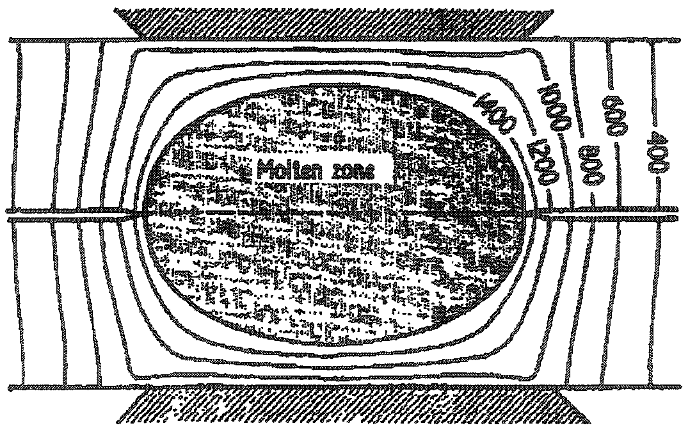

Figure 3.2 Theoretical temperature distribution (°C)

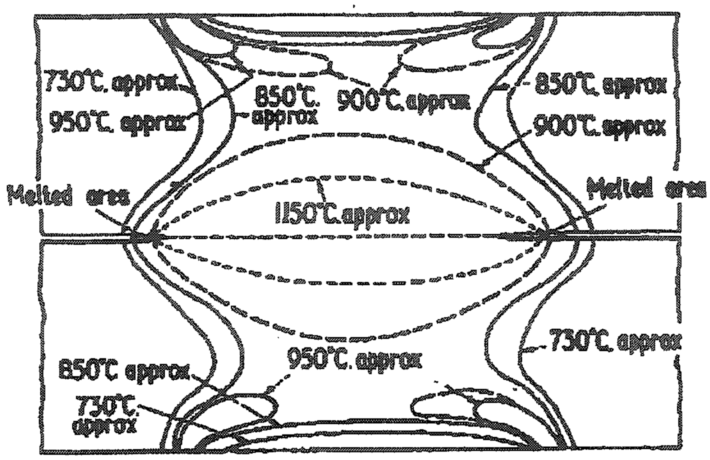

Figure 3.3 Experimental temperature distribution

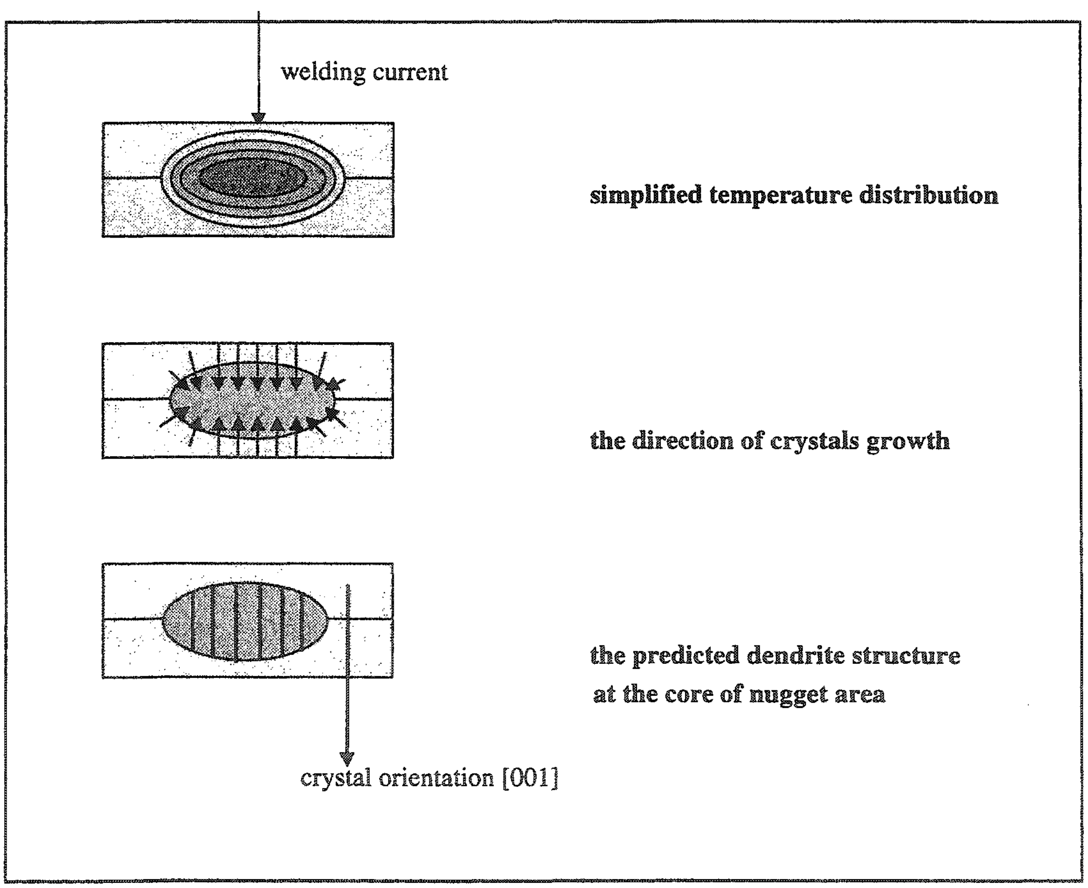

Figure 3.4 The assumed nugget structure in spot weld

Since acoustic waves propagate through the [100] direction of the spot weld nugget crystal in the core of the nugget, we can substitute the direction unit into equation 3.12 as l=1, m=0, and n=0. We can derive a simplified wave propagation model as:

$$\lambda_{11} = C_{11}$$
$$\lambda_{22} = \lambda_{33} = C_{44}$$

Solving the eigenvalue problem, then:

$$(C_{11} - \rho C^2)(C_{44} - \rho C^2) = 0 \quad \text{.....................(3.13)}$$

The wave speeds are:

$$C_L = \sqrt{\frac{C_{11}}{\rho}} \qquad C_{SH} = C_{SV} = \sqrt{\frac{C_{44}}{\rho}} \quad \text{.........................(3.14)}$$

The longitudinal wave speed and the direction calculated here is proven to be correct in Kupperman and Reimann's study [56]. However, the shear waves traveling across the dendrites region with the polarization direction parallel to the dendrites will have a different attenuation pattern compared to the shear waves propagating in other directions.

The dendrites in spot weld nuggets are long, cylindrical single crystals with orientation in the vertical [100] direction. Assuming the dendrite's cylindrical crystal is symmetric about the Z- axis (Figure 3.4), the general orthorhombic symmetry object can be reduced to be hexagonally symmetrical. The independent elastic constants are reduced from nine to five according to Kupperman and Reimann's study [56]. The five independent elastic constants can be calculated by the modified formula as:

$$\overline{C}_{11D} = \overline{C}_{22D} = \overline{C}_{11} + \frac{3\gamma C}{20}$$
$$\overline{C}_{33D} = \overline{C}_{11} + \frac{2\gamma C}{5}$$
$$\overline{C}_{44D} = \overline{C}_{55D} = \overline{C}_{44} - \frac{\gamma C}{5} \qquad \ldots\ldots\ldots\ldots\ldots\ldots\ldots\ldots(3.15)$$
$$\overline{C}_{66D} = \overline{C}_{44} + \frac{\gamma C}{20}$$
$$\overline{C}_{13D} = \overline{C}_{23D} = \overline{C}_{12} - \frac{\gamma C}{5}$$
$$\overline{C}_{12D} = \overline{C}_{12} + \frac{\gamma C}{20}$$

where γ is the texture anisotropy factor and

C can be calculated as: $C = C_{11} - C_{12} - 2C_{44}$.

Detailed description can be found in the literature [23] and [28].

For the spot weld type of anisotropy, an experiment is required to obtain these elastic constants. There are two ways to calculate these constants. The first one is to use static tensile testing and the second one is to use acoustic testing. Accordingly, the first method involves the following steps:

- Fabricate samples cut in three principle local directions,
- Apply tensile tests at different direction cosines,
- Measure the longitudinal elongation and the lateral contraction, and
- Use the strain-stress relationship to calculate the components of the stiffness matrix.

The second method, the acoustic testing method, starts with a fresh cut sample to allow precise directional measurement. Then the acoustical velocity is measured relative to a certain locally preferred solidification direction. Following this, begin with another fresh cut sample and measure another preferred solidification direction, and vice versa. While the directional acoustical velocities have been recorded, the elastic stiffness matrix can be obtained by the Christoffel equation in Table 3.1. Details of these procedures can be found in the study of Dewey *et al.* [23].

3.3.2 Wave propagation in other (non-core) regions of weld nugget

The previous section discussed acoustic wave propagation in the core of spot weld nuggets. Since the grain growth is in the [100] direction in the core region, the behaviors of acoustic waves can be anticipated. Nevertheless, in other regions of a weld nugget, the microstructures of equiaxed grain growth make the prediction of acoustic wave behaviors difficult. Due to the irregular nugget shape, the microstructures in non-core regions of the weld nugget are equiaxed yet randomly arranged. This kind of microstructure affects the pattern of acoustic wave propagation. Sometimes it will misguide the acoustic wave and return bias signals. The other major factor affecting acoustic wave propagation is the HAZ of the weld. The HAZ has usually been recrystallized and its microstructures have been changed (see detail in Chapter 2). The change in the microstructures will re-focus the acoustic beam and result in misinterpretation. Furthermore, the melted coating material will produce contact between the base metals and allow acoustic waves to pass through which may change the results of the analysis of the weld nuggets. In some cases, a deep indentation of weld nuggets re-focuses the acoustic beam and produces signal-free regions.

The irregular shape of the nugget raises an interpretation problem for the acoustic method mathematically. However, this study helps to clarify interpretation problems. The experimental model described in the next chapter is based on the knowledge acquired in this chapter and provides another feasible approach to this problem.

Chapter 4

Quantitative analysis of acoustic images

The intention here is to establish an experimental model to predict spot weld quality based on its acoustic information. As the acoustic information about spot welds has been acquired, it is not clear what kind of information in the image is important to determine weld quality and what is not. From the literature review in Chapter 2, some basic indications of a weld's quality already exist, e.g. nugget diameter (nugget size), surface indentation, and nugget penetration. Through quantitative study of the acoustic images introduced in this chapter, these indications can be studied and converted into acoustic parameters. By correlating the acoustic parameters and the results from experts and experiments, a reliable index of weld quality can be established.

The results of acoustic image analysis are sets of pixel-based pictures with abundant information that allows us to scrutinize the detail of every aspect of the metallurgical and acoustic properties of each spot weld in the study.

4.1 Acoustic validity study

The acoustic microscopy method shows promising results for detecting flaws in weld nuggets[84]. This method can provide the information about quality of spot weld nuggets by examining the non-homogeneous objects inside nuggets such as: bubbles, inclusions, explosive welds, and porosity. However, due to the unpredictable nature of nuggets, the acoustic images shown on the display device are not actual size. The non-homogeneous objects inside, and the surface indentation, guide the acoustic waves and provide a pseudo-acoustic-image for welded nuggets. Thus, the accuracy of this information about welded nuggets acquired acoustically should be examined before further study.

There are two different types of studies performed for the validity test of the acoustic method. The first one is to verify the results of the acoustic method by using another nondestructive method. The second one is to test the ability of the acoustic method by describing the detection of artifact defects. In the first test, the commonly used optical examination procedure is employed as the tool for verifying the result of the acoustic test. The advantages and disadvantages of these two methods are tabulated as follows.

Table 4.1 Advantages and disadvantages of nugget tests

	Advantage	Disadvantage
Acoustic test	internal examination of structure and nugget size	the measurement results need to be calibrated
Optical test	visual inspection of nugget size	only surface information is obtained

4.1.1 Nugget examination by nondestructive methods

This approach is aimed at the calibration between the optical method and the acoustic microscope method. Instead of peeling the spot weld samples, this approach works on "peeling nuggets". The procedures of this approach will be described as follows:

1. Cut and grind the welding coupons to nugget tablets.
2. Polish these samples from a selected side.
3. Perform acoustic inspection of spot weld samples from both sides.
4. Examine the peeled nuggets from the selected side by the optical method. Examine the peeled nugget from both sides by the acoustic method. The acoustic signal

windows should be set close to the selected side of the nugget. This step will help to examine the correlation between the acoustic method and the optical method.

5. Peel the nugget into thinner tablets, and repeat steps 2 through 4.
6. Continue peeling the nugget until the desired thickness has been reached.
7. Calibrate the results from the optical method and the acoustic microscope method.

4.1.2 Verification results of the nondestructive method

This study uses three types of welding coupons according to their stack up, and they are: Type 1 (0.03" stack on 0.045"), Type 2 (0.04" stack on 0.06") and Type 3 (0.06" stack on 0.07"). Two welds of different welding parameters were produced on Type 1, and two and four welds on Types 2 and 3, respectively. The results are illustrated in Figure 4.1.

The results show that in Type 1 and Type 2 the acoustic estimation of the nugget diameter is very close to the diameter determined by the optical method. For Type 3, with thicker base metals which need a longer heating process during welding, the HAZ region is larger than Type 1 and 2. The HAZ affects the microstructures while recrystallization will substantially affect both nondestructive tests. For optical examination, the HAZ reacts to the etching process, and produces larger images. On the other hand, a ring-shaped region is observed by acoustic method. These results reinforce the conclusion drawn in section 3.3.2.

Table 4.2 Results of estimated nugget diameter

	diameter	Diameter from back	optical diameter
Type 1 #1	5.71	5.76	5.75
Type 1 #2	4.96	5.31	5.49
Type 2 #1	5.92	6.22	6.02
Type 2 #2	4.88	5.34	5.80
Type 3 #1	7.78		7.79
Type 3 #2	5.70		7.30
Type 3 #3	4.96		7.05
Type 3 #4	3.58		5.77

(unit: mm)

4.1.3 Artifact flaws examination

This study uses four Type 3 stack up (0.06" stack on 0.07") welds. An artificial flaw 2mm in diameter and 1.5 mm in depth was made in each of the four welds. The SPSAM is used to examine these flaws. The results shown in Figure 4.2 demonstrate that the acoustic estimation of the flaw size is very close to the real flaw size in the core region of the nuggets.

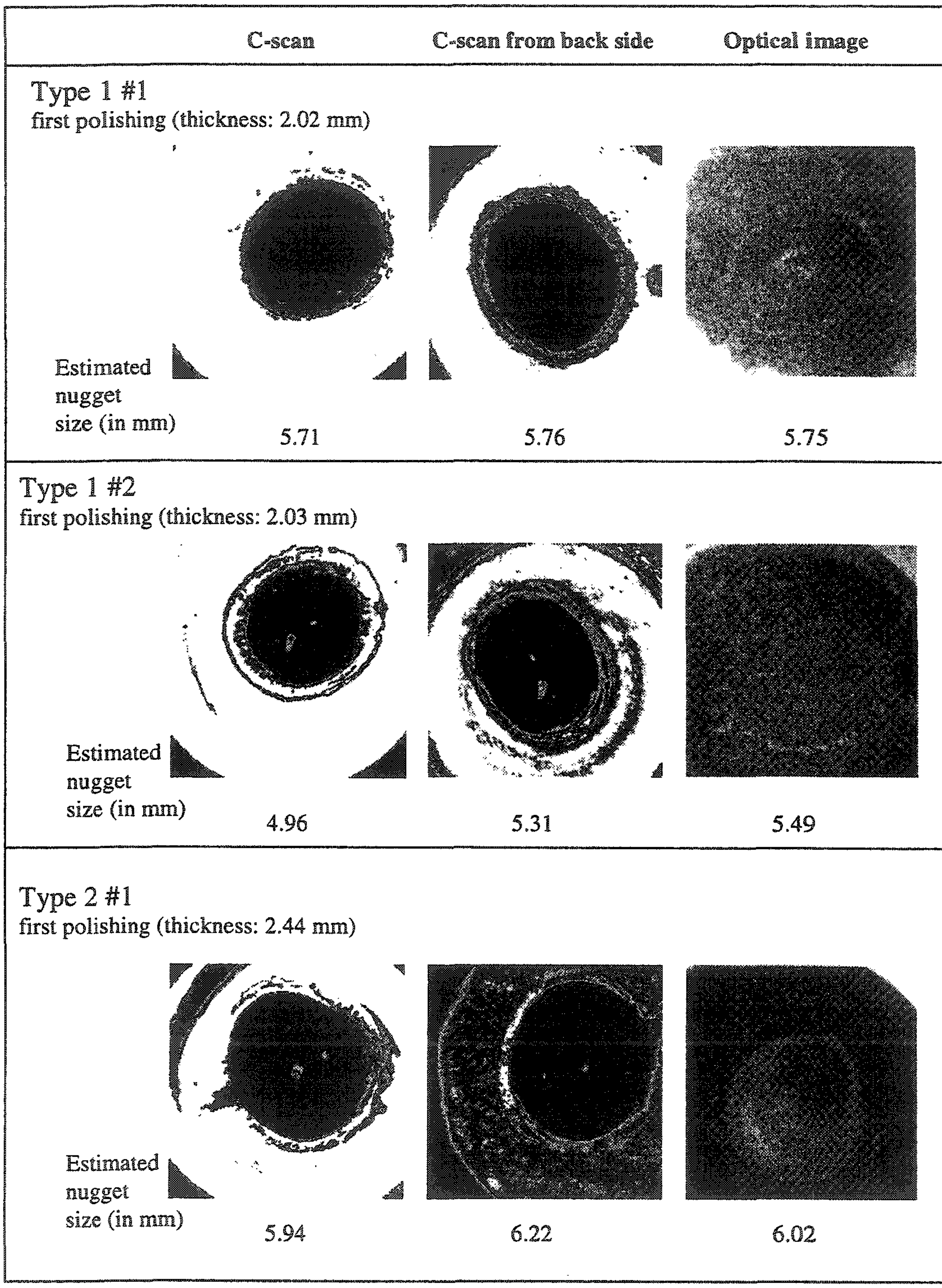

Figure 4.1 Nugget diameters estimated by acoustic and optical methods

	C-scan	C-scan from back side	Optical image
Type 2 #2 first polishing (thickness: 2.50 mm)		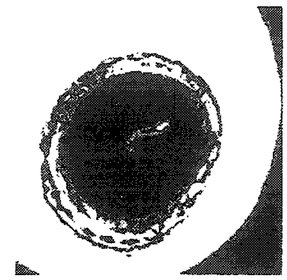	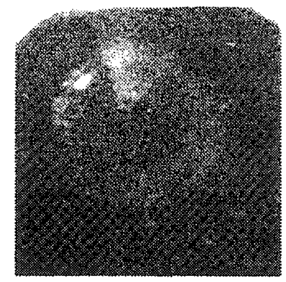
Estimated nugget size (in mm)	4.88	5.34	5.80
Type 3 #1 first polishing (thickness: 3.53 mm)	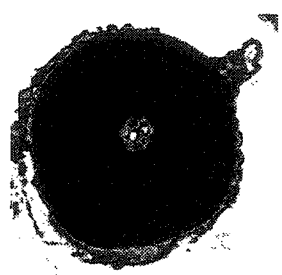		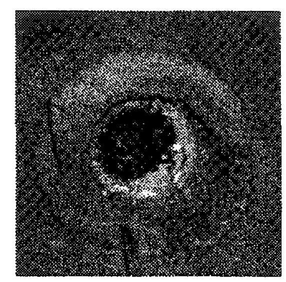
Estimated nugget size (in mm)	7.59		7.95
Type 3 #2 first polishing (thickness: 3.55 mm)			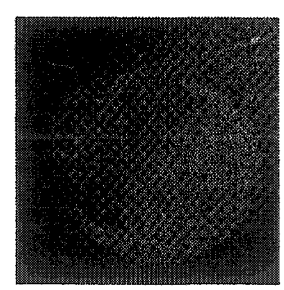
Estimated nugget size (in mm)	6.13		7.22

Figure 4.1 Nugget diameters estimated by acoustic and optical methods (continued)

C-scan	Optical image
Type 3 #3 first polishing (thickness: 3.57 mm) 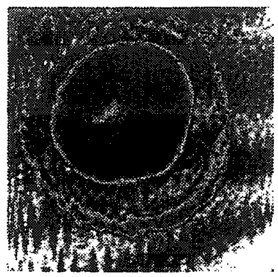 Estimated nugget size (in mm) 5.17	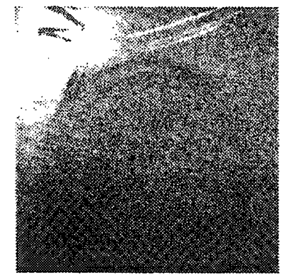 6.57
Type 3 #4 first polishing (thickness: 3.53 mm)  Estimated nugget size (in mm) 3.55	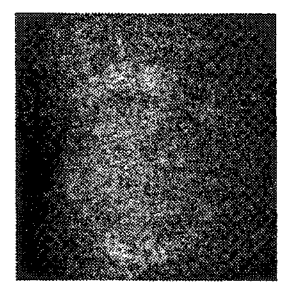 5.82
Type 3 #1 second polishing (thickness: 3.34 mm) 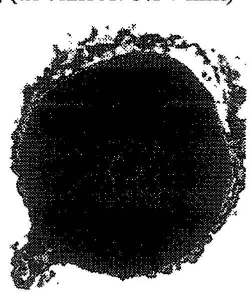 Estimated nugget size (in mm) 7.91	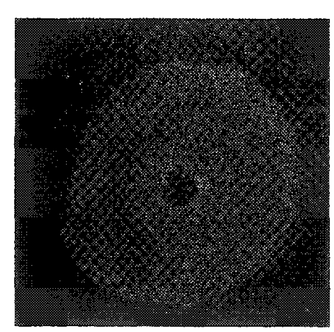 7.70

Figure 4.1 Nugget diameters estimated by acoustic and optical methods (continued)

C-scan	Optical image
Type 3 #2 second polishing (thickness: 3.38 mm) 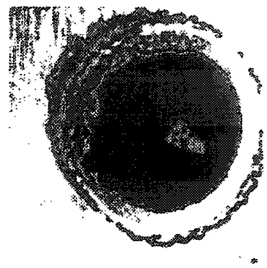 Estimated nugget size (in mm) 5.61	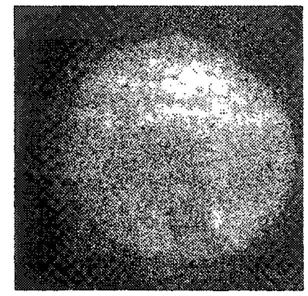 6.90
Type 3 #3 second polishing (thickness: 3.43 mm) 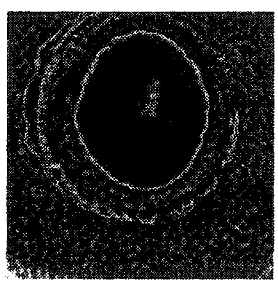 Estimated nugget size (in mm) 5.32	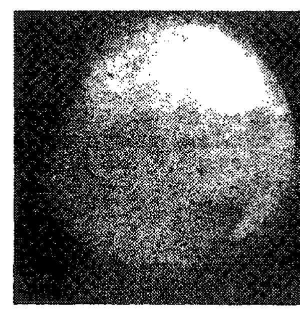 7.76
Type 3 #4 second polishing (thickness: 3.34 mm) 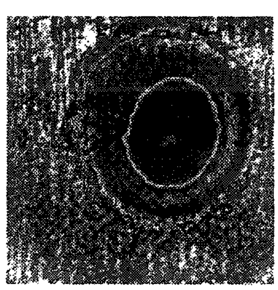 Estimated nugget size (in mm) 3.45	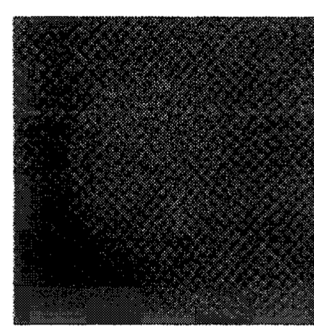 5.63

Figure 4.1 Nugget diameters estimated by acoustic and optical methods (continued)

C-scan	Optical image
Type 3 #1 third polishing (thickness: 3.15 mm)	
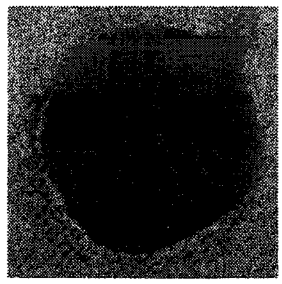	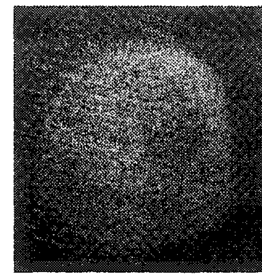
Estimated nugget size (in mm) 7.93	7.46
Type 3 #2 third polishing (thickness: 3.15 mm)	
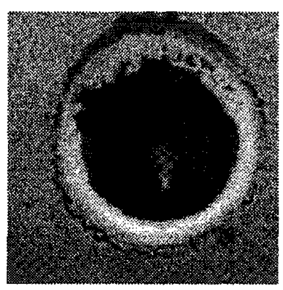	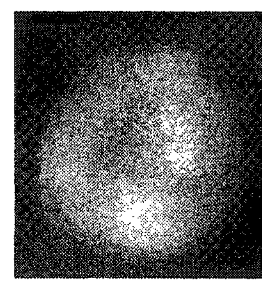
Estimated nugget size (in mm) 5.40	7.30
Type 3 #3 third polishing (thickness: 3.15 mm)	
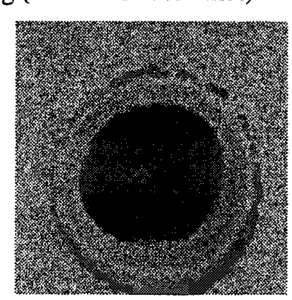	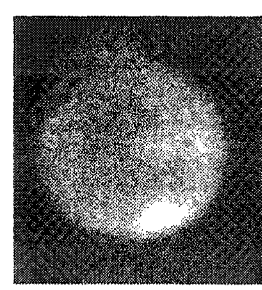
Estimated nugget size (in mm) 4.52	6.53

Figure 4.1 Nugget diameters estimated by acoustic and optical methods (continued)

	C-scan	Optical image
Type 3 #4 third polishing (thickness: 3.15 mm)	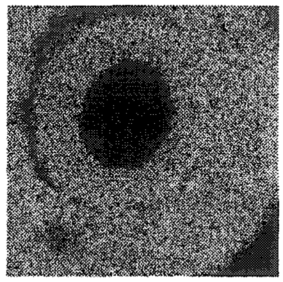	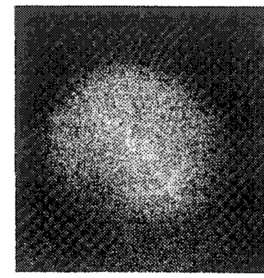
Estimated nugget size (in mm)	3.48	5.38
Type 3 #1 fourth polishing (thickness: 2.57 mm)	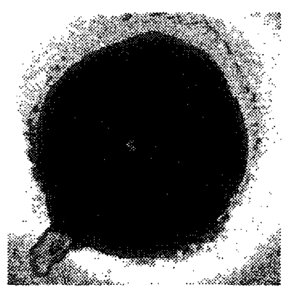	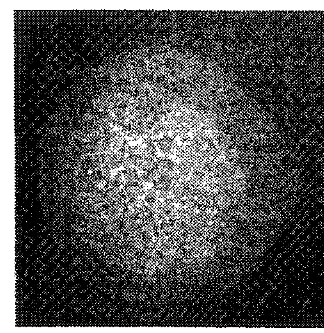
Estimated nugget size (in mm)	7.67	8.04
Type 3 #2 fourth polishing (thickness: 2.57 mm)	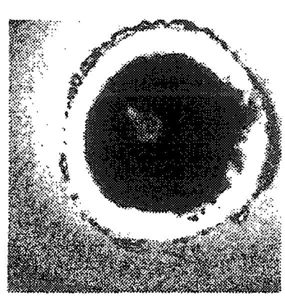	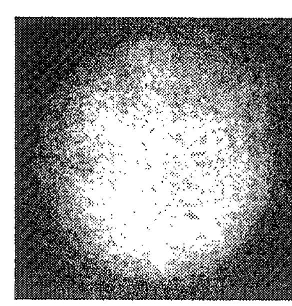
Estimated nugget size (in mm)	5.66	7.77

Figure 4.1 Nugget diameters estimated by acoustic and optical methods (continued)

	C-scan	Optical image
Type 3 #3 fourth polishing (thickness: 2.57 mm)		
Estimated nugget size (in mm)	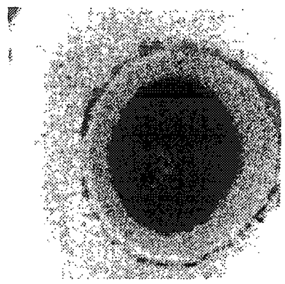 4.83	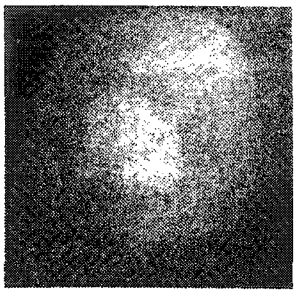 7.34
Type 3 #4 fourth polishing (thickness: 2.57 mm)		
Estimated nugget size (in mm)	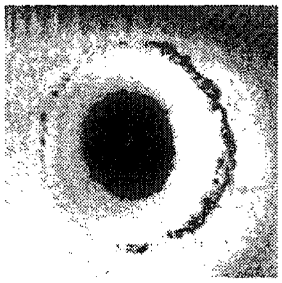 3.85	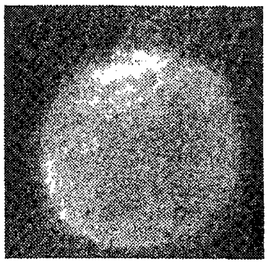 6.23

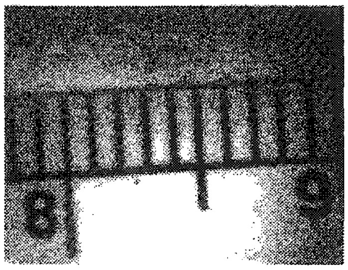

Scale of this study

Figure 4.1 Nugget diameters estimated by acoustic and optical methods (continued)

Acoustic image	Diameter of flaw
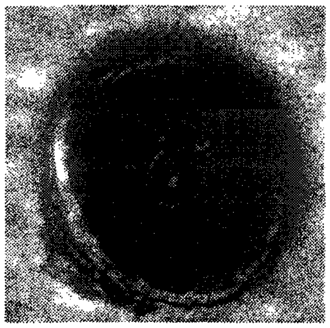	1.94 mm
	1.92 mm
	1.91 mm
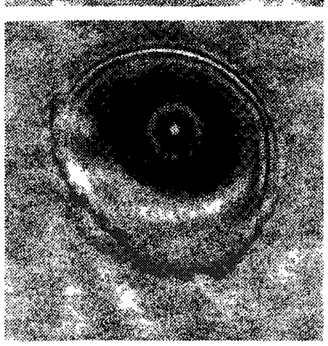	1.97 mm

Figure 4.2 Artifact flaw measurement by acoustic methods

4.2 Acoustic image study

To study the acoustic image, four practical steps are employed to convert the information into quantities for further studies.

4.2.1 Step 1: Mathematical morphology

Mathematical morphology was first introduced in 1964 by Serra [75]. This method is used to characterize geometric structure by numerical value. This method usually is used prior to image recognition and pattern identification to improve the geometric shapes of objects inside an image for further study. The purpose of the process is to filter out unnecessary information about the image and to reshape objects inside the image to fundamental geometry for pattern recognition.

The fundamental operations of morphology are dilation, erosion, opening and closing. The effect of the dilation (erosion) operator on an image is to enlarge (erode) the boundaries of selected objects. The opening (closing) operation is to perform erosion (dilation) then following by dilation (erosion). Two basic operators, dilation and erosion operators are used in this study to emphasize the discontinuities inside nuggets. The definition of dilation and erosion operations and their mathematical representation is listed in Table 4.3.

Table 4.3 Mathematical representations of dilation and erosion

	binary filter	gray-level filter
DILATION	Increase the geometrical area of an object by setting the background area pixel, which is adjacent to the object, to the same gray-level as that of the object.	Smooth small negative gray-level regions.
	$A \oplus B = \{t \in Z^2 : t = a + b, a \in A, b \in B\}$	$A \oplus B = \max[A(x+i, y+j) + B(i,j)]$
EROSION	Reduce the geometrical area of an object by setting the pixels at contour region to the gray-level of their background value.	Smooth small positive gray-level regions
	$A \Theta B = (A^c \oplus B^c)$	$A \Theta B = \min[A(x+i, y+j) - B(i,j)]$

Where $\oplus$ is the operator for dilation,

Θ is the operator for erosion,

A is an object inside an image, and a is a pixel in A,

B is a structural function or mask, and b is a member in a structural function, and

x, y are coordinators defined in A and B.

These two operations offer tools to study the combined effects of porous inclusion where multiple defects exist in a small region.

4.2.2 Step 2: Segmentation of images by thresholding

After the acoustic images have been readied for further examination by morphological processes, the thresholding method is proposed as the means to separate the interesting objects inside welds, such as weld nugget size, nugget shape, porosity, and inclusion. This algorithm converts a multi-gray-level image into an image containing fewer gray-level values. The operation defined for three gray-level regions for separating noise of image, nugget area, and discontinuities inside nuggets can be:

$$g(x,y) = \begin{cases} G_2 \ \text{if} \ f(x,y) > T_2 \\ G_1 \ \text{if} \ T_1 \le f(x,y) < T_2 \\ G_0 \ \text{if} \ f(x,y) \le T_1 \end{cases} \quad \text{........................}(4.1)$$

where $f(x,y)$ represents the original image; $g(x,y)$ is the image after thresholding; T_1 and T_2 are thresholding values; and G_0, G_1, and G_2 are the values of gray-level.

4.2.3 Step 3: Edge detection of acoustic images

The third proposed procedure for acoustic image study is edge detection. This process helps separate objects in acoustic images. The edges of objects can be distinguished by the discontinuities or abrupt changes in gray-level intensities. Since the gray-level numbers have already been reduced in the previous step, the edges between objects inside the weld nugget are quite clear. Edge detection is accomplished through the use of a range filter. The idea of a range filter is to calculate the difference between maximum and minimum gray-level values in a local region defined by a specific mask. The range filter can be defined as:

$$Range(A) = max\,[A(x+i,\, y+j)] - min\,[A(x+i,\, y+j)] \quad \text{......................}(4.2)$$

where $x+i$, $y+j$ are coordinators existing in image A, and i, j are defined in a special mask.

The special mask is the key of this operation, and it will decide what kind of pixel information will be included in the range operation.

4.2.4 Step 4: Area calculation in acoustic images

This operation calculates the number of pixels contained within an object in an acoustic image. Following the previous steps, the acoustic image becomes an image within which objects with well-defined boundaries appear. This algorithm can help to calculate the number of pixels of the nugget area, porosity, and inclusion, and later on, to convert this information into the real area. Besides area calculation, other geometrical measurement algorithms (e.g. maximum nugget diameter measurement and nugget surface indentation calculation) will be applied to collect the quantified information of acoustic images.

These algorithms proposed in section 4.3 are illustrated in Figure 4.3. A computer program written in JAVA language is developed to achieve this goal and the typical output carrying out these algorithms from this program is shown in Figure 4.4. Further analysis results are shown in Chapter 5.

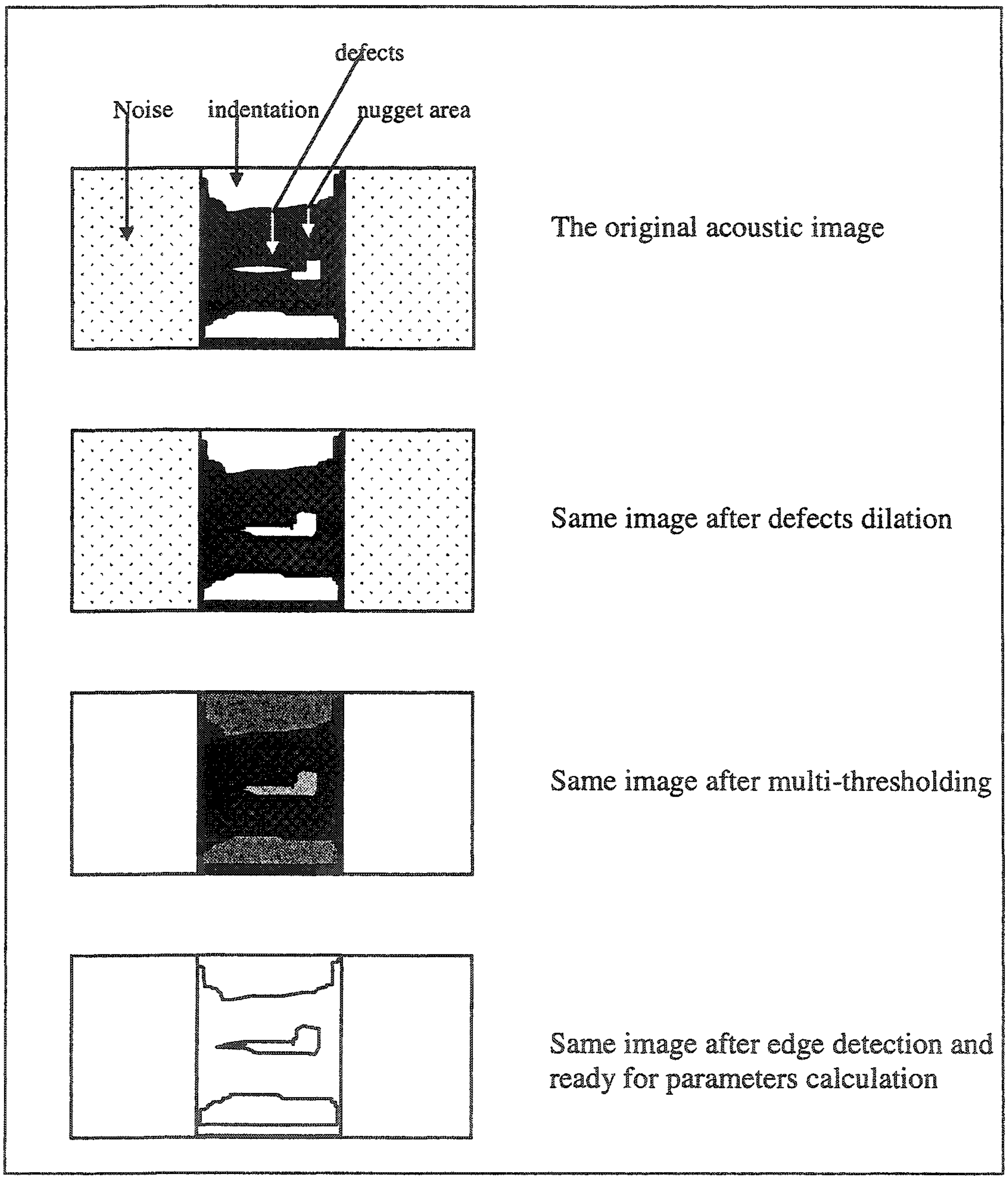

Figure 4.3 Procedures for quantitative analysis of acoustic images

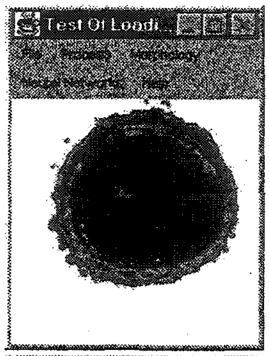

The original acoustic image

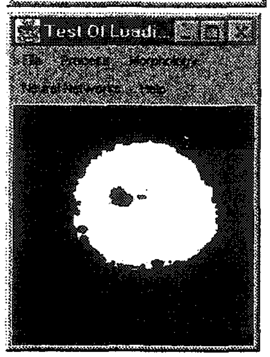

Same image after defects dilation

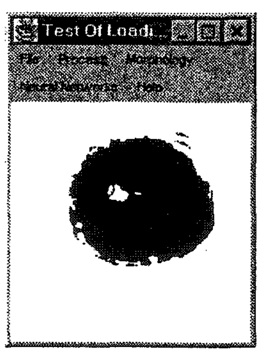

Same image after thresholding

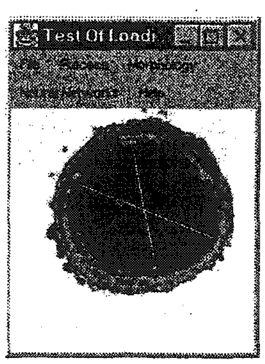

Same image after edge detection and ready for parameters calculation

Figure 4.4 Computer program for quantitative analysis of acoustic images

4.3 Data analysis

4.3.1 Analysis method I : Statistical correlation

The acoustic imaging method provides abundant information after image extraction. However, this information will consume a major part of the processing resource and is computationally exhausting. An important issue for this study is to select which parameters should enter the decision pool for determining weld quality. A fundamental study is performed to help obtain the list of essential parameters, e.g., nugget diameter, indentation, and inclusion inside nuggets. The ideal quality identifier is the strength of the weld nuggets. Nevertheless, the quantity is difficult to measure and will vary from process to process. Consequently, a substitute quantity – the diameter measured from the destructive test (peel test) - is used for analyzing the welding quality.

The procedures for obtaining these quantity factors are described as follows:

1. Choose a group of selected welding coupons for this experiment.
2. Capture the B-scan image from the newly developed acoustic device.
3. Select a group of parameters according to existing knowledge.
4. Conduct destructive tests on these samples.
5. Measure the nugget diameters of the peel test result.
6. Use the ANOVA technique to screen out the insignificant parameters.

7. Build up the nugget strength indicator by correlating significant parameters to the nugget diameters produced by peel tests.

For a three variable system, α, β, and γ are related to the nugget diameter S.

The linear model will be:

$$S = C_1 + C_2\alpha + C_3\beta + C_4\gamma \quad \text{.....................(4.3)}$$

The polynomial model will be:

$$S = C_1 + C_2\alpha + C_3\beta + C_4\gamma + C_5\alpha\beta + C_6\alpha\gamma + C_7\beta\gamma + C_8\alpha^2 + C_9\beta^2 + C_{10}\gamma^2$$

$$\text{.......................(4.4)}$$

where C_i, $i = 1 \sim 10$ are constant coefficients.

After the formulation, an ANOVA table can be established to investigate the significance of these variables. Thus, some of the insignificant parameters can be filtered out. The ANOVA provides the inferential procedure for testing the statistical hypothesis. One of the ways to judge the significance of each variable is by assessing the character of the F-score. A level of confidence for the significance test can be set as either 95% or 99% to select the variables which are to enter the next stage.

The next stage of analysis is to use either the linear multiple regression or the non-linear multiple regression method to establish the constants associated with acoustic parameters. A variety of commercial software exists for solving non-linear regression. Most of them follow this procedure:

1. Start the initial estimation for each variable, then generate the curve defined by the estimation.
2. Adjust variables to fit the curve closer to data points through algorithms, e.g., Marquardt method.
3. Further adjust the curve and make it closer to the data set. Once the pre-set error limit is reached, stop and report the result.

Through these procedures, a set of significant parameters will be determined and their coefficients found. Consequently, the diameter of the weld will be predictable through the cumulative relationship, which will be an indicator of the spot weld quality.

4.3.2 Analysis method II : Neural networks

Sometimes the assessment of a spot weld is made by a general description such as a good/marginal/bad weld instead of a more specific index, like bonding strength. The reason is that the general approach is usually the kind of criterion that can be easily adopted into industrial standards. For example, if we consider the variations among spot welds, including the materials, thickness and coating of base metal, or the type of electrode welding tip, the statistical analysis method may not check all the possibilities at one time and may need to be repeated for each different case. In such a situation, the artificial neural networks (ANN) analysis is an ideal analytical method.

ANN were originally designed as a model to simulate how the human brain works. The first ANN model was formulated in 1943 by McCulloch and Pitts. In 1949, Donald Hebb introduced Hebbian learning which states that changes in synaptic strengths are proportional to the activation of the neuron. In 1957, Frank Rosenblatt developed this idea into a two-layer network and established the perception convergence theorem. The next major step in the study of neural networks was the discovery of backpropagation by Werbos in 1974. Parker, in 1982, and Rumelhard and Hinton, in 1986, furthered the study of neural networks. Even today, neural network research flourishes, and new learning algorithms are developed every week.

The ANN is a simplified model that simulates human information passing behavior by artificial neurons. Each neuron has:

1) input and output which is related to the state of the neuron itself;
2) a threshold function to decide on the input-output relationship; and
3) unidirectional connection communication channels which carry numeric (as opposed to symbolic) data.

Figure 4.5 illustrates the abstract structure of a biological neuron. A brief explanation of some terms of Figure 4.5:

1. **Axon**: site where signals are transmitted between neurons by electrical pulses.

2. **Synapses**: pulses traveling in an axon from neuron to neuron.
3. **Soma (dendrites)**: found principally on a set of branching processes emerging from the cell body.

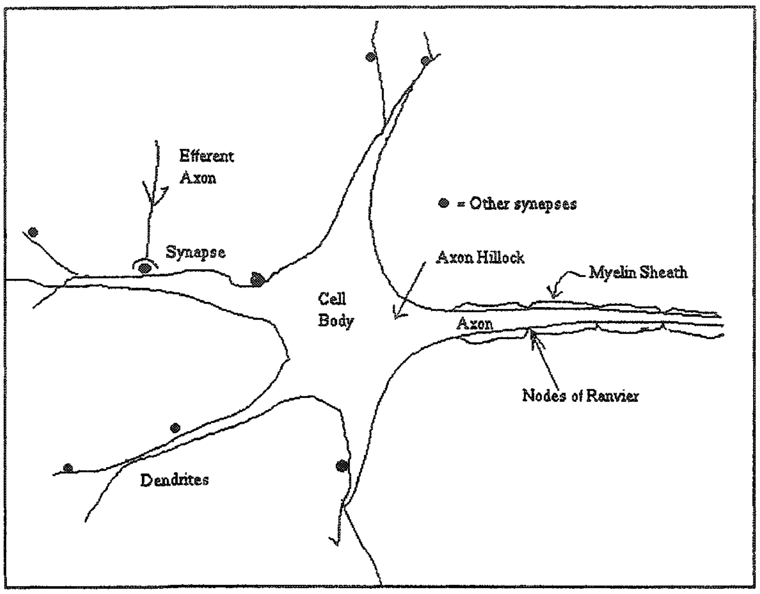

Figure 4.5 Biological neuron (following Gurney [40])

The process of signal transmitting is described by Gurney [40]:

> *"Each pulse occurring at a synapse initiates the release of a small amount of chemical substance or neurotransmitter which travels across the synaptic cleft and which is then received at post-synaptic receptor sites on the dendritic side of the synapse. The neurotransmitter becomes bound to molecular sites here which, in turn, initiates a change in the dendritic membrane potential. This post-synaptic-potential (PSP) change may serve to increase (hyperpolarise) or decrease (depolarise) the polarisation of the post-synaptic membrane. In the former case, the PSP tends to inhibit generation of pulses in the afferent neuron, while in the latter, it tends to excite the generation of pulses. The size and type of PSP produced will depend on factors such as the geometry of the synapse and the type of neurotransmitter. Each PSP will travel along its dendrite and spread over the soma, eventually reaching the base of the axon (axon-hillock). The afferent neuron sums or integrates the effects of thousands of such PSPs over its dendritic tree and over time. If the integrated potential at the axon-hillock exceeds a threshold the cell 'fires' and*

generates an action potential or spike which starts to travel along its axon. This then initiates the whole sequence of events again in neurons contained in the efferent pathway."

ANN learn from examples and usually have training rules whereby the weights of connections are adjusted on the basis of presented examples. Alternatively, the model can be illustrated in Figure 4.6.

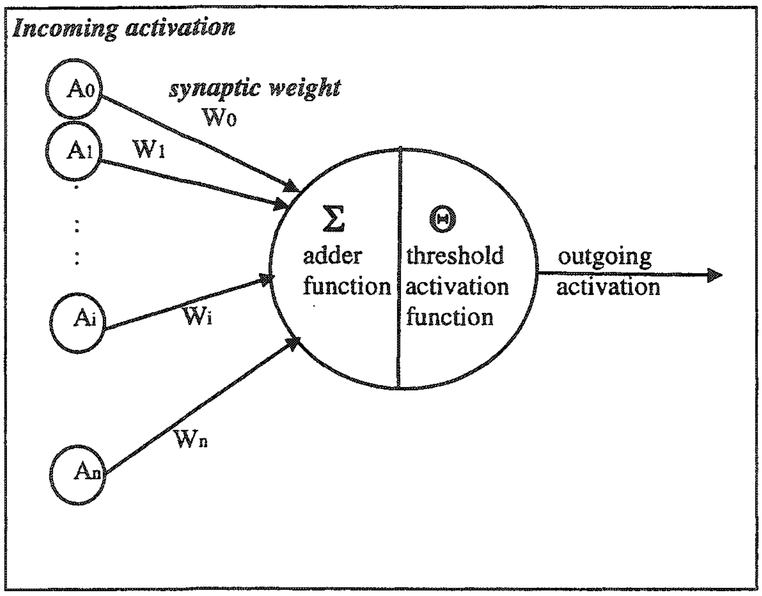

Figure 4.6 Diagram of abstract neuron model

The proposed neural networks model is a three layer feed-forward model trained with the backpropagation method with logistic function as the activation function. The logistic threshold function is:

$$f(x) = \frac{1}{1 + e^{-x}} \qquad \text{.......................(4.5)}$$

where $f(x)$ represents the output; and x is the input.

The backpropagation method is the most popular model in neural networks. By backward training the errors, it is a suitable approach for examining the problem for the following reasons:

1. It is easy to apply to a practical problem such as the problem examined. This algorithm has been proven as very robust for training multiple layer networks.
2. It is very effective when the relationship between input/output layers is nonlinear and the training data are abundant.

The abstract neural networks model of this study can be illustrated as follows.

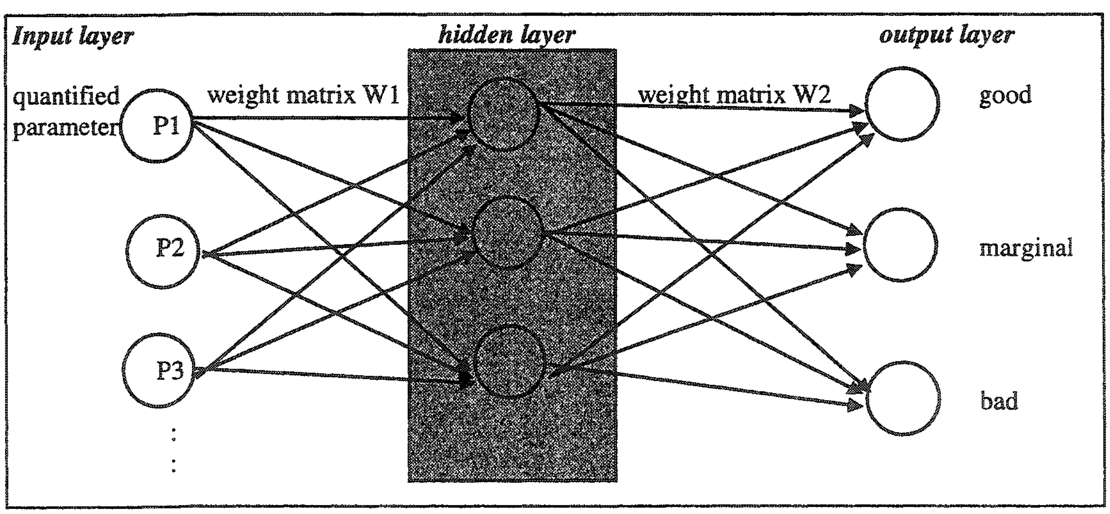

Figure 4.7 Proposed method, a multi-layer feed-forward net

Assume there are i quantified parameters, j hidden units, and three output units (representing good/marginal/bad welds). W_{ij} stands for the weight between input layer i-

th unit and *j*-th unit of the hidden layer. The activation function here has a special property such that $f'(x)=f(x)(1-f(x))$. The details of backpropagation algorithm were described in the literature [40][41][65], and the typical steps could be described as:

1. Compute the hidden layer neuron activation:

   The j-th hidden layer neural: $y_j = f((\sum_i x_i W_1[i][j]) + \theta_j)$

2. Compute the output layer neuron activation:

   The j-th output layer neural: $z_j = f((\sum_i y_i W_2[i][j]) + \tau_j)$

3. Compute the output layer error:

   output differences = (desired value) - (computed value)

   For the i-th component of error at the output layer:

   $e_i = z_i(1-z_i)(p_i - z_i)$

4. Compute the hidden layer error:

   For the i-th component of error at the hidden layer:

   $t_i = y_i(1-y_i)(\sum_j W_2[i][j]e_j)$

5. Adjust the weights for the second layer of the synapses:

   For the i-th neuron in the hidden layer and the j-th neuron in the output layer:

   $\Delta W_2[i][j] = \mu y_i e_j$

6. Adjust the weights for the first layer of the synapses:

   For the i-th neuron in the input layer and the j-th neuron in the hidden layer:

$$W_1[i][j] = \lambda x_i t_j$$

Notations:

x, y, z are vectors for the output neurons in the input layer, hidden layer, and output layer, respectively. W_1 and W_2 are weight matrices between the input/hidden layer and the hidden/output layer. *p* is the desired output vector. *e* and *t* are vectors for errors in the output and hidden layers. θ and τ are vectors of the threshold or bias value for the hidden layer and the output layer. μ and λ are learning rate parameters for the hidden layer and the output layer. Repeat steps 1 through 6 on all training data until the specified tolerance of the output error is reached.

The backpropagation network has the ability to learn any arbitrarily complex nonlinear mapping. With respect to the statistics method, the proposed feed-forward method with one hidden layer is a very close projection pursuit regression.

Chapter 5

Results

The examined specimens used in this study were produced under carefully controlled welding parameters (welding current, electrode pressure, and holding time) and identical metal conditions (e.g., surface coating, thickness). Due to the continuous hardware improvement, weld specimens were separated into three groups chronologically. The first group with C-scan images as their results was examined earlier by ultra-Short Pulse Scanning reflection Acoustic Microscope (SPSAM). The quality of these specimens was certified by experts from the best to the worst as setup, nominal, minimum, less than minimum, and stick weld, respectively. The minimum quality is the bottom line of an accepted weld. The second group with C-scan as their result was examined by SPSAM as well. This group was peel tested and served as the verification group to test the Artificial Neural networks (ANN) model built by group one. Later on, after the prototype of the hand-held microscope was born, newly arrived specimens, categorized as group three, were examined by both hand-held microscope and SPSAM.

This experiment started with applying nondestructive acoustic tests to specimens and recording all the acoustic information. Then destructive testing was conducted on the second and third groups of specimens for conventional nugget diameter measurement. Through destructive tests, the nugget size of each spot weld could be found. This information was then integrated into the results together with the parameters recognized by the proposed method in a later section. The experimental procedures for the specimens are listed in the following table:

Table 5.1 Detail of experiments

	Group one	Group two	Group three
Time	Early stage	Early stage	After the prototype of hand-held device was developed
Microscope(s) used	SPSAM	SPSAM	Hand-held device and SPSAM
Experiment procedure 1	Nondestructive only	Destructive and nondestructive	Destructive and nondestructive
Experiment procedure 2	Identified by expert for their quality (setup / nominal / minimum / less than minimum / stick)	Perform peel tests and measure the nugget diameters	Perform peel tests and measure the nugget diameters
Current status	Serve as the calibration coupon for nondestructive testing in industries	destroyed	destroyed
Result of collected data	Acoustic images and quality information (good/bad weld)	Acoustic images and quantity information (weld diameter)	Acoustic images and quantity information (weld diameter)
Number of specimens	390	13	46

5.1 Experimental results of group one

Two types of metal stack up were studied, and they are Type I (0.03" x 0.045") and Type II (0.04" x 0.06"). The criteria for identifying weld quality by experts for each metal stack up is based on the size of the weld nugget. The criteria are listed in table 5.2.

Table 5.2 Quality of weld (group I)

	Type I	**Type II**
Setup	*5.1 ±0.4*	*6.4 ±0.4*
Nominal	*4.4 ±0.4*	*5.6 ±0.4*
Minimum	*3.6 +0.4*	*4.8 + 0.4*
Less than minimum	*1.8 ±0.4*	*2.4 ±0.4*
Stick	*No nugget*	*No nugget*

(unit: mm)

The following table lists part of the result obtained by acoustic image measurement. The complete results are listed in Appendix I. Details of the measuring method were shown in Chapter 4, Section 2. Details of the analysis method were shown in Chapter 4, Section 3.

Table 5.3 Acoustic image analysis results of group I

	Result of image analysis			Experts' result	
TYPE I Stack up	Area	Max. diameter	Min. diameter	Nugget diameter	Quality
	14.0	4.5	3.3	1.9	Less than min.
	15.0	5.3	2.8	1.4	Less than min.
	18.0	5.7	3.0	2.1	Less than min.
	12.0	5.0	2.5	1.9	Less than min.
	16.0	5.0	2.5	2.1	Less than min.
	14.0	5.2	2.5	1.9	Less than min.
	11.0	5.0	2.5	1.7	Less than min.
	12.0	4.9	2.5	1.5	Less than min.
	16.0	5.3	2.5	1.7	Less than min.
	14.0	5.1	2.5	1.5	Less than min.
	14.0	4.9	2.5	2.0	Less than min.
	15.0	5.3	3.5	1.8	Less than min.
	14.0	5.1	3.3	1.8	Less than min.

These results involve the quality indicator (e.g. setup, nominal, minimum, less than minimum, stick) and will be adopted in the ANN model developed for this study. Among these specimens, 120 samples including 24 setup, 24 nominal, 24 minimum, 24 less than minimum, and 24 stick were chosen for each type of stack up to train the ANN. The other 75 samples for each type were used to test the neural networks model. In Type I stack up, all 75 samples match the actual weld quality of the ANN corresponding model. For the Type II stack up, 71 out of 75 samples match the weld quality of the corresponding ANN model. The results indicate a coherent performance for this model based on expert knowledge.

The results of Type II is plotted in Figures 5.1 to 5.3 according to the selected acoustic parameters (area, maximum nugget diameter, and minimum nugget diameter). It is observed that there exists no clear boundary between weld quality by considering a single parameter. For example, in Figure 5.1, the range of "minimum" quality and "less than minimum" are overlapped between 20 and 30. In other words, the quality of weld cannot be decided by a single acoustic parameter.

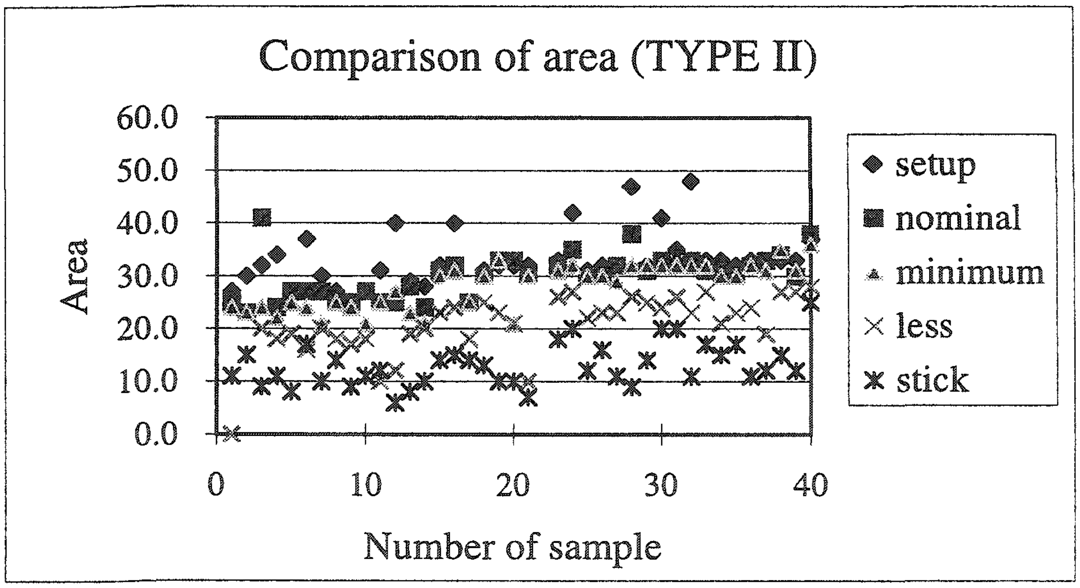

Figure 5.1 The distribution of weld qualities in terms of acoustic parameter 1

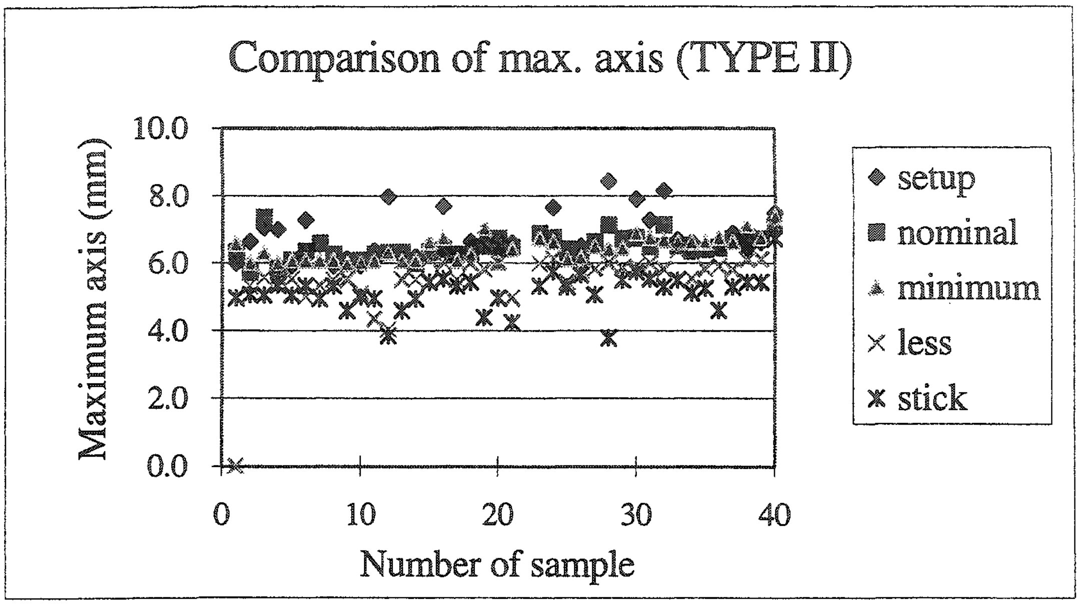

Figure 5.2 The distribution of weld qualities in terms of acoustic parameter 2

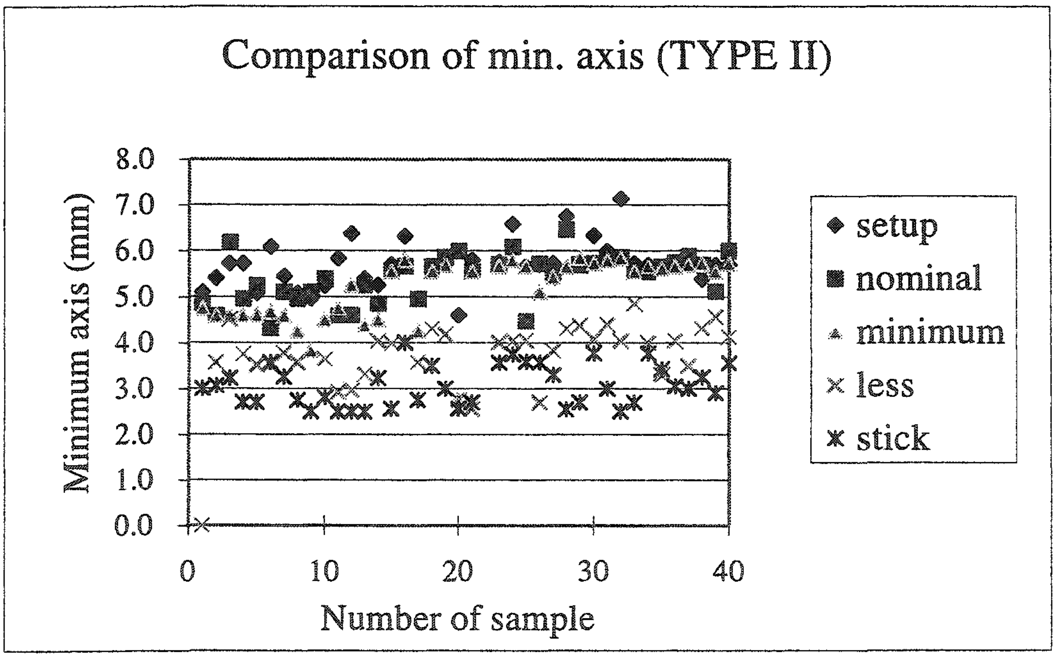

Figure 5.3 The distribution of weld qualities in terms of acoustic parameter 3

5.2 Experimental results of group two

One type of metal stack up (Type I, 0.03" x 0.045") was studied. This group of specimens was acoustically examined and peel tested. The acoustic C-scan images have been used to test the corresponding ANN model built by the specimens of group 1. The verification is 100% consistent to both (peel test and ANN) models. The results are listed in Table 5.4.

Table 5.4 Acoustic image analysis results of group II

	area	maximum axis	minimum axis	output	peel test diameter	weld quality	result
weld 78	31.0	6.7	5.5	good	5.65	setup	match
weld 81	42.0	7.3	6.3	good	5.5	setup	match
weld 82	38.0	7.6	6.0	good	5.5	setup	match
weld 86	24.0	6.0	4.5	good	5.5	setup	match
weld 88	22.0	5.8	4.3	good	4.45	nominal	match
weld 90	21.0	5.9	4.0	good	4.0	minimum	match
weld 92	21.0	5.7	4.3	good	3.65	minimum	match
weld 94	19.0	5.6	4.0	bad	3.5	less than	match
weld 96	19.0	5.7	3.8	bad	2.24	less than	match
weld 98	17.0	5.6	3.8	bad	2.2	less than	match
weld 100	15.0	5.2	3.8	bad	0	stick	match
weld 102	14.0	5.2	3.8	bad	0	stick	match
weld 104	0.0	0.0	0.0	bad	0	stick	match

5.3 Experimental results of group three

In this study, three parameters chosen for analyzing the weld quality are: surface indentation, nugget diameter measured from the acoustic method, and the total inclusion size inside the nugget. The data of these parameters and the results from the peel test are listed in Table 5.5. The experimental result is normalized and plotted in Figure 5.4 to provide visual assistance for choosing a proper interpretation of the weld quality:

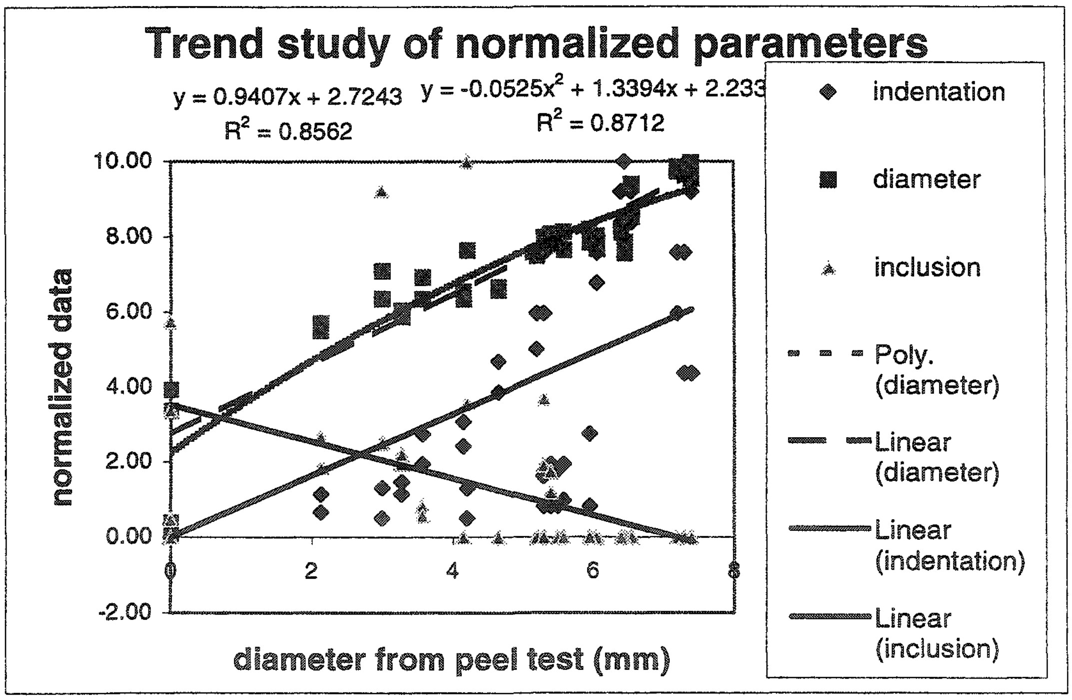

Figure 5.4 Study of acoustic measured parameter

Table 5.5 Experimental results

	Peel test	Acoustic parameters		
Sample number	diameter	Diameter (mm)	inclusion area	indentation
#1	0	2	0	5
#1_opp	0	1.77	0.45	3
#3	0	3.85	3.3	5
#3-opp	0	4.2	5.6	3
#6	2.13	5.18	1.8	10
#6_opp	2.13	5.3	2.6	7
#9	3.27	5.52	1.9	12
#9_opp	3.27	5.41	2.15	10
#10	3.57	6.06	0.8	20
#10_opp	3.57	5.7	0.55	15
#12	4.15	5.83	0	22
#12_opp	4.15	5.7	0	18
#14	4.65	5.9	0	32
#14_opp	4.65	5.85	0	27
#16	5.2	6.47	0	40
#16_opp	5.2	6.41	0	34
#17	5.3	6.57	0	50
#17_opp	5.3	6.63	0	40
#19	6.05	6.74	0	50
#19_opp	6.05	6.52	0	45
#23	6.55	7.59	0	55
#23_opp	6.55	7.06	0	60
#26	6.45	6.64	0	65
#26_opp	6.45	6.46	0	50
#27	6.4	6.8	0	60
#27_op	6.4	6.85	0	55
#57	3	6.16	2.45	6
#57_opp	3	5.7	9	11
#59	4.2	6.5	3.5	6
#59_opp	4.2	6.5	9.75	11
#61	5.3	6.71	3.6	8
#61_opp	5.3	6.65	1.85	13
#66	5.4	6.6	1.7	8
#66_opp	5.4	6.77	1.15	15
#67	5.5	6.64	0	8
#67_opp	5.5	6.75	0	14
#68	5.58	6.51	0	9
#68_opp	5.58	6.8	0	15
#70	5.95	6.63	0	8
#70_op	5.95	6.85	0	20
#72	7.2	7.8	0	40
#72_op	7.2	7.87	0	50
#73	7.3	7.84	0	30
#73_op	7.3	7.8	0	50
#74	7.4	7.68	0	30
#74_opp	7.4	7.96	0	60

There is no significant relationship between the normalized data and the diameter measured from the peel test. The only parameter capable of portraying the relationship is the distance between the weld boundaries, the order of which cannot be decided since the coefficient of determination (R^2) of the first and second order equations are so close. Therefore, both linear and nonlinear regression models are tested for determining the suitable model. Later on, the appropriate model is used to carry out the magnitude of the coefficients of the equation.

These three variable systems, α, β, and γ, where they represent indentation, acoustic diameter, and inclusion, respectively, are related to the diameter from peel test D.

Rewriting equation 4.3, the linear model would be:

$$D = C_0 + C_1\alpha + C_2\beta + C_3\gamma \quad \text{.....................(5.1)}$$

Rewriting equation 4.4, the polynomial model would be:

$$D = C_0 + C_1\alpha + C_2\beta + C_3\gamma + C_4\alpha^2 + C_5\beta^2 + C_6\gamma^2 + C_7\alpha\beta + C_8\beta\gamma + C_9\alpha\gamma \quad \text{.....................(5.2)}$$

where C_i, i =0~9 are constant coefficients.

The coefficients of the linear and nonlinear regression models are shown in the following table, and the results are plotted in Figure 5.5 and Figure 5.6, respectively. Figure 5.6 demonstrating the polynomial model with 10 constants is a closer prediction.

The F-score of this model is 170.36, which is substantially greater than the F-critical value of 2.17. Therefore, this regression model is useful in predicting the diameters measured by the peel test. The sum of the residual square is reasonably small at 4.28.

Table 5.6 Coefficients of linear and nonlinear models

Linear model									
C_0	C_1	C_2	C_3						
-3.340	0.0154	0.0791	0.0433						
Nonlinear model									
C_0	C_1	C_2	C_3	C_4	C_5	C_6	C_7	C_8	C_9
0.3962	0.2333	-1.050	-0.255	0.0008	0.2826	0.0201	-0.041	-0.029	0.0139

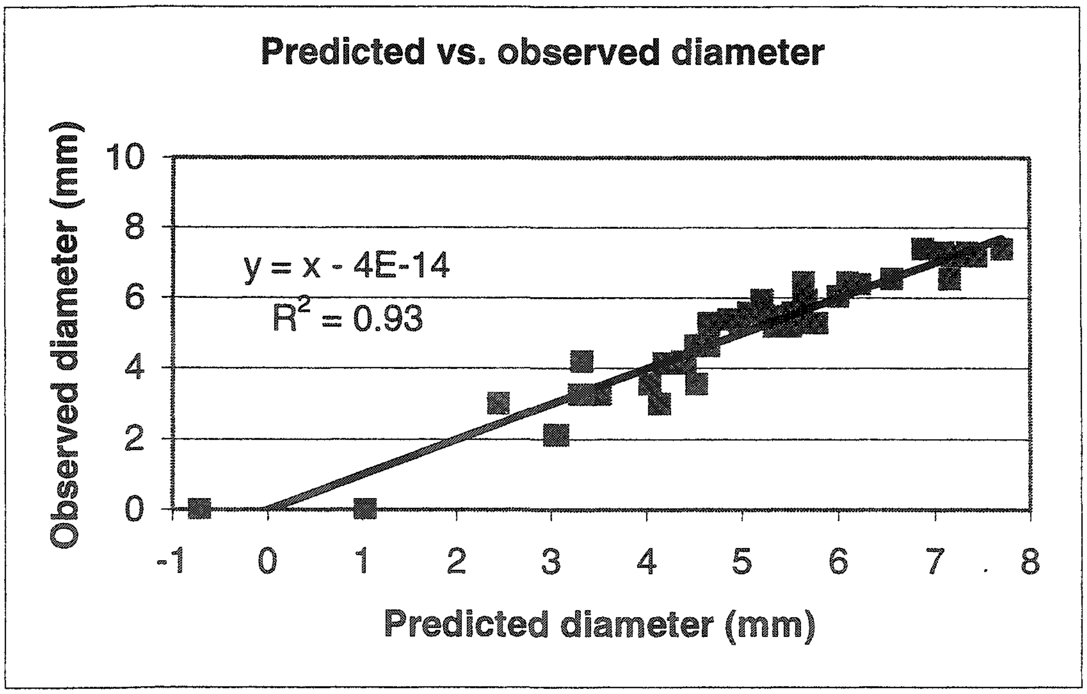

Figure 5.5 Predicted vs. observed diameter of linear model

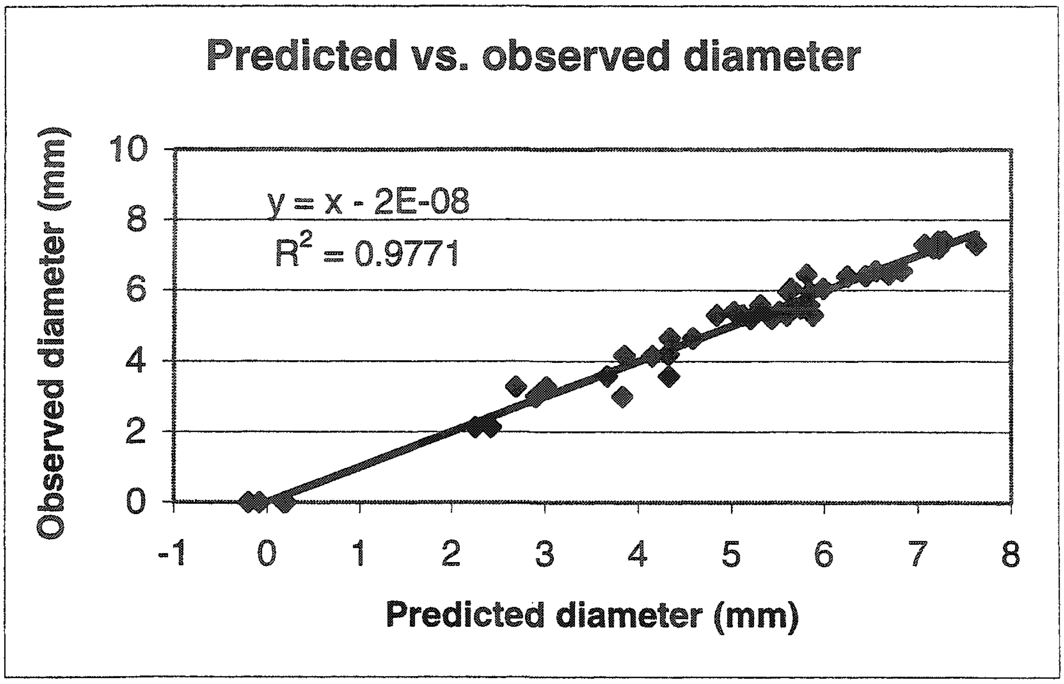

Figure 5.6 Predicted vs. observed diameter of nonlinear model

To reduce the calculation efforts of this model, a t-test for the statistical significance of each parameter is performed. The significance level is chosen as 95%, and the t-value is 1.645, which suggests that some of the terms are insignificant. Hence the reduced equation can be rewritten as:

$$D = C_0 + C_1\alpha + C_2\beta + C_3\alpha^2 + C_4\beta^2 + C_5\gamma^2 + C_6\alpha\beta \quad (5.3)$$

The coefficients are listed in the following table:

Table 5.7 Coefficients of linear and nonlinear models

Nonlinear model (after parameter screening)						
C_0	C_1	C_2	C_3	C_4	C_5	C_6
0.93835	0.31894	-1.66622	0.00044	0.34996	-0.00739	-0.04926

The new model provides an explanation without losing much of the generality of the observed diameter with the coefficient of determination equal to 0.969. The sum of the residual square is 5.755.

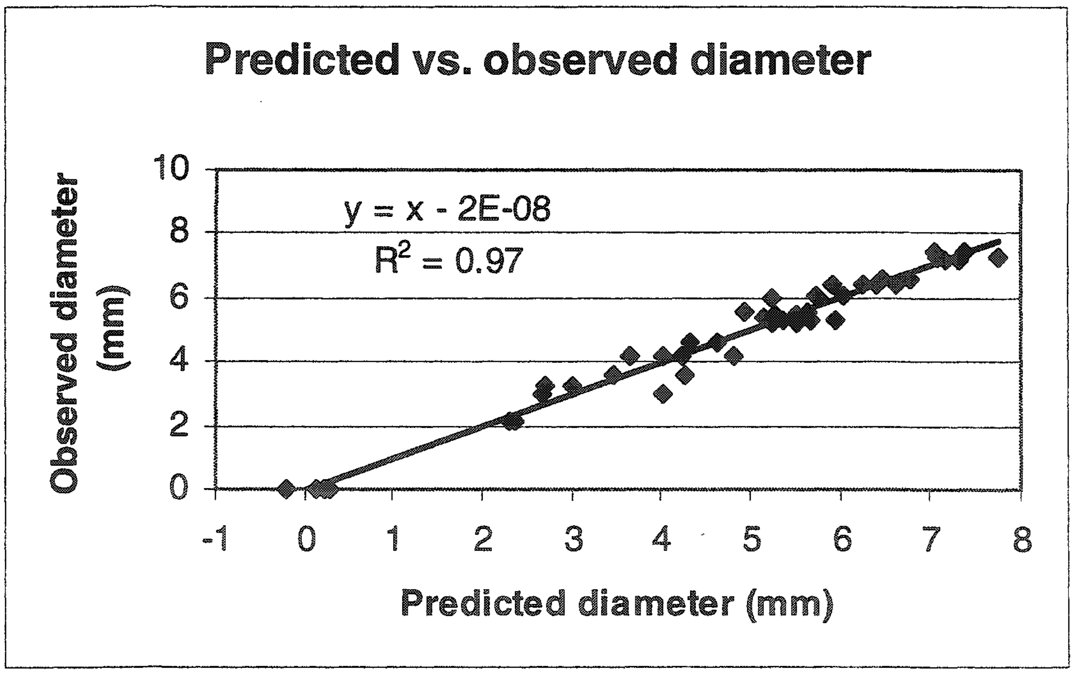

Figure 5.7 Predicted vs. observed diameter of nonlinear model with 6 parameters

Through these procedures, a set of significant parameters is determined and their coefficients can be retrieved. Consequently, the peel diameter of the weld will be predictable through the cumulative relationship, which will be an indicator of spot weld quality.

5.4 The developed software

JAVA is chosen to be the programming language to carry out the software system. The main reason for using JAVA is its portability. This software is able to run under most operation systems, e.g. Windows, UNIX, MacOS, and LINUX, without changing a single line of code. There are many other advantages to JAVA: JAVA is a programming language and platform; JAVA is an object-oriented language; JAVA supports internationalization; and JAVA is a multi-thread language.

There are two versions of the Acoustic Image Analysis software (AIA). The first version is the analyzer with image processing tools and neural networks training/ testing functions. Users can manipulate AIA by a pull down menu. Users can load images, perform basic image processing techniques, run default operations (thresholding / dilation / area calculation), prepare ANN training data, train ANN, prepare testing data, and test ANN results. The later version is aimed at performing spot weld quality examination on pre-trained ANN. Users can access file systems, perform the ANN test by clicking on one button on the toolbar. The following figures illustrate the user interface of these two versions of AIA:

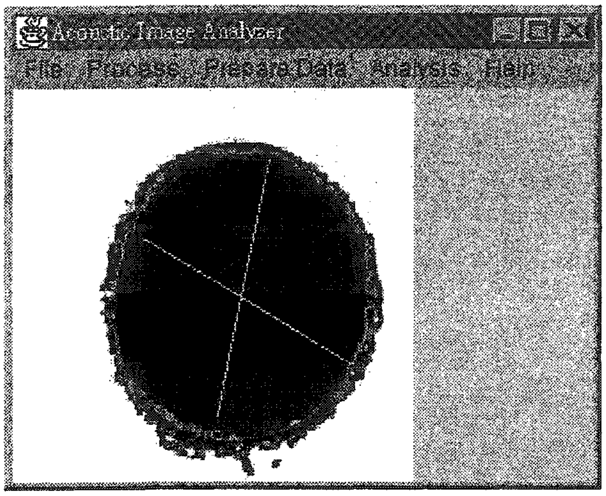

Figure 5.8 The user interface of Acoustic Image Analyzer (AIA)

Figure 5.9 The output screen shot of AIA

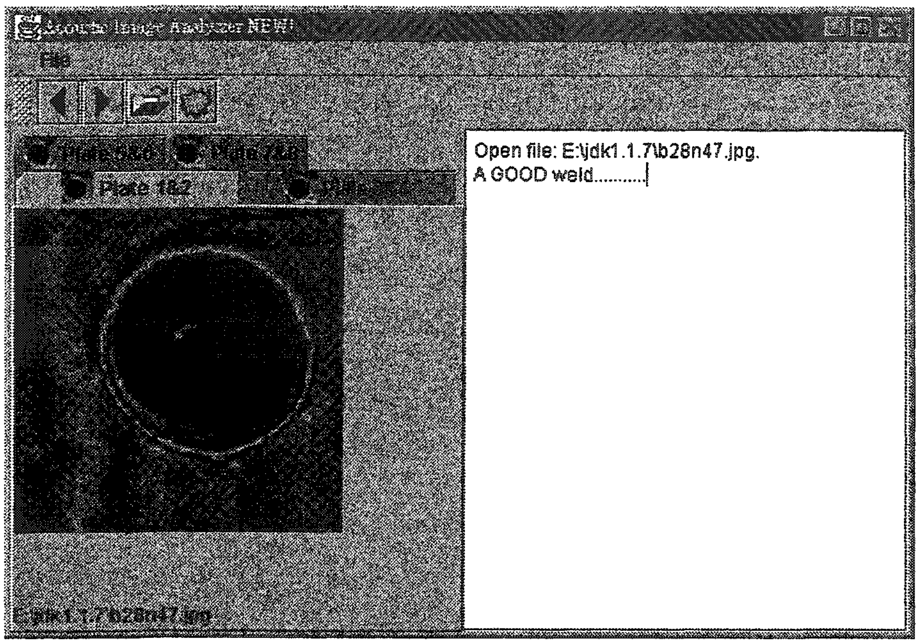

Figure 5.10 The screen shot of the newer version of Acoustic Image Analyzer (AIA2)

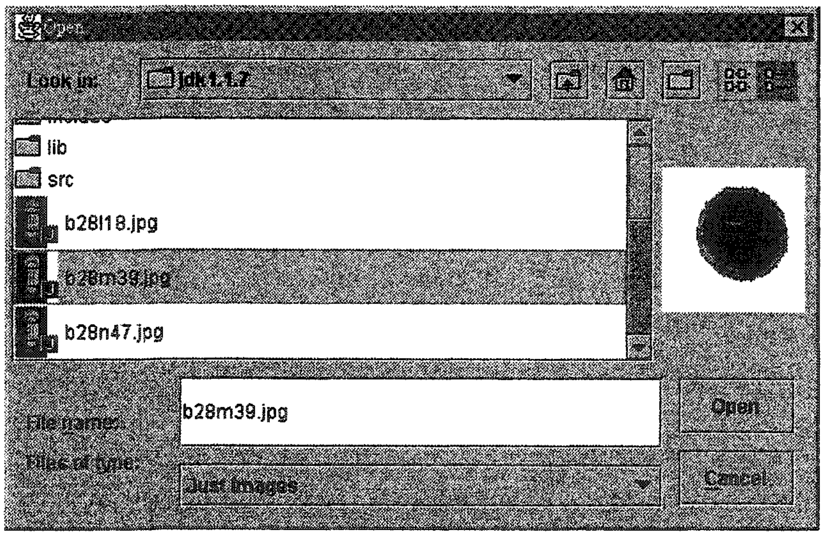

Figure 5.11 Other screen shot of AIA2

Chapter 6

Conclusion and future research

The spot weld process is the most popular joining mechanism in various industries. The quality of the spot weld is very important since it directly affects the quality of products and its performance in these industries. Due to the complicated physical properties of the spot weld, its quality is difficult to control. Most companies use an on-line welding parameters monitoring system (welding current, holding time, electronic force) with an off-line statistical sampling examination to ensure their product quality. This mechanism will fail for the following reasons:

1. The on-line parameter monitoring systems ignore many on-site errors such as the misalignment of weld tips, deterioration of the welding tip, electrical current oscillation, and fluctuation of the holding pressure.
2. The off-line inspection only offers a delayed response to the production line.
3. It is not an economic solution to reject a lot of high value products when mistakes happen.

The acoustic nondestructive method provides a feasible solution for spot weld quality inspection because it can examine the internal structures of spot welds. However, two problems prevent the current on-line application of the acoustic method. The first problem, involving the time-consuming scanning mechanism, can be solved by hardware renovation which is under development by The Center for Imaging Research and Advanced Materials Characterization. The second problem is that experienced operators are needed to operate the device and interpret the result. Even a skillful operator cannot operate the acoustic system and make a decision in an on-line fashion. This problem can be solved by building up a software program that is able to perform like an expert. Once reliable software is built, with the fast scanning hardware, every operator on the job site can be an expert in acoustic nondestructive testing.

The mathematical models reviewed in Chapter 3 provide a good fundamental knowledge of acoustic wave propagation in spot weld nuggets. However, due to the irregular shape of the nugget and the variation of materials, the mathematical model needs further work. An experimental approach is suggested in this study. This approach attempts to develop the correlation between acoustic images and the quality of spot welds.

In conclusion, the acoustic images were processed by using morphology techniques so that pre-set acoustic parameters could be acquired. Two methods, namely, statistical correlation and artificial neural networks (ANN), were used to build the correlation laws between the acquired acoustic parameters and the quality of spot welds. Conventionally, there are two ways to determine the quality of the spot weld, and they are the peel test, and opinions from experts, respectively. For weld quality obtained by the result of the peel test, a quantitative result is presented. This result is suitable for the statistical correlation study. On the other hand, for a qualitative result (good/bad weld indicator provided by experts), the ANN method which capable of manipulating boolean data, is a good choice. Both methods render excellent results for predicting weld quality.

Although statistical or related techniques are used in this research, this research is preferable to the conventional spot weld inspection method. The conventional examination method is only concerned with the statistical control of the periphery parameter and sampling techniques. By employing acoustic nondestructive inspection, which is able to acquire more internal information, this research provides a far more comprehensive analysis than the traditional statistical method. This study proves that an on-line acoustic examination is an achievable target. Through this approach, acoustic inspection of the spot weld can be applied as an on-line, feedback, real-time inspection device.

Further research based on this work could include:

1. Comprehensive anisotropic study at the non-core regions of weld nuggets.
2. Software development suitable for the next generation of the hand-held acoustic microscope.
3. Introduction of more acoustic parameters in the decision pool to determine the quality of spot welds, such as depth of penetration, profile of indentation, and shape of nugget.
4. An increase in the process speed of software by adding advanced functions to the hardware. For example, develop the hardware to measure the profile of indentation during scanning.
5. Apply more data to obtain higher statistical confidence results.

References

1. Achenbach, J. D., *Wave Propagation in Elastic Solids*, Elsevier Publish Co., 1973.

2. Acoff, V. L., and Thompson, R. G., "Effect of Postweld Heat Treatment on Ti-14Al-21Nb Fusion Zone Structure and Hardness", *Welding Journal*, Vol. 74, pp. 1s-9s, 1995.

3. Adler, L., Rose, J. H., and Mobley, C., "Ultrasonic Method to Determine Gas Porosity in Aluminum Alloy Casting: Theory and Experiment", *Journal of Applied Physics*, Vol. 59, No.2, pp. 336-346, 1986.

4. Arnold, K., and Gosling, J., *The JAVA programming language*, Addison Wesley Longman Inc., 1996.

5. Beersiek, J., Poprawe, R., Schulz, W., Gu, H.; Mueller, R. E., and Duley, W.W., "On-line monitoring of penetration depth in laser beam welding", *Proceedings of the 1997 Laser Materials Processing Conference*, ICALEO'97. Part 1 Vol. 83, No. Pt 1, pp. C30-C39 1997.

6. Bently, K. P., Greenwood, J. A., Knowlson, P., and Baker, R. G., "Temperature Distribution in Spot Welds", *British Welding Journal*, Vol. 10, June, pp. 613-619, 1963.

7. Bertram, L. A., "Flow Effects on the Solidification Environment in a GTA Spot Weld", *Journal of Engineering Materials and Technology*, Vol. 115, pp. 24-9, 1993.

8. Bhattacharya, S., Andrews, D. R., and Green, L. W., "In-process Quality Control of Spot Weld", *Metal Construction*, April, pp. 227-229 1975.

9. Briggs, A., *Acoustic Microscopy*, Clarendon Press, 1992.

10. Briggs, A., "Ceramic Fiber Composites", *Advance Materials & Processes*, Vol. 7, pp. 26-29, 1994.

11. Browne, D. J., Chandler, H. W., and Evans, J. T., "Computer Simulation of Resistance Spot Welding in Aluminum: Part I", *Welding Journal*, Vol. 74, pp. 339s-344s, 1995.

12. Browne, D. J., Chandler, H. W., and Evans, J. T. "Computer Simulation of Resistance Spot Welding in Aluminum: part II", *Welding Journal*, Vol. 74, pp. 417s-422s, 1995.

13. Bruckner, W. H., *Metallurgy of Welding*, Pitman Publishing Corporation, 1954.

14. Campione, M., and Walrath, K., *The JAVA tutorial*, second edition, Addison Wesley Longman Inc., 1998.

15. Chan, P, Lee, R., and Kramer, D. *The JAVA class libraries*, Second edition, Vol. 1, Addison Wesley Lonhman Inc, 1998.

16. Chan, P, Lee, R., and Kramer, D. *The JAVA class libraries*, Second edition, Vol. 2, Addison Wesley Lonhman Inc, 1998.

17. Chang, H. S., Cho, Y. J., Choi, S. G., and Cho, H. S., "A propotional Integral Controller for Resistance Spot Weld Using Nugget Expansion", *Transactions of the AMSE*, Vol. 111, pp. 332-336, 1989.

18. Cho, H. S., and Cho, Y. J., "A Study of The Thermal Behavior in Resistance Spot Welds", *Welding Journal*, Vol. 68, No. 6, pp. 236-244, 1989.

19. Colchester, A. C. F., and Hawkes, D. J., eds. *Information Processing in Medical Images*, 12th International Conference, IPMI '91 Proceeding, Springer-Verlag, 1991.

20. Connor, L. P. ed, *Welding Handbook*, American Welding Society, 1991.

21. De, A., Gupta, O. P., and Dorn, L., "An Experimental Study of Resistence Spot Welding in 1 mm Think Sheet of Low Carbon Steel", *Proceedings of the Institution of Mechanical Engineerings. Part B, Journal of Engineering Manufacture* Vol. 210, noB4, pp. 341-347, 1996.

22. Deschamps, M., and Som, A., "Acoustic Signature of Dispersive and Orthotropic Composites Using a Focused Microscope", *Journal of Acoustic Society of America*, Vol. 93, pp. 1374-1384, 1993.

23. Dewey, B. R., Adler, L., King, R. T., and Cook, K. V., "Measurement of Anisotropic Elastic Constants of Type 308 Stainless-Steel Electroslag Welds", *Experimental Mechanics*, Vol.17, No.11, pp. 420-426, 1977.

24. Dickinson, D. W., Franklin, J. E., and Stanya, A., "Characterization of Spot Welding Behavior by Dynamic Electrical Parameter Monitoring" *Welding Journal*, Vol. 59, No. 6, pp. 170-176, 1980.

25. Dix, A. F. J., "Metallurgy Study of Resistance Weld Nugget Formation and Stuck Welds", *British Welding Journal, January*, pp. 7-16, 1968.

26. Easterling, K., *Introduction to the Physical Metallurgy of Welding*, Butterworths, 1983.

27. Ekis, J. W., "Ultrasonic Examination for resistance Spot Welds of Filter Connectors", *Materials Evaluation*, Vol. 52, pp. 462-463, 1994.

28. Exner, H. E., and Hougardy, H. P., ed. *Quantitative Image Analysis of Microstructures*, Informationsgesellscgaft Verlag, 1988.

29. Froehlich, J. *http://rfhs8012.fh-regensburg.de/~sauer/jfroeh/diplom/e-index.html*

30. Fuerschbach, P. W., "Measurement and Prediction of Energy Transfer Effieiency in Laser Beam Welding", *Welding Journal*, Vol. 75, pp. 24s-34s, 1996.

31. Deary, D. M., *Graphic JAVA*, second edition, Sun Microsystems Press, 1997.

32. Gerry, K., "Aluminum/Steel Welding", *Automotive Industries*, Vol. 174, p. 44, 1994.

33. Gilmore, R. S., Glaeser, A. M., and Wade, J. C., "Calibrating Ultrasonic Images for The NDE Structural Materials", *ASME Transactions*, Vol. 116, July, pp. 640-646, 1994.

34. Gilmore, R. S., "Industrial ultrasonic imaging and microscopy", *Physics, D: Applied Physics, Vol. 29,* pp. 1389-1417, 1996.

35. Gornaja, S.P., and Aljoshin, N.P., "Attenuation of ultrasonic waves in austenitic steel welds", *Nondestructive Testing and Evaluation* Vol. 13, No. 3, pp. 149-168, 1997.

36. Gosling, J., Joy, B., and Steele, G., *The JAVA language specification*, Addison Wesley Longman Inc., 1996.

37. Gould, J. E., "An Examination of Nugget Development During Spot Welding, Using Both Experimental and Analytical Techniques" *Welding Journal*, Vol. 66, Number 1, pp. 1- 10, 1987.

38. Graham, I., and Jones, P. L., *Expert Systems Knowledge, Uncertainty and Decision*, Chapman and Hall Ltd., 1988.

39. Greenwood, J. A., "Temperatures in Spot Welding" *British Welding Journal*, Vol. 8, No. 6, pp. 316-322, 1961.

40. Gurney, K., Neural Nets, *http://www.shef.ac.uk/psychology/gurney/notes/contents.html*

41. Harvey, R. L., *Neural Network Principles*, Prentice Hall, 1994.

42. Hirsch, R. B., "Tip Force Control Equals Spot Weld Quality", *Welding Journal*, Vol. 72, pp. 57-60, 1993.

43. Houldcroft, P. T., *Welding Process Technology*, Cambridge University Press, 1977.

44. Howe, P., "Spot Weld Spacing Effect on Weld Button Size", *Sheet Metal Welding Conference*, paper C3, 1994.

45. *http://www.developer.com*

46. Irving, B., "Welding the Four Most Popular Aluminum Alloys", *Welding Journal*, Vol. 73, pp. 51-55, 1994.

47. Java programmer's FAQ, *http://www.best.com/pvdl/javafaq.html*

48. JavaWorld Magazine, *http:www.javaworld.com*

49. Johnson, K. I., "Resistance Welding Quality Control Techniques" *Metal Construction & British Welding Journal*, Vol. 5, No. 1, pp. 176-181, 1975.

50. Johnson, R. A., *Miller & Freund's Probability & Statistics for Engineers*, Prentice Hall, Inc., 1994.

51. Jou, M., Messler, R. W. Jr., and Li, C. J., "A Fuzzy System for Resistance Spot Welding Based on a Neural Network Model", *Sheet Metal Welding Conference*, paper C2, 1994.

52. Kaiser, J. G., Dunn, G. J., and Eagar, T. W., "The Effect of Electrical Resistance on Nugget Formation During Spot Welding", *Welding Journal*, Vol. 62, No. 6, pp. 167-174, 1982.

53. Kanne, W. R. Jr., Johnson, G. W. E., Braun, J. D., and Louthan, M. R. Jr., Ed., *Metallographic Characterization of Metals after Welding, Processing and Service*, ASM International, International Metallographic Society, Vol. 20, 1993.

54. Keyser, C. A., *Basic Engineering Metallurgy*, 2nd Edition, 1959.

55. Krauss, G., *STEELS: Heat Treatment and Processing Principles*, ASM International, 1990.

56. Kupperman, D. S., Reimann, K. J., "Ultrasonic Wave Propagation and Anisotropy in Austenitic Stainless Steel Weld Metal", *IEEE Transactions on Sonics and Ultrasonics*, Vol. SU-27, No. 1, pp. 7-15, 1980.

57. Lee, Y. C., Kim, J. O., and Acgenbach, J. D., "V(z) Curves of Layered Aniotropic Materials for the Line-focus Acoustic Microscope", *Journal of Acoustic Society of America*, Vol. 94, pp. 923-930, 1994.

58. Lancaster, J. F., *Metallurgy of Welding*, George Allan & Unwin Ltd., 1980.

59. Ledbetter, H. M., "Monocrystal Elastic Constants in The Ultrasonic Study of Welds", *Ultrasonics*, Vol. 23, January, pp. 9-13, 1985.

60. Lin, C. J., and Duh, J. G., "Influence of Weld Parameters on the Mechanical Properties of Spot Weld Fe-Mn-Al-Cr Alloy", *Journal of Materials Science*, Vol. 28, pp. 4767-4774, 1993.

61. Linnert, G. E., *Welding Metallurgy*, 3rd edition , American Welding Society, 1965.

62. Lott, A., "Ultrasonic Detection of Molten/Solid Interfaces of Weld Pools", *Material Evaluation*, Vol. 42, March, pp. 337-341, 1984.

63. Louthan, M. R. Jr., LeMay, I., and Vander Voort, G. F., Ed., *Welding, Failure Analysis, and Metallography*, ASM International, International Metallographic Society, Vol. 14, 1987.

64. Maev, R. G., Watt, D. F., Pan, R., Levin, L. M., and Maslov, K. I., "Development of High Resolution Ultrasonic Inspection Methods for Welding Microdefectoscopy", *Acoustic Imaging*, Edited by Tortoli, P., and Masotti, L., Vol.22, pp. 779-784, 1996.

65. Masters, T., *Practical Neural Recipes in C++*, Academic Press, Inc., 1993.

66. Nava-Rudiger, E., and Houlot, M., "Integration of real time quality control systems in a welding process", *Journal of Laser Applications* Vol. 9, No. 2, pp. 95-102, 1997.

67. Neid, H. A., "The Finite Element Modeling of the Resistance Spot Welding Process", *Welding Journal*, Vol. 63, pp. 123s-132s, 1984.

68. Ogilvy, J. A., "Ultrasonic Beam Profiles and Beam Propagation in an Austenitic Weld Using a Theoretical Ray Tracing Model", *Ultrasonics*, Vol. 24, November, pp. 337-347, 1986.

69. O'Neill, B., Maev, R., "Mathematical Methods for the Characterization of Ultrasound in Anisotropic Materials", Submitted to *Physics Review B*, September 1998.

70. Pal, K., and Cronin, D. L., "Static and Dynamic Characteristics of Spot Welded Sheet Metal Beams", *ASME Transactions*, Vol. 117, August, pp. 316-322, 1995.

71. Pan, R., *Modelling Weld Microstructure Development in Resistance Welded Cross Bars*, Thesis, university of Windsor, 1991.

72. Roset, C. A., and Rager, D. D., "Resistance Welding Parameter Profile for Spot Welding Aluminum", *Welding Journal*, Vol. 54, No. 12, pp. 530-536, 1974.

73. RWMA, *Resistance Welding Manual*, 4th Edition, Resistance Welder Manufacturers' Association, 1989.

74. Séférian, D., *The Metallurgy of Welding*, John Wiley and Sons Inc., 1962.

75. Serra, J., *Image Analysis and Mathematical Morphology*, Academic Press, 1982.

76. Shehata, M. T., Leduc, T. R., LeMay, I., and Louthan, M. R. Jr., Ed., *Metallographic Techniques and the Characterization of Composites, Stainless Steel, and Other Engineering Materials*, ASM International, International Metallographic Society, Vol. 22, 1995.

77. Snee, R. K., and Taylor, J. L., "Infra-red Monitoring of Resistance Spot Welding", *Metal Construction and British Welding Journal*, Vol. 4, No. 1, pp. 142-148, 1972.

78. Sokolowski, J. H., Maev, R. G., Lee, H., Maeva, E. Y., and Maslov, K. I., "Analysis of Casting Subsurface Structure Using Acoustic Microscopy", *Review of Progress in Quantitative Nondestructive Evaluation*, Vol. 18B, 1998 (in press).

79. Spinella, D. J., "Using Fuzzy Logic Determine Operating Parameters for Resistance Spot Welding for Aluminum", *Sheet Metal Welding Conference*, paper C5, 1994.

80. Taylor, J. L., "A New Approach to The Displacement Monitor in Resistance Spot Welding of Mild Steel Sheet", *Metal Construction*, pp. 72-75, 1987.

81. Tsai, C. L., Cheng, W. T., and Lee, H. T., "Modelling Strategy for Control of Welding-induced Distortion", Proceedings of the 1995 7th Conference on Modeling of Casting, Welding, and Advanced Solidification Processes, pp. 335-345, 1995.

82. Tsai, C. L., Dai, W. L., Papritan, J. C., and Dickinson, D. W., "Analysis and Development of a Real-Time Control Methodology in Resistance Spot Welding", *Welding Journal*, Vol. 70, pp. 339s-345s, 1991.

83. Tsai, C. L., Jammal, O. A., Papritan, J. C., and Dickinson, D. W., "Modeling of Resistance Spot Weld Nugget Growth", *Welding Journal*, Vol. 71, pp. 47s-54s, 1992.

84. *Ultrasonic Testing Handbook*, American Society for Nondestructive testing, 1991.

85. Utrata, D., Piela, S., and Nath, S., "Evaluation of Spot Welds by Various Techniques", *Reviews of Progress in Quantitative Nondestructive Evaluation*, Vol. 16, pp. 1207-1213, 1997.

86. Veidt, M., and Sachse, W., "Ultrasonic Point-Source/Point-Receiver Measurements in Thin Specimens", *Journal of Acoustic Society of America*, Vol. 96, No. 4, pp. 2318-2326, 1994.

87. Vlahopoulos, N., Allen, T., and Zhao, X., "Approach for modeling spot-welded joints in an energy finite element formulation", *Proceedings of the 1998 National Conference on Noise Control Engineering*. Part 1, Apr 5-9, pp. 347-352, 1998.

88. Yuasa, H., and Masazumi, K., "Inspection Device for Spot Weld Nugget", *Acoustic Imaging*, Edited by Tortoli, P., and Masotti, L., Vol.22, pp. 771-778, 1996.

Appendix I

Results of acoustic measurement

	Result of image analysis			Experts' result	
TYPE I Stack up	Area	Max. diameter	Min. diameter	Nugget diameter	Quality
	12.0	4.9	2.5	1.5	Less than min.
	16.0	5.3	2.5	1.7	Less than min.
	14.0	5.1	2.5	1.5	Less than min.
	14.0	4.9	2.5	2.0	Less than min.
	15.0	5.3	3.5	1.8	Less than min.
	14.0	5.1	3.3	1.8	Less than min.
	10.0	4.9	2.5	1.7	Less than min.
	10.0	5.4	2.5	1.4	Less than min.
	17.0	5.6	2.8	2.1	Less than min.
	15.0	5.0	3.5	1.8	Less than min.
	10.0	4.8	3.3	1.5	Less than min.
	14.0	4.6	3.2	1.9	Less than min.
	16.0	4.8	3.5	2.0	Less than min.
	10.0	4.6	3.2	1.4	Less than min.
	12.0	4.9	2.5	1.5	Less than min.
	15.0	5.0	3.5	1.7	Less than min.
	13.0	5.0	2.8	1.6	Less than min.
	13.0	4.6	3.2	1.8	Less than min.
	12.0	4.7	2.5	2.2	Less than min.
	11.0	4.6	2.8	1.8	Less than min.
	12.0	4.8	3.3	1.8	Less than min.
	16.0	5.2	3.2	1.8	Less than min.
	9.0	4.2	3.2	1.5	Less than min.
	8.0	4.2	2.5	1.9	Less than min.

	Result of image analysis			Experts' result	
TYPE I Stack up	Area	Max. diameter	Min. diameter	Nugget diameter	Quality
	14.0	4.8	2.5	1.7	Less than min.
	14.0	4.8	3.3	1.7	Less than min.
	5.0	3.5	2.5	1.6	Less than min.
	14.0	4.8	2.5	1.9	Less than min.
	15.0	4.7	3.3	1.8	Less than min.
	10.0	4.6	2.5	1.5	Less than min.
	13.0	4.7	3.3	1.7	Less than min.
	12.0	4.7	3.2	1.7	Less than min.
	24.0	5.8	5.0	4.0	Minimum
	24.0	5.8	4.2	4.0	Minimum
	24.0	6.1	4.4	4.0	Minimum
	24.0	5.7	4.9	4.0	Minimum
	23.0	6.0	4.5	4.0	Minimum
	23.0	6.3	4.0	4.0	Minimum
	23.0	6.0	4.0	3.9	Minimum
	24.0	6.0	4.8	4.0	Minimum
	27.0	6.1	5.0	3.9	Minimum
	23.0	5.7	4.8	4.0	Minimum
	26.0	6.1	5.1	3.9	Minimum
	25.0	5.8	5.0	3.9	Minimum
	24.0	5.8	5.0	3.9	Minimum
	23.0	6.1	4.0	3.9	Minimum
	25.0	6.1	4.8	4.0	Minimum
	24.0	5.8	5.0	4.0	Minimum

	Result of image analysis			Experts' result	
TYPE I Stack up	Area	Max. diameter	Min. diameter	Nugget diameter	Quality
	20.0	5.4	4.2	3.8	Minimum
	26.0	6.2	4.8	4.0	Minimum
	19.0	5.3	4.3	3.7	Minimum
	19.0	·4.9	4.3	3.9	Minimum
	19.0	5.2	3.8	4.0	Minimum
	24.0	6.0	4.8	4.0	Minimum
	22.0	5.5	4.7	4.0	Minimum
	20.0	5.4	4.0	4.0	Minimum
	20.0	5.1	4.4	4.0	Minimum
	19.0	5.1	4.5	4.0	Minimum
	19.0	5.3	4.2	3.9	Minimum
	19.0	4.9	3.8	3.9	Minimum
	22.0	5.5	4.3	3.9	Minimum
	20.0	5.3	4.3	3.7	Minimum
	19.0	5.2	4.2	3.7	Minimum
	18.0	5.0	3.5	4.0	Minimum
	20.0	5.1	4.6	4.0	Minimum
	19.0	5.1	4.2	4.0	Minimum
	20.0	5.3	4.5	4.0	Minimum
	19.0	5.1	4.3	4.0	Minimum
	19.0	5.1	4.5	3.9	Minimum
	19.0	5.1	4.4	3.9	Minimum
	21.0	5.4	4.0	4.0	Minimum
	25.0	5.8	4.5	4.6	Nominal

	Result of image analysis			Experts' result	
TYPE I Stack up	Area	Max. diameter	Min. diameter	Nugget diameter	Quality
	27.0	6.3	5.3	4.6	Nominal
	25.0	6.1	4.2	4.5	Nominal
	25.0	5.8	4.2	4.8	Nominal
	26.0	5.9	5.3	4.8	Nominal
	24.0	6.0	4.3	4.6	Nominal
	24.0	6.1	4.2	4.6	Nominal
	24.0	5.8	4.5	4.5	Nominal
	30.0	6.5	5.0	4.4	Nominal
	24.0	5.8	4.3	4.6	Nominal
	27.0	6.1	5.1	4.8	Nominal
	25.0	6.0	4.2	4.6	Nominal
	26.0	6.1	4.8	4.7	Nominal
	24.0	6.0	4.2	4.6	Nominal
	26.0	6.1	4.8	4.7	Nominal
	26.0	6.0	5.0	4.7	Nominal
	23.0	5.9	4.7	4.2	Nominal
	26.0	6.1	4.8	4.8	Nominal
	21.0	5.5	4.5	4.5	Nominal
	21.0	5.4	4.4	4.5	Nominal
	21.0	5.4	4.4	4.6	Nominal
	24.0	5.8	4.5	4.5	Nominal
	23.0	5.6	4.7	4.6	Nominal
	22.0	5.4	4.5	4.7	Nominal
	21.0	5.3	4.6	4.6	Nominal

	Result of image analysis			Experts' result	
TYPE I Stack up	Area	Max. diameter	Min. diameter	Nugget diameter	Quality
	25.0	6.1	4.9	4.6	Nominal
	23.0	5.7	4.8	4.7	Nominal
	20.0	5.2	4.5	4.5	Nominal
	23.0	5.5	4.8	4.5	Nominal
	22.0	5.4	4.5	4.6	Nominal
	21.0	5.4	4.2	4.6	Nominal
	21.0	5.4	4.5	4.4	Nominal
	20.0	5.1	4.5	4.7	Nominal
	20.0	5.1	4.5	4.6	Nominal
	23.0	5.5	4.8	4.1	Nominal
	20.0	5.2	4.5	4.1	Nominal
	21.0	5.2	4.7	4.0	Nominal
	20.0	5.3	4.5	4.0	Nominal
	27.0	6.0	5.3	4.6	Nominal
	32.0	8.1	5.5	5.2	Setup
	32.0	6.9	5.1	5.2	Setup
	26.0	6.0	5.1	5.2	Setup
	33.0	6.7	5.8	5.4	Setup
	28.0	6.0	5.4	5.2	Setup
	27.0	6.1	4.6	5.2	Setup
	27.0	6.3	4.5	5.1	Setup
	27.0	6.0	5.1	5.1	Setup
	38.0	7.3	5.8	5.4	Setup
	27.0	6.3	5.4	5.0	Setup

	Result of image analysis			Experts' result	
TYPE I Stack up	Area	Max. diameter	Min. diameter	Nugget diameter	Quality
	39.0	7.9	5.9	5.4	Setup
	28.0	6.0	5.5	5.4	Setup
	38.0	7.8	6.0	5.4	Setup
	28.0	6.2	4.7	5.1	Setup
	38.0	6.3	5.2	5.2	Setup
	28.0	6.1	5.5	5.3	Setup
	35.0	7.9	5.8	5.4	Setup
	31.0	7.8	5.5	5.4	Setup
	33.0	7.1	5.7	5.4	Setup
	33.0	7.5	5.7	5.3	Setup
	34.0	6.7	5.7	5.4	Setup
	27.0	6.0	5.1	5.1	Setup
	24.0	5.9	4.9	5.0	Setup
	23.0	5.5	4.8	4.9	Setup
	35.0	6.6	6.0	5.1	Setup
	31.0	7.0	5.4	5.2	Setup
	25.0	6.1	4.6	4.9	Setup
	36.0	7.1	5.5	4.9	Setup
	27.0	6.0	5.0	5.0	Setup
	23.0	5.9	4.8	5.1	Setup
	23.0	5.7	4.6	5.1	Setup
	20.0	5.1	4.3	4.7	Setup
	19.0	5.0	3.8	4.7	Setup
	33.0	6.4	5.1	4.9	Setup

	Result of image analysis			Experts' result	
TYPE I Stack up	Area	Max. diameter	Min. diameter	Nugget diameter	Quality
	35.0	7.1	5.8	4.8	Setup
	33.0	6.6	5.7	4.9	Setup
	34.0	7.6	5.7	4.9	Setup
	35.0	8.5	5.7	5.1	Setup
	28.0	6.4	5.3	4.7	Setup
	9.0	4.2	2.5	0.0	Stick
	11.0	5.0	3.2	0.0	Stick
	7.0	4.9	2.5	0.0	Stick
	7.0	4.2	2.5	0.0	Stick
	9.0	4.8	3.0	0.0	Stick
	3.0	3.8	2.5	0.0	Stick
	9.0	4.8	2.5	0.0	Stick
	2.0	3.5	2.5	0.0	Stick
	12.0	5.0	3.3	0.0	Stick
	8.0	4.3	2.8	0.0	Stick
	7.0	4.9	2.5	0.0	Stick
	9.0	4.6	3.1	0.0	Stick
	3.0	3.8	2.5	0.0	Stick
	9.0	4.6	2.5	0.0	Stick
	8.0	4.5	3.2	0.0	Stick
	11.0	5.2	3.1	0.0	Stick
	9.0	4.8	3.0	0.0	Stick
	10.0	4.8	3.3	0.0	Stick
	11.0	4.6	3.3	0.0	Stick

	Result of image analysis			Experts' result	
TYPE I Stack up	Area	Max. diameter	Min. diameter	Nugget diameter	Quality
	10.0	4.6	3.0	0.0	Stick
	8.0	4.5	3.0	0.0	Stick
	2.0	3.5	2.5	0.0	Stick
	8.0	4.0	2.7	0.0	Stick
	5.0	4.3	2.5	0.0	Stick
	9.0	4.3	3.1	0.0	Stick
	2.0	4.2	2.5	0.0	Stick
	1.0	3.5	2.5	0.0	Stick
	6.0	4.2	2.5	0.0	Stick
	8.0	4.0	2.5	0.0	Stick
	6.0	4.4	2.5	0.0	Stick
	5.0	4.5	2.7	0.0	Stick
	3.0	4.4	2.5	0.0	Stick
	7.0	4.2	2.7	0.0	Stick
	0.0	3.5	2.5	0.0	Stick
	10.0	4.5	3.0	0.0	Stick
	11.0	4.5	3.0	0.0	Stick
	5.0	4.2	2.5	0.0	Stick
	8.0	4.3	3.0	0.0	Stick
	6.0	3.9	2.8	0.0	Stick
	14.0	4.5	3.3	1.9	Less than min.
	15.0	5.3	2.8	1.4	Less than min.
	18.0	5.7	3.0	2.1	Less than min.
	12.0	5.0	2.5	1.9	Less than min.

	Result of image analysis			Experts' result	
TYPE I Stack up	Area	Max. diameter	Min. diameter	Nugget diameter	Quality
	16.0	5.0	2.5	2.1	Less than min.
	14.0	5.2	2.5	1.9	Less than min.
	11.0	5.0	2.5	1.7	Less than min.

	Result of image analysis			Experts' result	
TYPE II Stack up	Area	Max. diameter	Min. diameter	Nugget diameter	Quality
	15.0	5.4	3.3	0.0	Stick
	12.0	5.4	2.9	0.0	Stick
	25.0	6.7	3.6	0.0	Stick

	Result of image analysis			Experts' result	
TYPE II Stack up	Area	Max. diameter	Min. diameter	Nugget diameter	Quality
	0.0	0.0	0.0	2.5	Less than min.
	15.0	5.3	3.6	2.1	Less than min.
	20.0	5.6	4.5	2.8	Less than min.
	18.0	5.6	3.8	2.4	Less than min.
	19.0	5.5	3.5	2.4	Less than min.
	16.0	5.0	3.5	2.4	Less than min.
	20.0	5.3	3.8	2.0	Less than min.
	18.0	5.5	3.6	2.0	Less than min.
	17.0	5.5	2.5	2.0	Less than min.
	18.0	5.1	3.6	2.1	Less than min.
	10.0	4.3	2.9	2.5	Less than min.
	12.0	4.0	3.0	2.3	Less than min.
	19.0	5.5	3.3	2.3	Less than min.
	20.0	5.5	4.0	2.0	Less than min.
	23.0	6.1	4.0	2.5	Less than min.
	24.0	6.0	4.0	2.8	Less than min.
	18.0	5.5	3.6	2.0	Less than min.
	25.0	6.0	4.3	2.6	Less than min.
	23.0	5.8	4.2	2.8	Less than min.
	21.0	6.0	2.8	2.3	Less than min.
	10.0	5.0	2.5	2.8	Less than min.
	26.0	6.0	4.0	2.7	Less than min.
	27.0	6.1	4.0	2.8	Less than min.
	22.0	5.4	4.0	2.4	Less than min.

	Result of image analysis			Experts' result	
TYPE II Stack up	Area	Max. diameter	Min. diameter	Nugget diameter	Quality
	23.0	5.8	2.7	2.4	Less than min.
	23.0	5.8	3.8	2.2	Less than min.
	26.0	6.0	4.3	1.8	Less than min.
	25.0	5.9	4.4	1.8	Less than min.
	24.0	5.9	4.1	1.8	Less than min.
	26.0	6.0	4.4	1.5	Less than min.
	23.0	5.8	4.0	1.9	Less than min.
	27.0	6.4	4.8	1.7	Less than min.
	21.0	5.5	4.0	1.7	Less than min.
	23.0	5.8	3.3	1.6	Less than min.
	24.0	5.9	4.0	1.9	Less than min.
	19.0	5.8	3.5	1.8	Less than min.
	27.0	6.1	4.3	1.5	Less than min.
	27.0	6.1	4.6	1.7	Less than min.
	28.0	7.1	4.1	1.7	Less than min.
	24.0	6.6	4.8	4.8	Minimum
	23.0	6.0	4.6	4.8	Minimum
	24.0	6.3	4.6	4.8	Minimum
	22.0	6.0	4.6	4.8	Minimum
	25.0	6.1	4.6	4.8	Minimum
	24.0	6.1	4.7	5.1	Minimum
	21.0	6.1	4.6	4.8	Minimum
	25.0	6.1	4.3	5.0	Minimum
	24.0	6.0	3.8	4.8	Minimum

	Result of image analysis			Experts' result	
TYPE II Stack up	Area	Max. diameter	Min. diameter	Nugget diameter	Quality
	21.0	6.0	4.5	4.8	Minimum
	25.0	6.1	4.8	5.0	Minimum
	27.0	6.3	5.2	5.0	Minimum
	23.0	6.1	4.4	4.8	Minimum
	21.0	6.1	4.5	4.8	Minimum
	30.0	6.6	5.5	5.2	Minimum
	31.0	6.8	5.8	5.2	Minimum
	25.0	6.1	4.3	5.0	Minimum
	30.0	6.3	5.5	5.2	Minimum
	33.0	7.0	5.7	5.2	Minimum
	21.0	6.0	2.8	5.2	Minimum
	30.0	6.4	5.5	5.2	Minimum
	31.0	6.7	5.7	5.2	Minimum
	32.0	6.6	5.8	5.1	Minimum
	30.0	6.1	5.7	5.2	Minimum
	30.0	6.2	5.1	5.2	Minimum
	29.0	6.5	5.4	4.0	Minimum
	32.0	6.4	5.7	3.9	Minimum
	32.0	6.5	5.8	3.9	Minimum
	32.0	6.9	5.7	3.9	Minimum
	32.0	6.8	5.8	3.7	Minimum
	32.0	6.7	5.8	3.7	Minimum
	32.0	6.6	5.5	4.0	Minimum
	30.0	6.6	5.7	4.0	Minimum

	Result of image analysis			Experts' result	
TYPE II Stack up	Area	Max. diameter	Min. diameter	Nugget diameter	Quality
	30.0	6.6	5.6	4.0	Minimum
	32.0	6.8	5.7	4.0	Minimum
	31.0	6.6	5.7	4.0	Minimum
	35.0	7.1	5.7	3.9	Minimum
	31.0	6.8	5.5	3.9	Minimum
	36.0	7.4	5.7	4.0	Minimum
	25.0	6.3	4.8	5.2	Nominal
	23.0	5.7	4.6	5.0	Nominal
	41.0	7.4	6.2	5.2	Nominal
	24.0	5.8	4.9	5.2	Nominal
	27.0	6.1	5.2	6.0	Nominal
	27.0	6.4	4.3	5.3	Nominal
	27.0	6.6	5.1	5.3	Nominal
	25.0	6.3	4.9	5.2	Nominal
	25.0	6.1	5.1	5.4	Nominal
	27.0	6.1	5.4	5.3	Nominal
	25.0	6.3	4.6	5.3	Nominal
	25.0	6.3	4.6	5.3	Nominal
	28.0	6.3	5.2	5.7	Nominal
	24.0	6.0	4.8	5.3	Nominal
	31.0	6.3	5.5	5.8	Nominal
	32.0	6.4	5.7	5.9	Nominal
	25.0	6.3	4.9	5.2	Nominal
	30.0	6.3	5.7	6.0	Nominal

	Result of image analysis			Experts' result	
TYPE II Stack up	Area	Max. diameter	Min. diameter	Nugget diameter	Quality
	33.0	6.5	5.9	5.9	Nominal
	33.0	6.7	6.0	5.6	Nominal
	30.0	6.5	5.5	5.8	Nominal
	32.0	6.9	5.7	5.8	Nominal
	35.0	6.8	6.1	6.0	Nominal
	30.0	6.4	4.5	5.9	Nominal
	30.0	6.4	5.7	5.9	Nominal
	32.0	6.6	5.5	4.6	Nominal
	38.0	7.1	6.5	4.7	Nominal
	31.0	6.7	5.7	4.5	Nominal
	33.0	6.8	5.7	4.5	Nominal
	32.0	6.5	5.8	4.6	Nominal
	33.0	7.1	5.9	4.6	Nominal
	31.0	6.5	5.5	4.4	Nominal
	31.0	6.4	5.5	4.7	Nominal
	30.0	6.4	5.7	4.6	Nominal
	32.0	6.5	5.8	4.1	Nominal
	33.0	6.7	5.9	4.1	Nominal
	34.0	6.8	5.7	4.0	Nominal
	30.0	6.7	5.1	4.0	Nominal
	38.0	7.1	6.0	4.6	Nominal
	27.0	6.0	5.1	5.9	Setup
	30.0	6.6	5.4	6.0	Setup
	32.0	7.0	5.7	6.0	Setup

	Result of image analysis			Experts' result	
TYPE II Stack up	Area	Max. diameter	Min. diameter	Nugget diameter	Quality
	34.0	7.0	5.7	6.1	Setup
	27.0	5.9	5.1	6.0	Setup
	37.0	7.3	6.1	6.1	Setup
	30.0	6.6	5.4	6.1	Setup
	27.0	5.9	5.1	6.0	Setup
	25.0	6.1	5.0	6.0	Setup
	27.0	5.9	5.2	6.0	Setup
	31.0	6.4	5.8	6.1	Setup
	40.0	8.0	6.4	6.3	Setup
	29.0	6.3	5.4	6.0	Setup
	28.0	6.2	5.2	6.1	Setup
	32.0	6.5	5.7	6.0	Setup
	40.0	7.7	6.3	6.5	Setup
	25.0	6.3	4.9	6.0	Setup
	31.0	6.6	5.5	6.3	Setup
	32.0	6.6	5.7	6.0	Setup
	32.0	6.4	4.6	6.2	Setup
	32.0	6.6	5.8	6.0	Setup
	33.0	6.7	5.8	6.1	Setup
	42.0	7.6	6.6	6.1	Setup
	31.0	6.1	5.7	6.1	Setup
	32.0	6.5	5.7	6.1	Setup
	32.0	6.6	5.7	5.2	Setup
	47.0	8.4	6.8	4.9	Setup

	Result of image analysis			Experts' result	
TYPE II Stack up	Area	Max. diameter	Min. diameter	Nugget diameter	Quality
	32.0	6.6	5.7	4.9	Setup
	41.0	7.9	6.3	5.0	Setup
	35.0	7.3	6.0	5.1	Setup
	48.0	8.2	7.1	5.1	Setup
	33.0	6.7	5.7	4.7	Setup
	33.0	6.6	5.7	4.7	Setup
	32.0	6.5	5.7	4.9	Setup
	33.0	6.5	5.7	4.8	Setup
	33.0	6.9	5.7	4.9	Setup
	33.0	6.5	5.4	4.9	Setup
	33.0	6.6	5.7	5.1	Setup
	37.0	7.5	5.7	4.7	Setup
	11.0	5.0	3.0	0.0	Stick
	15.0	5.1	3.1	0.0	Stick
	9.0	5.0	3.2	0.0	Stick
	11.0	5.3	2.7	0.0	Stick
	8.0	5.0	2.7	0.0	Stick
	17.0	5.3	3.6	0.0	Stick
	10.0	4.9	3.3	0.0	Stick
	14.0	5.3	2.8	0.0	Stick
	9.0	4.6	2.5	0.0	Stick
	11.0	5.0	2.8	0.0	Stick
	12.0	4.9	2.5	0.0	Stick
	6.0	3.9	2.5	0.0	Stick

	Result of image analysis			Experts' result	
TYPE II Stack up	Area	Max. diameter	Min. diameter	Nugget diameter	Quality
	8.0	4.6	2.5	0.0	Stick
	10.0	4.9	3.2	0.0	Stick
	14.0	5.4	2.5	0.0	Stick
	15.0	5.5	4.0	0.0	Stick
	14.0	5.3	2.8	0.0	Stick
	13.0	5.4	3.5	0.0	Stick
	10.0	4.4	3.0	0.0	Stick
	10.0	5.0	2.5	0.0	Stick
	7.0	4.2	2.7	0.0	Stick
	18.0	5.3	3.6	0.0	Stick
	20.0	5.75	2.6	0.0	Stick
	12.0	5.3	3.6	0.0	Stick
	16.0	5.7	3.6	0.0	Stick
	11.0	5.1	3.3	0.0	Stick
	9.0	3.8	2.5	0.0	Stick
	14.0	5.5	2.7	0.0	Stick
	20.0	5.8	3.8	0.0	Stick
	20.0	5.5	3.0	0.0	Stick
	11.0	5.3	2.5	0.0	Stick
	17.0	5.5	2.7	0.0	Stick
	15.0	5.1	3.8	0.0	Stick
	17.0	5.3	3.4	0.0	Stick
	11.0	4.6	3.1	0.0	Stick
	12.0	5.3	3.0	0.0	Stick

Appendix II

AIA program source code

```
//------------------------------------------------------------------------
// L_Img.java:
//              load image with menu bar
//              use image-filters method
//------------------------------------------------------------------------
import java.awt.*;
import java.io.*;
import java.awt.event.*;
import ImageFilterBase;
import BinaryFilter;
import EdgeDetectionFilter;
import GrayImageFilter;
import BrighterImage;
import ImageDilationFilter;
import java.awt.image.*;

public class AIA extends Frame implements WindowListener
{
// MenuBar definitions
        MenuBar mb;
//------------------------------------------------------------------------
// Menu and Menu item definitions
//------------------------------------------------------------------------
        Menu m1;        // File
        MenuItem FileOpen; // Open
        MenuItem FileSave;  // Save
        MenuItem CloseItem; // Close
        Menu m5;        // Process
        MenuItem OriginalImg; //back to original
        MenuItem ImgGray;  //Gray Image
        MenuItem ImgBrightness;      // Brightness
        MenuItem ImgHistogram;       // Histogram
        MenuItem morph_dilation;     // Dilation/Erosion
        MenuItem morph_threshold; // Thresholding
        MenuItem morph_edge;         // Edge Detection
        MenuItem morph_calculation;          // Area Calculation
        MenuItem morph_perform;  // Perform
        Menu m15;     // Preparing data for analysis
        MenuItem morph_training;     // Prepare data for training
        MenuItem morph_test;         // Prepare data for testing (NN or statstics)
        Menu m18;     // Analysis (NN-training, NN-testing, statistics)
        MenuItem NN_Training;        // NN-Training
        MenuItem NN_Test;  // NN-Testing
        MenuItem stat; // use statistics method
        MenuItem once; // one image-one button do it once
```

```
        Menu m23;     // Help
        MenuItem About;       // About

// dialog for open more files ----------------- need rework for better interface
        M_dialog message1= new M_dialog(this, " ");

//------------------------------------------------------------------------
// Display panel definition
//------------------------------------------------------------------------
        Panel westPanel;  // Image Canvas definitions

//------------------------------------------------------------------------
// MenuItem Listener
//------------------------------------------------------------------------
        private MenuItemListener menuItemListener = new MenuItemListener();

//------------------------------------------------------------------------
// Other variables
//------------------------------------------------------------------------
        static String filename_now,filename_last;
        int times=0; int count1=0;
        getImg PicCanvas1;
        BPNet networks;
        double diameter;
        double[] temp1=new double[3];
        double[] temp3=new double[3];
        double[][] testing_matrix=new double[50][3];

//------------------------------------------------------------------------
// Class constructor
//------------------------------------------------------------------------
        public AIA()
        {
                super ( " ");
                setSize( new Dimension( 500, 300 ) );
                setResizable( true );
                addWindowListener( this );      // Add listeners.
                networks = new BPNet (3,50,1,0.1,1.0,1000000);
                // Instant of neural networks class
                // BPNet(noi,noh,noo,learning_rate,min_sse,max_cycle)
                makeGUI();      // Make the GUI.
        }

//------------------------------------------------------------------------
// Method of graphic user interface
```

```
//------------------------------------------------------------------------
        private void makeGUI()
        {
                mb = new MenuBar();

//--------------------------------------------------------------------
// Create menu and menu items and assign to menubar
//--------------------------------------------------------------------
                m1 = new Menu("File");
                mb.add(m1);
                        FileOpen = new MenuItem("Open");
                        m1.add(FileOpen);
                        FileSave = new MenuItem("Save");
                        m1.add(FileSave);
                        CloseItem = new MenuItem("Close");
                        m1.add(CloseItem);
                m5 = new Menu("Process");
                mb.add(m5);
                        OriginalImg = new MenuItem("Back to Original Image");
                        m5.add(OriginalImg);
                        ImgGray = new MenuItem("Gray Image");
                        m5.add(ImgGray);
                        ImgBrightness = new MenuItem("Brighten Image");
                        m5.add(ImgBrightness);
                        ImgHistogram = new MenuItem("Histogram");
                        m5.add(ImgHistogram);
                        morph_dilation = new MenuItem("Dilation/Erosion");
                        m5.add(morph_dilation);
                        morph_threshold = new MenuItem("Thresholding");
                        m5.add(morph_threshold);
                        morph_edge = new MenuItem("Edge Detection");
                        m5.add(morph_edge);
                        morph_calculation = new MenuItem("Area Calculation");
                        m5.add(morph_calculation);
                        morph_perform = new MenuItem("Perform");
                        m5.add(morph_perform);
                m15 = new Menu("Prepare Data");
                mb.add(m15);
                        morph_training = new MenuItem("Training Data");
                        m15.add(morph_training);
                        morph_test = new MenuItem("Testing Data");
                        m15.add(morph_test);
                m18 = new Menu("Analysis");
                mb.add(m18);
                        NN_Training = new MenuItem("Training");
```

```
                m18.add(NN_Training);
                NN_Test = new MenuItem("Testing");
                m18.add(NN_Test);
                stat = new MenuItem("Statistics");
                m18.add(stat);
                once = new MenuItem("Do it once");
                m18.add(once);
        m23 = new Menu("Help");
                mb.add(m23);
                About = new MenuItem("About");
                m23.add(About);

        setMenuBar (mb);

//-----------------------------------------------
// Create image canvas
//-----------------------------------------------
    westPanel = new Panel();
    westPanel.setLayout(new BorderLayout());
    add(westPanel);
    westPanel.setBackground (Color.yellow);

//-----------------------------------------------
// Make action listener
//-----------------------------------------------
        FileOpen.addActionListener(menuItemListener);
        FileSave.addActionListener(menuItemListener);
        CloseItem.addActionListener(menuItemListener);
        OriginalImg.addActionListener(menuItemListener);
        ImgGray.addActionListener(menuItemListener);
        morph_threshold.addActionListener(menuItemListener);
        morph_edge.addActionListener(menuItemListener);
        ImgBrightness.addActionListener(menuItemListener);
        morph_dilation.addActionListener(menuItemListener);
        morph_calculation.addActionListener(menuItemListener);
        morph_perform.addActionListener(menuItemListener);
        NN_Training.addActionListener(menuItemListener);
        NN_Test.addActionListener(menuItemListener);
        morph_training.addActionListener(menuItemListener);
        morph_test.addActionListener(menuItemListener);
        stat.addActionListener(menuItemListener);
        once.addActionListener(menuItemListener);

      }
```

```
   public void windowClosing( WindowEvent event ) { dispose(); }
   public void windowOpened( WindowEvent event ) {}
   public void windowIconified( WindowEvent event ) {}
   public void windowDeiconified( WindowEvent event ) {}
   public void windowClosed( WindowEvent event ) {}
   public void windowActivated( WindowEvent event ) {}
   public void windowDeactivated( WindowEvent event ) {}


//-----------------------------------------------
// Main program
//-----------------------------------------------
   public static void main(String args[])
        {

                AIA win = new AIA();

                win.addWindowListener( new WindowAdapter()
                {
                        public void windowClosed (WindowEvent event) {
                        System.exit(0);}
                });

     win.setTitle("Acoustic Image Analyzer   "); //+filename_now);
     win.show();
   }


//-----------------------------------------------
// Define action for different listener
//-----------------------------------------------
        class MenuItemListener implements ActionListener
        {
                public void actionPerformed(ActionEvent e)
                {
// menu for "File"
                        String command = e.getActionCommand();
                                if ( command.equals("Close") )
                                {
                                        dispose();
                                        System.exit(0);
                                }
                                else if ( command.equals("Open") )
                                {
```

```
                                        filename_now=loadFile("Open Image File .......");

                                        show();
                                }
                                else if ( command.equals("Save") )
                                        saveFile(false);
// menu for "Image Processing"
                                else if (command.equals("Back to Original Image") )
                                        PicCanvas1.imgBack();
                                else if (command.equals("Brighten Image") )
                                        PicCanvas1.brightenImg();
                                else if (command.equals("Gray Image")  )
                                        PicCanvas1.gray();
                                else if (command.equals("Thresholding") )
                                        PicCanvas1.thresholding();
                                else if (command.equals("Edge Detection") )
                                        PicCanvas1.edge_detect();
                                else if (command.equals("Dilation/Erosion") )
                                        PicCanvas1.dilation();
                                else if (command.equals("Area Calculation") )
                                        PicCanvas1.area_calculation();
                                else if (command.equals("Perform") )
                                        PicCanvas1.morph_perform();
// menu for "Analysis"
                                else if (command.equals("Training"))
                                {
                                        double error;
                                        networks.set_init();
                                        error=networks.training();
                                        System.out.println(" The SSE is...." + error);
                                }
                                else if (command.equals("Testing"))
                                        networks.test();
//  menu for "Prepare Data"
                                else if (command.equals("Training Data"))
// under preparing data
                                        prepare_training_data();
                                else if (command.equals("Testing Data"))
// under preparing data
                                        prepare_testing_data();
                        }
                }

//  Method 1  <loadfile>
                private String loadFile (String fdtitle)
```

```
        {
                FileDialog fd = new FileDialog( this, fdtitle, FileDialog.LOAD );
                fd.setFile("*.*");
                fd.show();
                String currentFile, filename_1 = null;
                if (( currentFile = fd.getFile()) != null)
                {

                        filename_1 = fd.getDirectory() + currentFile;
                        westPanel.removeAll();
                        PicCanvas1 = new getImg(filename_1);
                        westPanel.add(PicCanvas1);
                        fd.dispose();
                }
                return filename_1;
        }

// Method 2  <savefile>
        private String saveFile(boolean in)
        {
                String temp_filename=null;
                FileDialog fd1 = new FileDialog( this, "Save File", FileDialog.SAVE );
                fd1.setFile("*.*");
                fd1.show();
                String currentFile1= null;
                while (in=true)  // when int=1, <type 1> save as text file
                {
                        if (( currentFile1 = fd1.getFile()) != null)
                        {
                                temp_filename = fd1.getDirectory() + currentFile1;
                                fd1.dispose();
                        }
                        break;
                }
                while (in=false) // indicate the file is a gif file, <type 2> need gifEncoder
to save it
                {break;}
                System.out.println("the file will be save as....."+temp_filename);
                return temp_filename;

                // Save file data...
        }

// Method 3  <prepare_training_data>
        private void prepare_training_data()
```

```
        {
                filename_last=filename_now;
//              message1.show();
                show();
                message1.show();
                temp1=PicCanvas1.morph_perform1();
                N_dialog message2= new N_dialog(this, " ");
        }

// Method 4  <prepare multi-data for testing >
        private void prepare_testing_data()
        {
                M1_dialog message2= new M1_dialog(this, " ");
                show();
                temp3=PicCanvas1.morph_perform1();
        }


//--------------------------------------------------------------
// Inner class getImg; mainly for image processing
//--------------------------------------------------------------
        public class getImg extends Canvas
    {
                private Image image;
// constructor 1 for images from file
                public getImg(String filename)
                {
                        image = Toolkit.getDefaultToolkit().getImage(filename);
                        repaint();
                }
                public void paint(Graphics g)
                {
                        g.drawImage(image, 0, 0, this);
                }

// Method 1  <override update>
                public void update(Graphics g)
                {
                        paint(g);
                }

// Method 2  <update an image >
                public void refresh()
                {
                        Graphics g = this.getGraphics();
```

```
                paint(g);
        }

// Method 3  <bring back an image >
        private void imgBack()
        {
                image = Toolkit.getDefaultToolkit().getImage(filename_now);
                repaint();
        }

// Method 4  < gray image filter >
        private void gray()
        {
                FilteredImageSource source =
                        new FilteredImageSource(image.getSource(),
                        new GrayImageFilter());
                image=createImage(source);
                repaint();
        }

// Method 5  < thresholding image filter >
        private void thresholding()
        {
                FilteredImageSource source =
                        new FilteredImageSource(image.getSource(),
                        new BinaryFilter(0.1));
                image=createImage(source);
                repaint();
        }

// Method 6  < brighten image filter >
        private void brightenImg()
        {
                FilteredImageSource source =
                        new FilteredImageSource(image.getSource(),
                        new BrighterImage());
                image=createImage(source);
                repaint();
        }

// Method 7  < image edge detection filter >
        private void edge_detect()
        {
                FilteredImageSource source =
                        new FilteredImageSource(image.getSource(),
```

```
                        new EdgeDetectionFilter(20));
                image=createImage(source);
                repaint();
        }

// Method 8  < image delation filter >
        private void dilation()
        {
                FilteredImageSource source =
                        new FilteredImageSource(image.getSource(),
                        new ImageDilationFilter());
                image=createImage(source);
                repaint();
        }

// Method 9   perform a set of morph on one image, for demonstration
        private void morph_perform()
        {
                        FilteredImageSource source =
                                new FilteredImageSource(image.getSource(),
                                new BinaryFilter(0.1));
                        image=createImage(source);
                        //repaint();
                        FilteredImageSource source1 =
                                new FilteredImageSource(image.getSource(),
                                new ImageDilationFilter());
                        image=createImage(source1);
                        //repaint();
                        FilteredImageSource source2 =
                                new FilteredImageSource(image.getSource(),
                                new AreaCalculationFilter());
                        image=createImage(source2);
                        repaint();
        }

// Method 10   perform a set of morph on one image, pass the parameters of
//             an image for further usage
        private double[] morph_perform1()
        {
                double[] temp5=new double[3];
                FilteredImageSource source =
                                new FilteredImageSource(image.getSource(),
                                new BinaryFilter(0.1));
                image=createImage(source);
                //repaint();
```

```
                        FilteredImageSource source1 =
                                    new FilteredImageSource(image.getSource(),
                                    new ImageDilationFilter());
                        image=createImage(source1);
                        //repaint();
                        FilteredImageSource source2 =
                                    new FilteredImageSource(image.getSource(),
                                    new AreaCalculationFilter());
                        image=createImage(source2);
                        temp5=AreaCalculationFilter.Cal();
                        return temp5;
                  }

// Method 11  <calculate image parameters
                  private void area_calculation()
                  {
                        FilteredImageSource source =
                              new FilteredImageSource(image.getSource(),
                              new AreaCalculationFilter());
                        image=createImage(source);
                        repaint();
                  }
            }

//-----------------------------------------------------------------------------
// Inner class M_dialog; for preparing training data
//          interacting with user for
//1. processing more images
//2. call class N_dialog for result entering
//3. save training data
//-----------------------------------------------------------------------------
            class  M_dialog extends Dialog implements ActionListener
            {
                  int count=0;
                  double[][] training_matrix;
                  double[][] m_analysis=new double[200][4];
                  public M_dialog( Frame frame, String title)
                  {
                super(frame,  "Analysis more images? ", true);
                    Button b1, b2;
                        add(b1 = new Button("YES"), BorderLayout.WEST);
                        add(b2 = new Button("NO"), BorderLayout.EAST);
                b1.addActionListener(this);
                        b2.addActionListener(this);
                pack();
```

```
            show();
        }
        public void actionPerformed(ActionEvent evt)
        {
                String what = evt.getActionCommand();

// Choose YES  to proceed for next image and enter the target for this analysis
                if ("YES".equals(what))
                {
                        dispose();
                        System.out.println("true is pressed");
                        times++;
                        System.out.println("the yes button have been pressed for ...
                        "+times+" ... times");
                        System.out.println("=============================
                        ================");
                        System.out.println("processing ...... the file in progress
                        is......"+filename_now);
// Display parameters
                        for (int i =0; i<3; i++)
                        {
                                m_analysis[times-1][i]=temp1[i];
                                System.out.println("the                    parameters
                                are....."+temp1[i]);
                        }
                        m_analysis[times-1][3]=diameter;
// Display prepared matrix for saving
                        System.out.println("Please use file dialog to enter the
                        NEXT file you want to analysis ...");
                        filename_now=loadFile("Open NEXT Image File for Pre-
                        processing .......");
                }

// Choose NO to save parameters and target value for training
                else if ("NO".equals(what))
                {
                        dispose();
                        System.out.println("false is pressed");
                        while (times > 0)
                        //      break;
                        {
//
// ------------------------------------------------------------------------------------------
----
                                training_matrix=new double[200][4];
```

```
for (int i=1;i<times-1;i++)
{
        System.out.println("matrix save for outputs
        is....."+m_analysis[i][0]
        +"..."+m_analysis[i][1]+"..."+m_analysis[i][
        2]+"..."+m_analysis[i+1][3]);
        training_matrix[i-1][0]=m_analysis[i][0];
        training_matrix[i-1][1]=m_analysis[i][1];
        training_matrix[i-1][2]=m_analysis[i][2];
        training_matrix[i-1][3]=m_analysis[i+1][3];
}
for (int i=1;i<times-1;i++)
{
        System.out.println("for saving matrix
        is....."+training_matrix[i-1][0]
        +"..."+training_matrix[i-
        1][1]+"..."+training_matrix[i-
        1][2]+"..."+training_matrix[i-1][3]);
}
//..............................................................................................................................

// Ask an file dialog to save training data

String filename2=saveFile(true);
System.out.println("the file will be save
as...this....."+filename2);
FileOutputStream file_out;
DataOutputStream data_out;
try
{
        file_out = new
FileOutputStream(filename2);
        data_out = new DataOutputStream(file_out);
        data_out.writeInt(times-2);
        for (int i=0; i<times-2;i++)
// write parameters ( three of them) and target (one)
        {
                for (int j=0;j<4;j++)
                {
                        data_out.writeDouble(trainin
                        g_matrix[i][j]);
                }
        }
        data_out.close();
```

```
                                        }
                                        catch (IOException e)
                                        {
                                                System.out.println(e);
                                        }
//                                      times=0;
                                        break;
                                }
                        }
                }
        }
//=========================================
//--------------------------------------------------------------------------------
// Inner class M1_dialog; for preparing testing data
//          interacting with user for
//1. processing more images
//2. save data
//--------------------------------------------------------------------------------
        class  M1_dialog extends Dialog implements ActionListener
        {
                public M1_dialog( Frame frame, String title)
                {
                        super(frame,  "Analysis more images? ", true);
                        Button b1, b2;
                        add(b1 = new Button("More?"), BorderLayout.WEST);
                        add(b2 = new Button("Stop!"), BorderLayout.EAST);
                        b1.addActionListener(this);
                        b2.addActionListener(this);
                        pack();
                        show();
                }
                public void actionPerformed(ActionEvent evt)
                {
                        String what = evt.getActionCommand();

// Choose More  to proceed for next image
                        if ("More?".equals(what))
                        {
                                dispose();
                                System.out.println("more is pressed!!");
                                count1++;
                                System.out.println("the MORE button have been pressed
                                for ... "+count1+" ... times");
                                System.out.println("==============================
                                ===============");
```

```
                                System.out.println("Please use file dialog to enter the
                                NEXT file you want to test ...");
                                filename_now=loadFile("Open NEXT Image for file
                                preparation .......");
// Display parameters
                                for (int i =0; i<3; i++)
                                {
                                        testing_matrix[count1-1][i]=temp3[i];
                                        System.out.println("the i-th pair of parameters
                                        are....."+testing_matrix[count1-1][i]);
                                }
                        }

// Choose Stop to save parameters for training
                        else if ("Stop!".equals(what))
                        {
                                dispose();
                                System.out.println("STOP acquairing images");
                                System.out.println("the number of data set is......
"+count1);
                                while (count1 > 0)
                                {
                                        for (int m=0;m<count1;m++)
                                        {
                                                System.out.println("for saving matrix
                                                is....."+testing_matrix[m][0]
                                                +"..."+testing_matrix[m][1]+"..."+testing_m
                                                atrix[m][2]+"...");
                                        }
//...........................................................................................................................

// Ask an file dialog to save training data
                                        String filename2=saveFile(true);
                                        System.out.println("the file will be save
                                        as...this....."+filename2);
                                        FileOutputStream file_out;
                                        DataOutputStream data_out;
                                        try
                                        {

                                                file_out = new
FileOutputStream(filename2);
                                                data_out = new DataOutputStream(file_out);
                                                data_out.writeInt(count1-1);
```

```
                                        for (int i=1; i<count1;i++)
// write parameters ( three of them) and target (one)
                                        {
                                                for (int j=0;j<3;j++)
                                                {
                                                        data_out.writeDouble(testing
                                                        _matrix[i][j]);
                                                        System.out.println("  training
                                                        matrix          is          ......"
                                                        +testing_matrix[i][j]);
                                                }
                                        }
                                        data_out.close();
                                }
                                catch (IOException e)
                                {
                                        System.out.println(e);
                                }
//                              count1=0;
                                break;
                        }
                }
        }
}


//==========================================
        class N_dialog extends Dialog implements ActionListener
        {
                TextField t;
                public N_dialog( Frame frame, String title)
                {
                        super( frame,"Entering the target value for.... "+filename_last);
                        t=new TextField(50);
                        t.addActionListener(this);
                        add(t,BorderLayout.NORTH);
                        pack();
                        show();
                }

                public void actionPerformed(ActionEvent evt)
                {
                        String value1=t.getText();
                        System.out.println("you entered....."+value1);
                        try
```

```
                        {
                                Double d=Double.valueOf(value1);
                                diameter=d.doubleValue();
                        }
                        catch (NumberFormatException e)
                        {
                                System.err.println("Could not convert string to number
                                "+value1);
                        }
                        dispose();
                }
        }
}
```

```
//package piola.imagefilters;

import java.awt.*;
import java.awt.image.*;

// java class by Roberto Piola (http://www.ilpiola.it/roberto)

//  an abstract filter that reads a whole image, and performs something
//  on it before giving it to its consumer; its subclasses MUST define
//  method do_action() (the action to do on the whole image after it has
//  been loaded)
//  two examples of subclasses can be found in
//  http://www.ilpiola.it/roberto/imagefilters/EdgeDetectionFilter.java
//  and in
//  http://www.ilpiola.it/roberto/imagefilters/ImageSmootherFilter.java



    public abstract class ImageFilterBase extends ImageFilter
    {
        //protected          static          ColorModel          defaultRGB          =
ColorModel.getRGBdefault();
        protected ColorModel defaultRGB = ColorModel.getRGBdefault();

        protected int raster[],newraster[];
        protected int width,height;
        public ImageFilterBase()
        {
            super();
        }
        // method 1
      public void setDimensions(int w, int h)
        {
       width=w;
            height=h;
            raster=new int[width*height];
            newraster=new int[width*height];
            consumer.setDimensions(width,height);
        }

        // method 2
        public void setColorModel(ColorModel model)
        {
          consumer.setColorModel(defaultRGB);
        }
```

```
// method 3
public void setHints(int hintflags)
{
        consumer.setHints(TOPDOWNLEFTRIGHT
         | COMPLETESCANLINES
         | SINGLEPASS
         | (hintflags & SINGLEFRAME));
}

// method 4
public void setPixels(int x, int y, int w, int h, ColorModel model,
 byte pixels[], int off, int scansize)
{

        int srcoff = off;
        int dstoff = y * width + x;
        for (int yc = 0; yc < h; yc++)
        {
                for (int xc = 0; xc < w; xc++)
                {
                        raster[dstoff++]  =  model.getRGB(pixels[srcoff++]
                        & 0xff);
                }
                srcoff += (scansize - w);
                dstoff += (width - w);
        }
}

// method 5
public void setPixels(int x, int y, int w, int h, ColorModel model,
 int pixels[], int off, int scansize)
{
        int srcoff = off;
        int dstoff = y * width + x;
        if (model == defaultRGB)
        {
                for (int yc = 0; yc < h; yc++)
                {
                        System.arraycopy(pixels, srcoff, raster, dstoff, w);
                        srcoff += scansize;
                        dstoff += width;
                }
        }
        else
```

```
                {
                        for (int yc = 0; yc < h; yc++)
                        {
                                for (int xc = 0; xc < w; xc++)
                                {
                                        raster[dstoff++]                         =
                                        model.getRGB(pixels[srcoff++]);
                                }
                                srcoff += (scansize - w);
                                dstoff += (width - w);
                        }
                }
        }

        // method 6
        public void imageComplete(int status)
        {
                if (status == IMAGEERROR || status == IMAGEABORTED)
                {
                        consumer.imageComplete(status);
                        return;
                }
                DoProcess();
                consumer.setPixels(0,  0,width,height,  defaultRGB,  newraster,
                0,width);
                consumer.imageComplete(status);
                raster=null;  // try to deallocate it
                newraster=null;
        }

        abstract public void DoProcess();
        // it has to copy width X height pixels from raster[] to newraster[]...
}
```

```
import java.awt.*;
import java.awt.image.*;


    public class GrayImageFilter extends RGBImageFilter
    {

        public GrayImageFilter()
        {
  canFilterIndexColorModel = true;
        }

        public int filterRGB(int x, int y, int rgb)
        {
            DirectColorModel cm =
                (DirectColorModel)ColorModel.getRGBdefault();

            int   alpha = cm.getAlpha(rgb);
            int   red   = cm.getRed  (rgb);
            int   green = cm.getGreen(rgb);
            int   blue  = cm.getBlue (rgb);
            int   mixed = (red + green + blue) / 3;

            red   = blue = green = mixed;
            alpha = alpha << 24;
            red   = red   << 16;
            green = green << 8;

            return alpha | red | green | blue;
        }
    }
```

```
import java.awt.*;
import java.awt.image.*;


        public class ImageDilationFilter extends ImageFilterBase
        {
                public ImageDilationFilter()
                {
                        super();
                        //degree=th;
                }

                // method
                public void DoProcess()
                {
            int i,j,k,x,y;
                        /* initialize a black background */
                        for(y=0; y<height; y++)
                        for(x=0; x<width; x++)
                newraster[y*width+x]=0xffffffff;
                        /* first pass: in the horizontal direction */
                        for(y=1; y<height-1; y++)
                        for (x=1;x<width-1; x++)
                        {

                                k=y*width+x;
                                for (j=-1;j<1;j++)
                                for (i=-1;i<1;i++)
                                {
                                        if (raster[x+i+(y+j)*width] > 0xff000000)
                                        {
                                        //      newraster[x+i+(y+j)*width]=0xff000000;
                                        //      newraster[k]=0xffffffff;
                                                newraster[k]=0xff000000;
                                        }
                                }
                        }
                }
        }
```

```
/* Build up a 3 layers neural networks
input layer neuron =4
hidden layer neuron =3
output layer neuron =1 */
// by Hsu-Tung Lee June 25, 1998

import java.io.*;
import java.util.* ;
import java.awt.*;

public class BPNet extends Frame
{
int nop; // number of training pattern
int noi, noh, noo; // number of input, hidden, output neurons
double input[], output[], hidden[], target[], error[];
// matrix store the value of input, hidden, output, and target neuron
double weight_1[][], weight_2[][];
// weight matrix between input/hidden and hidden/output
double bias_1[], bias_2[]; // bias of hidden layer and output layer
double i_pattern[][], t_pattern[][]; // all input pattern and all target pattern
double learning_rate, min_sse, sse;
// double mc, moment;
//int max_cycle=1000000000;
double hidden_d[], output_d[]; // delta of hidden and output neuron
double weight1_d[][], weight2_d[][]; // weight matrix difference
double bias1_d[], bias2_d[]; // bias difference
long counter, cycle,max_cycle;
//double decre=0.95, incre=1.05; // increase/decrease rate of learning rate

public BPNet(int noi, int noh, int noo, double learning_rate, double min_sse, long
max_cycle)
// constructor
{
this.noi=noi; this.noh=noh; this.noo=noo;
this.learning_rate=learning_rate; this.min_sse=min_sse;
this.max_cycle=max_cycle;
weight_1=new double[noi][noh];
weight_2=new double[noh][noo];
bias_1=new double[noh];
bias_2=new double[noo];
}

// STEP 0. initialize weight and bias matrices, call once
void set_init()
{
```

```
for (int i = 0; i < noi; i++)
{
for (int j = 0; j < noh; j++)
{
weight_1[i][j] = (double)Math.random()*2.0-1.0;
weight_1[i][j]);
}
}
for (int i = 0; i < noh; i++)
{
for (int j = 0; j < noo; j++)
{
weight_2[i][j] = (double)Math.random()*2.0-1.0;
weight_2[i][j]);
}
}
for (int k = 0; k < noh; k++)
{
bias_1[k] = (double)Math.random()*2.0-1.0;
}
for (int k = 0; k < noo; k++)
{
bias_2[k] = (double)Math.random()*2.0-1.0;
}
}


public double training()
{
double temp[]; // temp matrix for matrix mutiply
error = new double[noo];
hidden_d = new double[noh];
output_d = new double[noo];
weight1_d = new double[noi][noh];
weight2_d = new double[noh][noo];
bias1_d = new double[noh];
bias2_d = new double[noo];
input = new double[noi];
target = new double[noo];
hidden = new double[noh];
output = new double[noo];

// ===== read in all input and target patterns for training
FileInputStream file_in1;
DataInputStream data_in1;
```

```
FileDialog fd = new FileDialog( this, "Open Training File", FileDialog.LOAD );
fd.setFile("*.dat");
fd.show();
String currentFile, filename = null;
if (( currentFile = fd.getFile()) != null)
{
filename = fd.getDirectory() + currentFile;
fd.dispose();
}
try
{
file_in1 = new FileInputStream(filename);
data_in1 = new DataInputStream(file_in1);
nop=data_in1.readInt();
nop=nop-1;
//----------------------------------------------------------
i_pattern = new double[nop][noi];
t_pattern = new double[nop][noo];
for ( int i=0; i < nop; i++)
{
for ( int j=0; j < noi; j++)
{
i_pattern[i][j]=data_in1.readDouble();
i_pattern[i][j]);
}
for (int k=0;k<noo;k++)
{
t_pattern[i][k]=data_in1.readDouble();
t_pattern[i][k]);
}
}
data_in1.close();
}
catch (IOException e)
{
System.out.println(e);
}


for (int i=0; i<nop;i++)
{
if (t_pattern[i][0]<4.8)
t_pattern[i][0]=0;
else
```

```
t_pattern[i][0]=1;
}

cycle=0;
sse=10.0;
counter=0;
long iii=1;
//        STEP 1.  while stop condition is false
while (sse > min_sse && cycle< max_cycle)
{
cycle++;
while (cycle==iii && iii<100000000000)
{
System.out.println("this is cycle number......    "+cycle);
System.out.println("the is sse is ......    "+sse);
iii=iii+100;
break;
}
sse=0;
// STEP 2. loop for each training patterns
for (int l=0; l<nop; l++)
{
counter++;
// STEP 3. prepare for next training pair ==============================
for (int i=0; i<noi;i++)
{
input[i]=i_pattern[l][i];
}
for (int i=0; i<noo;i++)
{
target[i]=t_pattern[l][i];
target[i]);
}
// STEP 4. feed forward processing (input to hidden layer )================
temp = multiply(input, weight_1, noi, noh);
for (int i=0; i<noh; i++)
{
hidden[i] = sigmoid(temp[i]+bias_1[i]);
}
// STEP 5. feed forward processing (hidden to output layer )================
temp = multiply(hidden, weight_2, noh, noo);
for (int i=0; i<noo; i++)
{
output[i] = sigmoid(temp[i]+bias_2[i]);
}
```

```
// STEP 6. backpropagtion of error
// calculate error for the first time ==============================
for (int i=0; i<noo; i++)
{
error[i]=target[i]-output[i];
sse+= error[i]*error[i];
}
// error information term (delta of output layer) ====================
output_d = delta(output, error, noo);
// error information term (delta of hidden layer) ====================
hidden_d = delta(hidden, output_d, weight_2, noh, noo);

// STEP 7. calculate weight and bias correction term ====================
// calculate correction terms of weight matrix #2 and bias #2
for (int i=0; i< noh; i++)
{
for (int j=0; j< noo; j++)
{
weight2_d[i][j] = learning_rate*hidden[i]*output_d[j];
}
}
for (int i=0; i< noo; i++)
{
bias2_d[i] = learning_rate*output_d[i];
}
// calculate correction term of weight matrix #1 and bias #1
for (int i=0; i< noi; i++)
{
for (int j=0; j< noh; j++)
{
weight1_d[i][j] = learning_rate*input[i]*hidden_d[j];
}
}
for (int i=0; i< noh; i++)
{
bias1_d[i] = learning_rate*hidden_d[i];
}
// STEP 8. update weights and bias
for ( int i=0; i< noh; i++)
{
bias_1[i] = bias_1[i] + bias1_d[i];
for (int j=0; j< noi; j++)
{
weight_1[j][i] = weight_1[j][i] + weight1_d[j][i];
```

```
}
for ( int i=0; i< noo; i++)
{
bias_2[i] = bias_2[i] + bias2_d[i];
for (int j=0; j< noh; j++)
{
weight_2[j][i] = weight_2[j][i] + weight2_d[j][i];
}
}
}
// end of an epoch ---------------------------------------------------
}
// end of while loop (the stop condition) -----------------------------------

// STEP 9. write output information ============================
if (cycle>=max_cycle)
System.out.println("Exceed maximum learning cycle......");
else
{
FileDialog fd1 = new FileDialog( this, "Save File", FileDialog.SAVE );

fd1.setFile("*.*");
fd1.show();
String currentFile1, filename2= null;
if (( currentFile1 = fd1.getFile()) != null)
{
filename2 = fd1.getDirectory() + currentFile1;
fd.dispose();
}


FileOutputStream file_out;
DataOutputStream data_out;
try
{
file_out = new FileOutputStream(filename2);
data_out = new DataOutputStream(file_out);
for (int i=0; i<noi;i++) // write weight_1
{
for (int j=0;j<noh;j++)
{
data_out.writeDouble(weight_1[i][j]);
System.out.println(" weight_1 matrix is ......" +weight_1[i][j]);

}
```

```
}
for (int i=0; i<noh;i++) // write bias_1
{
data_out.writeDouble(bias_1[i]);
System.out.println(" bias_1 matrix is ......."+ bias_1[i]);
}
for (int i=0; i<noh;i++) // write weight_2
{
for (int j=0;j<noo;j++)
{
data_out.writeDouble(weight_2[i][j]);
System.out.println(" weight_2 matrix is ......."+ weight_2[i][j]);
}
}
for (int i=0; i<noo;i++) // write bias_2
{
data_out.writeDouble(bias_2[i]);
System.out.println(" bias_2 matrix is ......"+ bias_2[i]);
}

//System.out.println("Size of file written: " + data_out.size());
data_out.close();
}

catch (IOException e)
{
System.out.println(e);
}
}
System.out.println(" training epoch are....... " +counter);
System.out.println(" new training sets are........"+nop);
return sse;

}
// end of training

double sigmoid(double f)
{
if (f < -50)
return 0.0;
else if (f > 50)
return 1.0;
else
return (1/(1+Math.exp(-f)));
}
```

```
//
//     output layer  only.
//
private double[] delta( double[] out, double[] err, int n)
{
double[] delta= new double[n];
for (int i=0;i<n;i++)
{
delta[i]=out[i]*(1-out[i])*err[i];
}
return delta;
}

//
//    hidden layer
//
private double[] delta( double[] out, double[] d, double[][] w, int n, int m)
{

double[] delta = new double[n];
double[] err = new double[n];
for (int i=0; i<n; i++)
{
for (int j=0; j<m; j++)
{
err[i]+=w[i][j]*d[j];
}
}
for (int i=0;i<n;i++)
{
delta[i]=out[i]*(1-out[i])*err[i];
}
return delta;
}

//
// matrices multiply (AxB)
//
private double[] multiply(double[] A, double[][] B, int n, int m)
{
double[] C = new double[m];
for (int i=0; i<m; i++)
{
C[i]=0;
for (int j=0; j<n; j++)
```

```
{
C[i] += A[j]*B[j][i];
}
}
return C;
}
public void test()
{
FileInputStream file_in, file_in1;
DataInputStream data_in, data_in1;
//===============================================================
//              NOTICE!!!!!!!!
//              this section is to assign the test result from image processing
//              REMEMBER to modify image processing program to make this temp.
matrix for
//              testing parameters
//===============================================================
double[] result_in = new double[noi];
String[] result;
double[] result_out = new double[noo];
double[] result_h = new double[noh];
double[] temp;
int not; // number of testing sets

// Read in the pre-prapare weight file for testing

FileDialog fd1 = new FileDialog( this, "Open Trained Weight File", FileDialog.LOAD );
fd1.setFile("*.dat");
fd1.show();
String currentFile1,filename1 = null;
if (( currentFile1 = fd1.getFile()) != null)
{
filename1 = fd1.getDirectory() + currentFile1;
fd1.dispose();
}
try
{
file_in = new FileInputStream(filename1);
data_in = new DataInputStream(file_in);

for (int i=0; i<noi;i++) // read weight_1
{
for (int j=0;j<noh;j++)
{
weight_1[i][j]=data_in.readDouble();
```

```
}
}
for (int i=0; i<noh;i++) // read bias_1
{
bias_1[i]=data_in.readDouble();
bias_1[i]);
}
for (int i=0; i<noh;i++) // read weight_2
{
for (int j=0;j<noo;j++)
{
weight_2[i][j]=data_in.readDouble();
is ......."+ weight_2[i][j]);
}
}
for (int i=0; i<noo;i++) // read bias_2
{
bias_2[i]=data_in.readDouble();
bias_2[i]);
}
data_in.close();
}
catch (IOException e)
{
System.out.println(e);
}
// Read in the pre-prapare file for testing

FileDialog fd = new FileDialog( this, "Open Testing File", FileDialog.LOAD );
fd.setFile("*.dat");
fd.show();
String currentFile,filename = null;
if (( currentFile = fd.getFile()) != null)
{
filename = fd.getDirectory() + currentFile;
fd.dispose();
}
try
{
file_in1 = new FileInputStream(filename);
data_in1 = new DataInputStream(file_in1);
not=data_in1.readInt();
result= new String[not];
for ( int n=0; n < not; n++)
{
```

```
for ( int j=0; j < noi; j++)
{
result_in[j]=data_in1.readDouble();
}
System.out.println(n+"-th  INPUTS     "+result_in[0]+"    .....    "+result_in[1]+"    .....
"+result_in[2]);
// feed forward processing (input to hidden layer )================
temp = multiply(result_in, weight_1, noi, noh);
for (int i=0; i<noh; i++)
{
result_h[i] = sigmoid(temp[i]+bias_1[i]);
}
// feed forward processing (hidden to output layer )================
temp = multiply(result_h, weight_2, noh, noo);
for (int i=0; i<noo; i++)
{
result_out[i] = sigmoid(temp[i]+bias_2[i]);
System.out.println(" The output of this analysis is......" + result_out[i]);
}
// Assign result value
for (int i=0; i<noo; i++)
{
if (result_out[i]<0.91)
result[n]="BAD";
else
result[n]="GOOD";
System.out.println("The result can be interpretate as a    "+result[n]+"   weld!!!");
}
System.out.println("==========================================");
}
data_in1.close();
}
catch (IOException e)
{
System.out.println(e);
}
}
}
```

VITA AUCTORIS

NAME:	Hsu-Tung Lee
PLACE OF BIRTH	Keelung, Taiwan, R.O.C.
YEAR OF BIRTH	1967
EDUCATION	Chung-Yuan Christian University, Chung-Li, Taiwan 1984-1988 B.Sc.
	The Ohio State University, Ohio, U.S.A. 1992-1995, M.Sc.
	University of Windsor, Windsor, Ontario 1996-1999, Ph.D.